

### **Photocopy and Use Authorization**

In presenting this thesis in partial fulfillment of the requirements for an advanced degree at Idaho State University, I agree that the Library shall make it freely available for inspection. I further state that permission for extensive copying of my thesis for scholarly purposes may be granted by the Dean of the Graduate School, Dean of my academic division, or by the University Librarian. It is understood that any copying or publication of this thesis for financial gain shall not be allowed without my written permission.

Signature \_\_\_\_\_

Date \_\_\_\_\_

**Performance Improvements to the  
Portal Evaluation Tank,  
Characterization and Analysis of  
Nuclear Power Plant Component Flooding Tests**

By

Antonio Tahhan

A thesis

submitted in partial fulfillment

of the requirements for the degree of

Master of Science in the Department of Nuclear Engineering

Idaho State University

Spring 2018

## **Committee Approval**

To the Graduate Faculty:

The members of the committee appointed to examine the thesis of Antonio Tahhan find it satisfactory and recommend it be accepted.

---

Dr. Chad Pope  
Major Advisor

---

Dr. Bruce Savage  
Committee Member

---

Dr. Brian Williams  
Graduate Faculty Representative

## Acknowledgments

I would like to thank first Dr. Imel and Dr. Gougar, they were the first professors I talked to when returning to ISU to get a Masters' Degree, they took me back with open arms and I am in debt for that.

I also want to thank Dr. Pope, for allowing me to join his flooding research group, offering me the assistantship that allowed me to keep studying at ISU, and for his support during all the time I have spent working on the project. Alongside Dr. Pope, I would like to thank Dr. Savage who has provided continued guidance, support and help at all steps of the project; finally, I would like to thank Dr. Williams for agreeing on being part of the Committee reviewing my thesis.

Additionally, I would like to thank Cody Muchmore, Alison Wells, Sneha Suresh and Rojin Tuladhar for all the help they provided in preparation for each and every one of the experiments.

To conclude, I would like to thank the CFEL team, for their all their feedback; all of you have been instrumental in this achievement.

## Vita

Antonio was born in Coro, a small city in the coastal area of Venezuela, the same place where his mom was born. He lived with his mom and dad in Caracas through most of his life. There he attended school, he attended pre-school through high school at Colegio San Agustín - el Paraíso, where he graduated with honors in 2010.

After high school, Antonio came to the United States to obtain his bachelor's degree, he was sure he wanted to obtain an engineering degree, and selected ISU as the university he would attain his Bachelors in Nuclear Engineering. Four years later, he graduated with a double major in Nuclear and Mechanical Engineering with honors from ISU; where he would return to in 2016 to start his Master's Degree.

Throughout his life Antonio has been surrounded by people who have helped him achieve everything that he has done, from his family and professors to his friends, he is grateful for all the opportunities he has had and hopes to be able to make proud all of them.

# Table of Contents

List of Figures .....	vii
List of Tables .....	xiii
List of Abbreviations .....	xiv
Abstract .....	xv
Introduction .....	1
The Portal Evaluation Tank .....	5
Pre-Mods Configuration .....	5
Post-Mods Configuration .....	9
Instrumentation Description.....	15
Pre-Mods Instrumentation.....	15
General Equipment.....	15
Measurement Instrumentation .....	15
Safety Instrumentation.....	16
Software.....	16
Connections .....	17
Post-Mods Instrumentation .....	18
General Equipment.....	18
Measurement Instrumentation .....	18
Safety Instrumentation.....	20
Software.....	20
Connections .....	21
Experiments, Results and Analysis.....	23
Pre-Mods Experiments, Results and Analysis .....	23

Frame Construction .....	23
Experiments .....	26
PET Improvements .....	41
Pressure and Flowrate Behavior Predictions .....	43
Flow3D Simulations (Courtesy of Gregory Roberts).....	44
SolidWorks Simulations .....	51
Flowrate-Behavior Experiment .....	55
Post-Mods Experiments, Results and Analysis.....	57
Post-Mods Hollow-Core Door Experiments .....	57
Post-Mods Steel Door Experiments.....	67
Data Processing Analysis .....	100
Leak Rate and Water Depth Dependency .....	106
Summary and Conclusions.....	116
Future Work .....	122
Bibliography .....	126
Appendix #1: Flygt Pump, Performance Curve & Specs .....	128
Appendix #2: Global Pump, Performance Curve & Specs .....	131
Appendix #3: PACTware Interface .....	133
Appendix #4:CR1000 Interface: Device Configuration Utility, Shortcut & PC200W .....	141
Appendix #5: Additel Land Wireless & Additel 680 Wireless Transmitter Setup.....	155
Appendix #6: Saving Experiment Results into Excel Workbook .....	161

## List of Figures

Figure 1. Door from Inside the Fukushima-Daiichi NPP .....	1
Figure 2. Fort Calhoun NPP flooded by the Mississippi River .....	2
Figure 3. Flooded Fukushima NPP Control Room .....	3
Figure 4. Picture of the PET, Bishwo Bandari Up Front .....	5
Figure 5. Top mounted PET instrumentation/safety equipment .....	6
Figure 6. Hollow-Core Door Experiments - Global Pump - Experiment Model .....	8
Figure 7. 12 in. PET Opening at the Top .....	9
Figure 8. Electrical Box at the Top of the PET .....	10
Figure 9. Approximate Model of the Updated PET 12 in. Piping.....	11
Figure 10. Continuation Pipe Segment Inside the PET .....	12
Figure 11. Piping Air & Pressure Relief Valves with Water Collection System in Place.....	13
Figure 12. Air Relief Valve Positioned Within its Surrounding Duct.....	14
Figure 13. PET Pre-Mods - Piping & Instrumentation Diagram .....	16
Figure 14. ABB Watermaster Flowmeters - Downstream 12 in. & 8 in. ....	19
Figure 15. PET Post-Mods - Piping & Instrumentation Diagram .....	20
Figure 16. Mismatched Size Frame .....	24
Figure 17. Inner-frame installed inside the PET.....	25
Figure 18. Hollow-Core Door Experiment #1 - Outward Opening Door, Depth Results .....	27
Figure 19. Experiment #1 - Outward Opening Door Showing Leakage Underneath from Bowing Effect .....	28
Figure 20. Plywood Strip Screwed to Bottom End of Frame .....	29



Figure 21. Hollow-Core Door Experiments #2 & #3 - Outward Opening Doors, Water Depth Results .....	30
Figure 22. Broken Door, Result of Experiment #2 .....	31
Figure 23. Broken Door, Result of Experiment #2 .....	32
Figure 24. Hollow-Core Door Experiments #4 & #5 - Inward Opening Doors, Water Depth .....	33
Figure 25. Hollow-Core Door Experiment #1 - Flow Information.....	37
Figure 26. Hollow-Core Door Experiment #3 - Flow Information.....	37
Figure 27. Hollow-Core Door Experiment #3 - Flow Information, Zoomed In .....	38
Figure 28. Hollow-Core Door Experiment 4 – Flow Information .....	39
Figure 29. Hollow-Core Door Experiment 5 – Flow Information .....	39
Figure 30. Flow3D Simulation #1 PET View .....	44
Figure 31. Flow3D Simulation #1 PET Pressure Prediction .....	45
Figure 32. Flow3D Simulation #2 PET View .....	46
Figure 33. Flow3D Simulation #2 PET Pressure Behavior .....	47
Figure 34. Flow3D Simulation #3 PET View .....	48
Figure 35. Flow3D Simulation #3 Piping System Pressure Behavior .....	49
Figure 36. SolidWorks PET Simulation Model.....	52
Figure 37. SolidWorks Simulation 'PET Average Total Pressure' Results .....	53
Figure 38. Hollow-Core Door - Experiment #6 - Initial Valve Configuration .....	58
Figure 39. Hollow-Core Door - Experiment #7 - Initial Valve Configuration .....	58
Figure 40. Hollow-Core Door Experiments #6 & #7 - PET Water Height.....	62
Figure 41. Hollow-Core Door Experiment #6 - Flow Information.....	65

Figure 42. Hollow-Cor Door Experiment #7 - Flow Information.....	67
Figure 43. Welded wood stud anchors, with holes for screws.....	69
Figure 44. Screwed Double Wood Studs into Anchors.....	69
Figure 45. (left) Top section of the stud inner frame. (right) Bottom section of the inner frame	70
Figure 46. Steel door frame and wall.....	71
Figure 47. Steel Door Experiments #1, #2 & #3 - Initial Valve Configuration.....	72
Figure 48. Steel Door Experiments #1, #2 & #3 - PET Water Height .....	73
Figure 49. Steel Door Experiment #1 - Flow Information.....	75
Figure 50. Steel Door Experiment #2 - Flow Information.....	76
Figure 51. Steel Door Experiment #3 - Flow Information.....	76
Figure 52. Steel Door Experiment #4 - Initial Valve Configuration.....	78
Figure 53. Steel Door Experiment #5 - Initial Valve Configuration.....	78
Figure 54. Steel Door Experiment #4 & #5 - PET Water Height.....	79
Figure 55. Steel Door Experiment #4 - Flow Information.....	80
Figure 56. Steel Door Experiment #5 - Flow Information.....	81
Figure 57. Steel Door Experiments #6, #7 & #8 - Initial Valve Configuration.....	82
Figure 58. Steel Door Experiment #6, #7 & #8 - PET Water Height.....	82
Figure 59. Steel Door Experiment #6 - Flow Information.....	83
Figure 60. Steel Door Experiment #7 - Flow Information.....	84
Figure 61. Steel Door Experiment #8 - Flow Information.....	84
Figure 62. Steel Door Experiment #9 - Initial Valve Configuration.....	85
Figure 63. Steel Door Experiment #9, #10 & #11 - PET Water Height.....	86

Figure 64. Bent Deadbolt, Result of Experiment #9 .....	87
Figure 65. Steel door experiment #9 - Flow Information .....	88
Figure 66. Steel Door Experiment #10 - Initial Valve Configuration.....	89
Figure 67. Steel Door Experiment #10 – Flow Information .....	90
Figure 68. Bent Deadbolt, Result of Experiment #10 .....	92
Figure 69. Steel Door Experiment #11 - Initial Valve Configuration.....	93
Figure 70. Steel Door Experiment #11 - Flow Information.....	94
Figure 71. Experiment #11 - Post-Experiment Door State .....	95
Figure 72. Deadbolt Comparison - Experiments #9 #10 left, Experiment #11 right .....	96
Figure 73. Steel Door Experiment #12 - Initial Valve Configuration.....	97
Figure 74. Experiment #12 - PET Water Height .....	98
Figure 75. Steel Door Experiment #12 - Flow Information.....	99
Figure 76. Steel Door Experiment #10 - Fill Rate Data-Processing Methods Comparison .....	100
Figure 77. Steel Door Experiment #10 - Leak Rate Data-Processing Methods Comparison .....	101
Figure 78. Steel Door Experiment #11 - Fill-Rate Data Processing Methods Comparison .....	101
Figure 79. Steel Door Experiment #11 - Leak-Rate Data Processing Methods Comparison ....	102
Figure 80. Hollow-Core Door Experiments - Leak Rate vs. PET Water Depth .....	107
Figure 81. Steel Door Experiments - Zoomed Leak Rate vs. PET Water Depth, Global Pump Incl. .....	108
Figure 82. Steel Door Experiment #10 - Depth Data Comparison.....	110
Figure 83. Steel Door Experiment #11 - Depth Data Comparison.....	111
Figure 84. Steel Door Experiment #10 - Leak Rate Analysis Comparison.....	114

Figure 85. Steel Door Experiment #11 - Leak Rate Analysis Comparison.....	115
Figure 86. PACTware Welcome Screen.....	133
Figure 87. PACTware- adding the HART modems.....	134
Figure 88. PACTware - Add HART modem DTM .....	134
Figure 89. PACTware – HART Communication Device.....	135
Figure 90. Device 'Parameters' Screen .....	136
Figure 91. PACTware - Add Flowmeter DTM .....	137
Figure 92. PACTware - Connecting to Flowmeters .....	138
Figure 93. PACTware - 'Archive' Screen .....	139
Figure 94. PACTware - 'Archive' Save Settings.....	140
Figure 95. Device Configuration Utility - Welcome Screen .....	142
Figure 96. Device Configuration - Connected to the CR1000 .....	143
Figure 97. Device Configuration - 'Logger Control' Screen .....	144
Figure 98. Device Configuration - 'Data Monitor' Screen .....	144
Figure 99. ShortCut - Welcome Screen.....	145
Figure 100. ShortCut - Datalogger Selection Screen.....	146
Figure 101. ShortCut - Sensor/General Measurements Selection Screen.....	146
Figure 102. ShortCut - Output Setup Screen .....	147
Figure 103. ShortCut - Output Select Screen .....	148
Figure 104. ShortCut - Save Screen.....	149
Figure 105. ShortCut - Wiring Diagram Screen .....	150
Figure 106. ShortCut - Wire Text Screen .....	150

Figure 107. PC200W - Welcome Screen .....	151
Figure 108. PC200W - Adding a Datalogger.....	152
Figure 109. PC200W - Connecting to a Datalogger .....	153
Figure 110. PC200W - Saving the Data .....	154
Figure 111. Additel 680 Pressure Transmitter- Turning On transmission .....	156
Figure 112. Additel 680 Pressure Transmitter - Selecting Channel .....	156
Figure 113. Additel Land Wireless - Channel Selection .....	157
Figure 114. Additel Land Wireless Transmitters Screen.....	158
Figure 115. Additel Land Wireless - Start to Record.....	159
Figure 116. Additel Land Wireless - Password Screen.....	159
Figure 117. Additel Land Wireless - Export/Save Data .....	160
Figure 118. Excel - Copying a Worksheet.....	161
Figure 119. Excel - Selecting the Position of the New Worksheet .....	162
Figure 120. Excel - Renaming the New Worksheet .....	162

## List of Tables

Table 1. System Flowrate Behavior #1 – Fragment of the Entire Data Collected .....	56
Table 2. CR1000 Raw Data - Fragment of Data Collected for SD - Experiment #11 .....	60
Table 3. Flowmeter Data - Recorded vs. Created .....	63
Table 4. CampBell Scientific vs Omega Depth Sensor Data Comparison .....	74
Table 5. Steel Door Experiment #10 - Quantification of Results from Different Data Processing Methods.....	104
Table 6. Steel Door Experiment #11 - Quantification of Results from Different Data Processing Methods.....	104
Table 7. Steel Door Experiment #10 - Depth Data Analysis Comparison .....	112
Table 8. Steel Door Experiment #11 - Depth Data Analysis Comparison .....	113
Table 9. Summary of Results from PET Steel Door Experiments.....	117
Table 10. Summary of Results from PET Hollow Core Door Experiments.....	118

## List of Abbreviations

CFEL	Component Flooding Evaluation Laboratory
DS	Downstream
EXP	Experiment
FM1	Flowmeter #1. Upstream 12 in. flowmeter
FM2	Flowmeter #2. Downstream 12 in. flowmeter
FM3	Flowmeter #3. Downstream 8 in. flowmeter
GPM	gallons per minute
HCD	Hollow-Core Door
NPP	Nuclear Power Plant
PET	Portal Evaluation Tank
PRA	Probabilistic Risk Assessment
SD	Steel Door
US	Upstream

# Abstract

## Performance Improvements to the Portal Evaluation Tank, Characterization and Analysis of Nuclear Power Plant Component Flooding Tests

Thesis Abstract – Idaho State University (2018)

The purpose of the work described in this thesis was to connect the PET to an available 60 HP pump, through a piping system that would allow control and measurement of the flow into the tank and perform experiments on nuclear power plant components. The experiments showcased the successful increase of the PET capabilities, in both, the flowrates achieved, and in the control the piping system provided the researchers to direct the water flow. The experiments on metal doors demonstrated how much more reliable they are when compared to the previously tested hollow-core doors, needing higher flowrates, at least twice those of the hollow-core doors to achieve the water depths that induced failures. The failures in these cases were also different than in hollow-core door experiments; in one test the door ended permanently bent with twisting of the deadbolt assembly, in two tests the deadbolt was bent and separated from the rest of the locking assembly, and in the remaining eight experiments, all performed with the deadbolt unlocked, the failure was achieved by the door popping open.



## Introduction

The tsunami that struck the Fukushima-Daiichi Nuclear Power Plant, located in the Fukushima prefecture of Japan in March 2011, served as a reminder of the many dangers power plants and structures in general are subjected to during an emergency event; as seen Figure 1, which shows the damage inside the Fukushima Daiichi NPP after the tsunami. The damage created by this tsunami was measured in billions of dollars (World Nuclear Association, 2017) and claimed thousands of lives. The tsunami caused the meltdown of three of the six reactors present at the NPP and the release of radioactive materials to the environment.



Figure 1. Door from Inside the Fukushima-Daiichi NPP

In the nuclear industry several accident-based scenarios are studied for each power plant before its construction, to understand the behavior of the plant during the event, and try to prevent any catastrophes, see Figure 2, which shows the Fort-Calhoun NPP after a flood from the

Mississippi river; of those scenarios, flooding occurrences are ones of great importance for the nuclear industry, especially after tsunami events. However, there is little to no data regarding the behavior and reliability of NPP components once they are or have been in contact with water (Szilard, et al., 2015); therefore, the regulations governing these scenarios are not up to the standards they should be.



*Figure 2. Fort Calhoun NPP flooded by the Mississippi River*

The lack of data and understanding regarding component usage and reliability under flooding conditions is a major problem; exacerbated only by the fact that NPP face flooding events more commonly than may be thought, i.e. in the U.S. NPPs have faced almost 20 flooding or near flooding events in the past 40 years (Wells, 2016).

To help solve this problem, the construction of CFEL is under way. CFEL will be the place where experiments of component assemblies and subassemblies will be tested under different

flooding conditions, including water rise, water jets and spray and wave impact. These experiments will provide the necessary data to build component reliability models, which will in turn increase the ability to accurately characterize the risk of flooding events.

There are two main types of components that CFEL is interested in producing reliability curves for; those are mechanical components, such as door, pipes, pipe feedthroughs; and electrical components, such as batteries and switchboards, see Figure 3 below, showing a NPP room of electrical components flooded. In the case of doors, in some power plants, low leakages through door gaps are not considered as flooding risks (Slack, Internal Flooding Flood Area Definition, 2014), and only air-lock doors are considered for PRA flooding scenarios, and even then, they are assumed to remain intact; in the case of switchboards, most of them are assumed to fail once the water level in a flooding event reaches it (Slack, Internal Flooding Walkdown Sumary Report, 2014).



*Figure 3. Flooded Fukushima NPP Control Room*

The scope of CFEL represents a large undertaking, which is why the process has been divided into two research focused tasks, and two construction focused tasks, which are not part of this study. The first construction task is the development of the PET which will be the main focus of this thesis, while the second construction mission is the construction of the actual laboratory. The research tasks of CFEL include the research of component fragility model to be used to analyze the data collected from the experiments; and the integration of smoothed particle hydrodynamic simulations into the component fragility models.

The purpose of this thesis is to implement enhancements to the PET that will allow the execution of pressurized experiments on the desired components. It was learned from the previously executed array of experiments on hollow-core doors, that the flowrate of water into the tank in scenarios with high-leakage, were not enough to fill the tank and conduct pressurized experiments. The second objective of this thesis is to make pressurized experiments on components more directly used in NPPs; as mentioned above, the first set of experiments were produced on hollow-core doors; the new experiments will be performed on steel doors. The final objective of this thesis is to characterize the flowrate and pressure behavior of the PET under different flow conditions.

## The Portal Evaluation Tank

### Pre-Mods Configuration

The design of the full-scale experiments started with the design and construction of the PET. The PET is a steel tank, with an extended semi-cylindrical shape; it has height of 8 ft., a total length of 12 ft. and a width of 8 ft; the diameter of the circular section 8 ft; shown in Figure 4. The tank has a square opening to the semi-cylindrical section of side of length of 7.5 ft., enclosed by steel angles of 3 in. on each side. The PET contains an antechamber 2 ft. wide, which is also surrounded by angles 3 in. wide. The PET has the capacity to hold approximately 2,000 gallons of water.



*Figure 4. Picture of the PET, Bishwo Bandari Up Front*



The PET has three openings used for inlet and outlets. Two of them are 3 in. openings located at each side; the last one is an opening 2 in. in diameter located at the bottom and used as a drain. The tank also has four 2 in. openings at the top; one of them was used to locate a pressure transmitter, two of them were used for safety instruments, a pressure relief valve set to go off at 6 psi, and an air relief valve; the last opening was used as a conduit through which the wires for the instrumentation located inside the tank could pass through. All of the top-mounted instrumentation is shown in Figure 5.



*Figure 5. Top mounted PET instrumentation/safety equipment*

In the cylindrical section, the PET contains a small 1 ft. x 1 ft. plexiglass window, to allow viewing what takes place inside. The PET is placed on the floor through 4 adjustable bases, the legs are screwed in, so that the height at which the tank sits from the floor can be slightly modified to level the tank.

At the top of the tank, a steel bar extends into the antechamber; this bar is used to hold an ultrasonic transducer and video-recording instrumentation.

At the bottom angle of the antechamber, centered in the middle, there is a v-notch weir, which in conjunction to an ultrasonic transducer can be used to calculate the leakage rate from the enclosed section.

In this configuration the PET was connected to a Global submersible pump, located inside a water reservoir containing approximately 8,000 gallons; the pump is capable of producing water flowrates up to 300 gpm. The connection was made through PVC piping 3 in. in diameter, to one of the PET side inlets; the piping configuration is shown Figure 6, and contained two ball valves, one that allowed flow into the PET, and another valve that directed the water flow towards the PET, or towards the return line, back into the water reservoir.

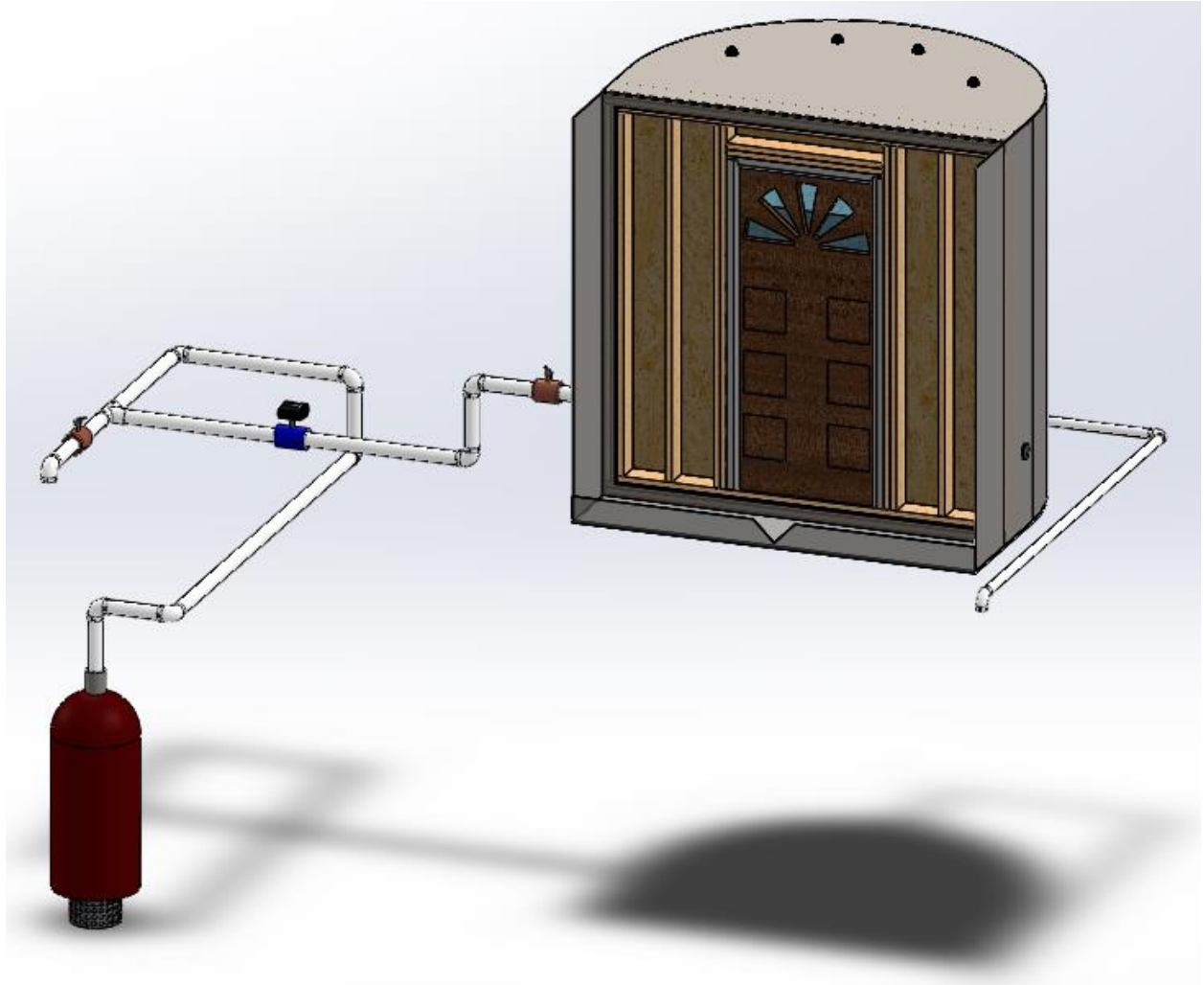


*Figure 6. Hollow-Core Door Experiments - Global Pump - Experiment Model*

The PET setup also consisted of an electromagnetic flowmeter that measured the water flowrate into the tank, a depth sensor placed inside the tank measured the height of the water column in it, while the ultrasonic transducer, was used in conjunction with the V-weir to measure the leakage rate from the experiment setup.



## Post-Mods Configuration

The design of the PET itself did not have many design changes. The only difference was the addition of a 12 in. opening with a flange at the top of the tank, shown below. This opening was used to connect the tank to the new piping system.



*Figure 7. 12 in. PET Opening at the Top*

All of the other openings in the PET remained unchanged. Instrumentation changes included the addition of a second depth sensor inside the PET and addition of water resistant LED light inside the tank. The instruments connected through three of the four top openings remained unchanged, however, the conduit used as a passthrough for the wiring of the instrumentation has now been sealed, to allow for pressurized experiments.

All electronic connections of the instruments have also been placed in a water-tight electrical box at the top of the PET, see Figure 8.



*Figure 8. Electrical Box at the Top of the PET*

Inside the tank there are two depth sensors, they are used to measure the water level inside the tank, and also produce some other information such as water temperature. There is also an ultrasonic transducer connected to the PET, it is only used in experiments with very low leakage, and it measures the height of the water column flowing through a v-notch weir.

The rest of the modifications were done to the piping system. The PET was connected to a Flygt 60 HP pump that was already present in the water reservoir. This pump was connected to the flume located in the laboratory, a piping network had already been put in place to connect the two equipment pieces. To connect the PET to the existing piping network, new 12 in. PVC piping sections were used, similarly, new piping sections were used to connect the PET back to the water reservoir. An approximate model of the new PET system is shown in Figure 9.

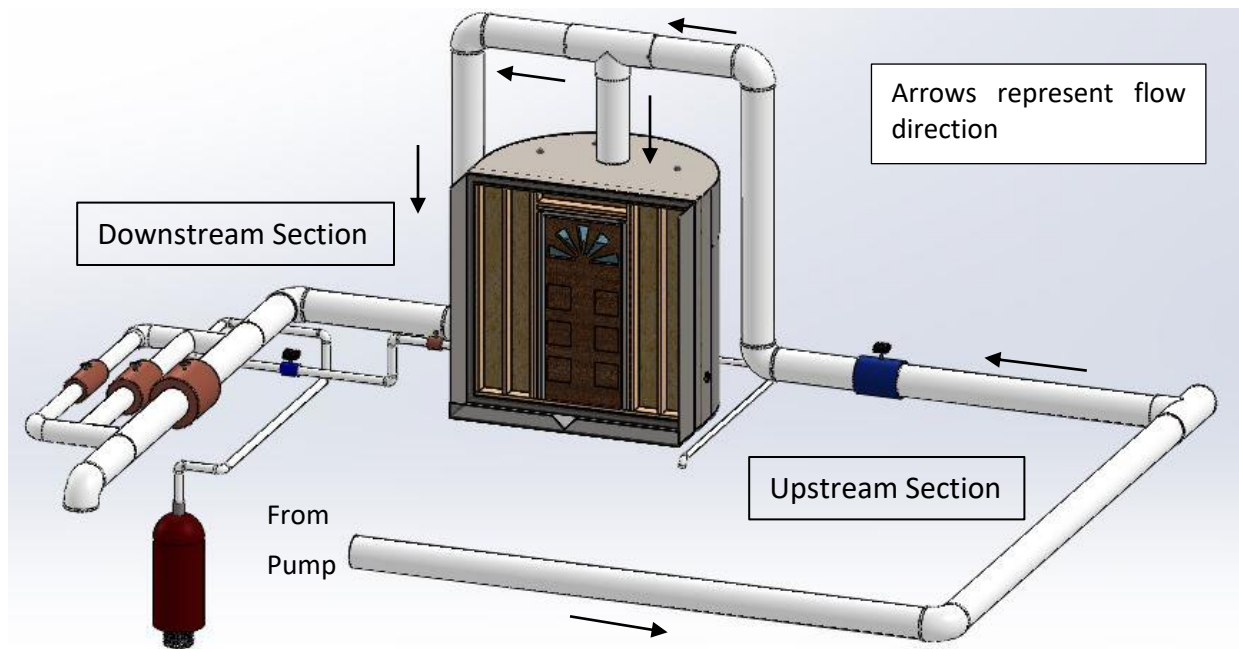
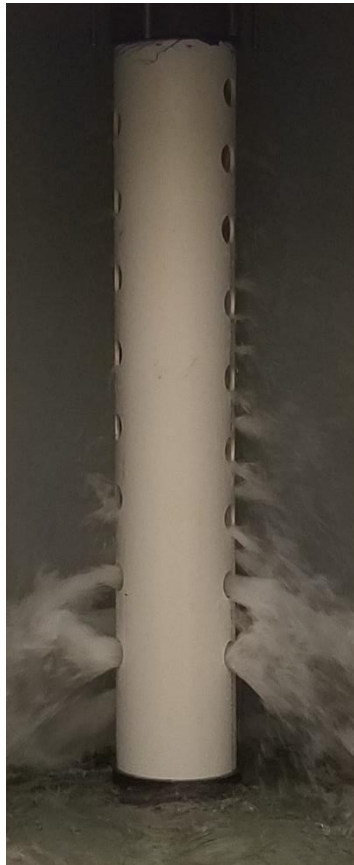


Figure 9. Approximate Model of the Updated PET 12 in. Piping

The piping section that goes from the pump to the PET will be called the 'Upstream Section', it is connected to a return line, that conveys the water back into the reservoir; and contains two electromagnetic flowmeters, a 12 in. and an 8 in. one. Butterfly valves are used to direct the water flow to each flowmeter. At the top of the PET, the upstream piping is connected to a 'Tee Joint', some of the water flows into the PET, while the rest flows back to the reservoir, through what is called the 'Downstream Section' of the piping network.

The Downstream Section consists of two flowmeters of the same size as the ones in the upstream section, it contains 3 distinct piping lines, of sizes of 12 in; 8 in. and 6 in. Each line contains a butterfly valve used for two functions; the first one is to adjust the water flow into the tank while it is filling with water, and the second is to be used in conjunction with the valve in the return line, to adjust the water pressure and flowrate in the system when the tank is full with water. For a detailed piping and instrumentation diagram see Figure 15.

Inside the PET a continuation of the 12 in. pipe goes from the top to the bottom of the tank, Figure 10. This pipe section has holes drilled around it to try and evenly distribute the water flow into the tank. Control of the flow into the PET, is achieved through a series of valves located in the upstream and downstream section of the tank.



*Figure 10. Continuation Pipe Segment Inside the PET*

The PVC pipes are also fitted with their own pressure and air relief valves for safety purposes. A 'Water Collection System', Figure 11, was fitted to all pressure and air relief valves; the system consisted in enclosing the pressure relief valves, and surrounding the air relief valves with ducts; the enclosure and the ducts would direct the flow from the activation of the safety valves down into funnels, connected through 1 in. clear tubing, and flowing down into the testing area, right in front of the PET.



*Figure 11. Piping Air & Pressure Relief Valves with Water Collection System in Place*

The two different methods for enclosing the safety valves were devised given their flow patterns. The velocity of the water flow being ejected from air relief valves, is lower than the velocity of the water being ejected by pressure relief valves, so a duct surrounding the valve should be able to contain and direct the flow downwards, see Figure 12; for pressure relief valves, a total enclosure of the valve was necessary. The enclosure was made using PVC pipe of 6 in. in diameter, which should be wide enough to allow all the flow from the safety valve to flow downwards in case it is triggered. Below are pictures of the valves within their enclosures.



*Figure 12. Air Relief Valve Positioned Within its Surrounding Duct*

The flowmeters can be used in several configurations; the most common setup however, is to connect the 12 in. flowmeter in the upstream section of the piping, together with the flowmeters of the downstream section.

It is important to note that the flowmeters in the upstream section of the piping cannot work in conjunction. This is because they were placed too close to each other, and the electromagnetic fields of one can affect the other.

## Instrumentation Description

### Pre-Mods Instrumentation

The measurement and safety instrumentation used for the experiment setup described in section Pre-Mods Configuration, are stated below. A complete piping and instrumentation diagram is also shown in Figure 13. PET Pre-Mods - Piping & Instrumentation Diagram.

### General Equipment

- 1) Global 4GSUBHD75 submersible high-volume dewatering pump.
- 2) MicroFlex HART USB Modem

### Measurement Instrumentation

- 1) Campbell Scientific CS 451 Depth Pressure Transducer
- 2) Campbell Scientific CR1000 Measurement and Control Datalogger
- 3) Khrone Optiflux 2000 3 in. Electromagnetic Flowmeter
- 4) Khrone IFC 050 Signal Converter
- 5) Additel 680 Wireless Pressure Transducer
- 6) Omega LVU 800 Series Ultrasonic Transmitter
- 7) Omega OMCP101A Current Datalogger

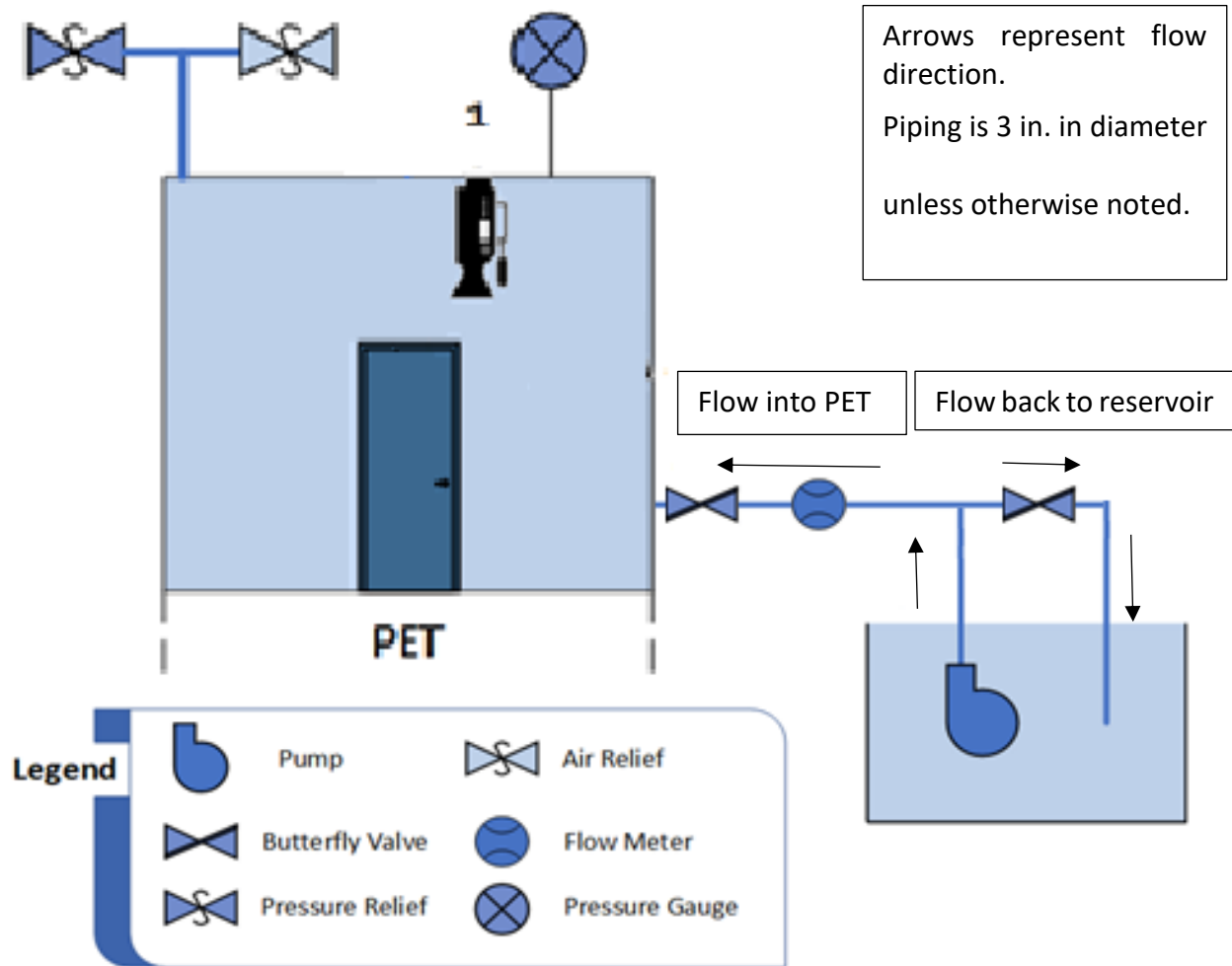


Figure 13. PET Pre-Mods - Piping & Instrumentation Diagram

#### Safety Instrumentation

- 1) Pressure Relief Valve.
- 2) Air relief valve.

#### Software

- 1) PACTware v5.0
- 2) PC200W v4.5
- 3) ShortCut v3.2
- 4) Omega OM-CP-IFC200 Data Recorder Software for Windows



5) CodeWrights GMBH Communications DTM

6) MicroFlex Generic HART DTM 6

## Connections

The Khrono EM Flowmeter is connected to the computer through the Microflex HART Modem, and it is operated software called PACTware.

PACTware, is a 'manufacturer and fieldbus independent software for operating field instruments' (PACTware, n.d.); to do this, several DTM packages must be uploaded to the PACTware interface, to recognize the hardware it is connected to. In these experiments, two DTMs were used, the first DTM allowed PACTware to connect to the HART modem, while the second one allowed PACTware to connect to the flowmeter.

In this case, there was a single flowmeter connected to a single HART modem, which made the connection to PACTware straightforward. More detailed instructions on how to proceed with PACTware are present in **Appendix #3: PACTware Interface**

The CS451 depth sensor was connected to the CR1000 datalogger. The software packages Shortcut, PC200 and Device Configuration are used in conjunction to achieve the connection. As explained in **Appendix #4:CR1000 Interface: Device Configuration Utility, Shortcut & PC200W**, the Device Configuration Tool, is the first software used to make sure there is a connection between the CR1000 and the computer, once that is achieved, Shortcut is used to connect the computer to the datalogger, and send the datalogger the program that will tell it how to interpret the data measured by the sensor. Since both the sensor and the datalogger are Campbell Scientific, Shortcut provides the wiring diagram to connect the sensor to the datalogger.

The program created in ShortCut tells the datalogger how often to record data, and what data to record. For these experiments, the datalogger sampled data every second, but only stored data consistently every four seconds; if the time interval for storing data was selected any lower, the datalogger would have memory problems that caused to miss data points and have uneven storage intervals; the selected 4 second storage interval, was the lowest time interval that produced consistent data without causing memory problems, and collecting data at consistent intervals was characteristic desired in the system in order to facilitate the posterior analysis of the data. The sampled data consisted of the water depth and temperature, while the recorded data consisted on the average, maximum, minimum and sample water depths.

Finally, PC200W is used as the tool to record the data from the datalogger. A more detailed description on how to use this software packages is included in **Appendix #4:CR1000 Interface: Device Configuration Utility, Shortcut & PC200W**.

#### Post-Mods Instrumentation

The measurement and safety instrumentation used for the experiment setup described in section Post-Mods Configuration, are stated below. A complete piping and instrumentation diagram is also shown in Figure 15.

#### General Equipment

- 1) Flygt NS-series pump
- 2) MicroFlex HART USB Modem

#### Measurement Instrumentation

- 1) Campbell Scientific CS 451 Depth Pressure Transducer

- 2) Campbell Scientific CR1000 Measurement and Control Datalogger
- 3) Two 12 in. ABB Watermaster Series Electromagnetic Flowmeters, see Figure 14
- 4) Two 8 in. ABB Watermaster Series Electromagnetic Flowmeters, see Figure 14
- 5) Additel 680 Wireless Pressure Transducer
- 6) Omega LVU 800 Series Ultrasonic Transmitter
- 7) Omega OMCP101A Current Datalogger
- 8) Omega PX437-015GI Water Level Sensor

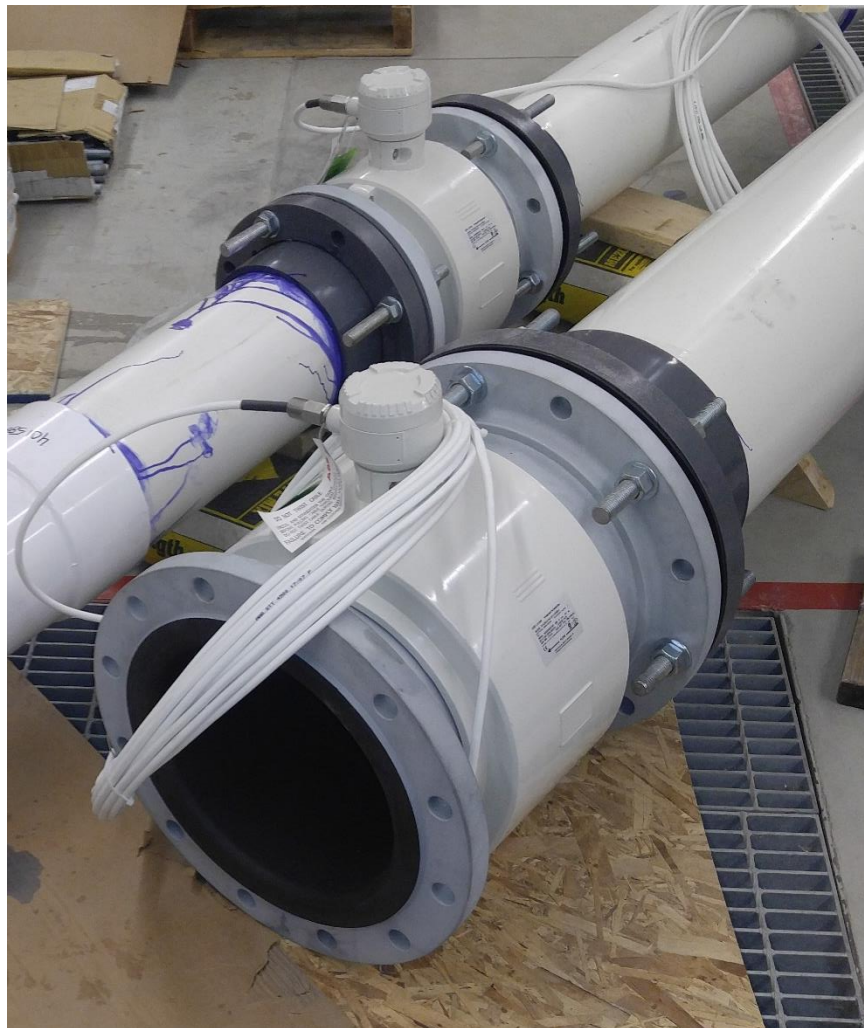


Figure 14. ABB Watermaster Flowmeters - Downstream 12 in. & 8 in.

## Safety Instrumentation

- 1) Two pressure relief valves, one for the PET, and one for the piping system.
- 2) Two air relief valves, one for the PET, and one for the piping system.

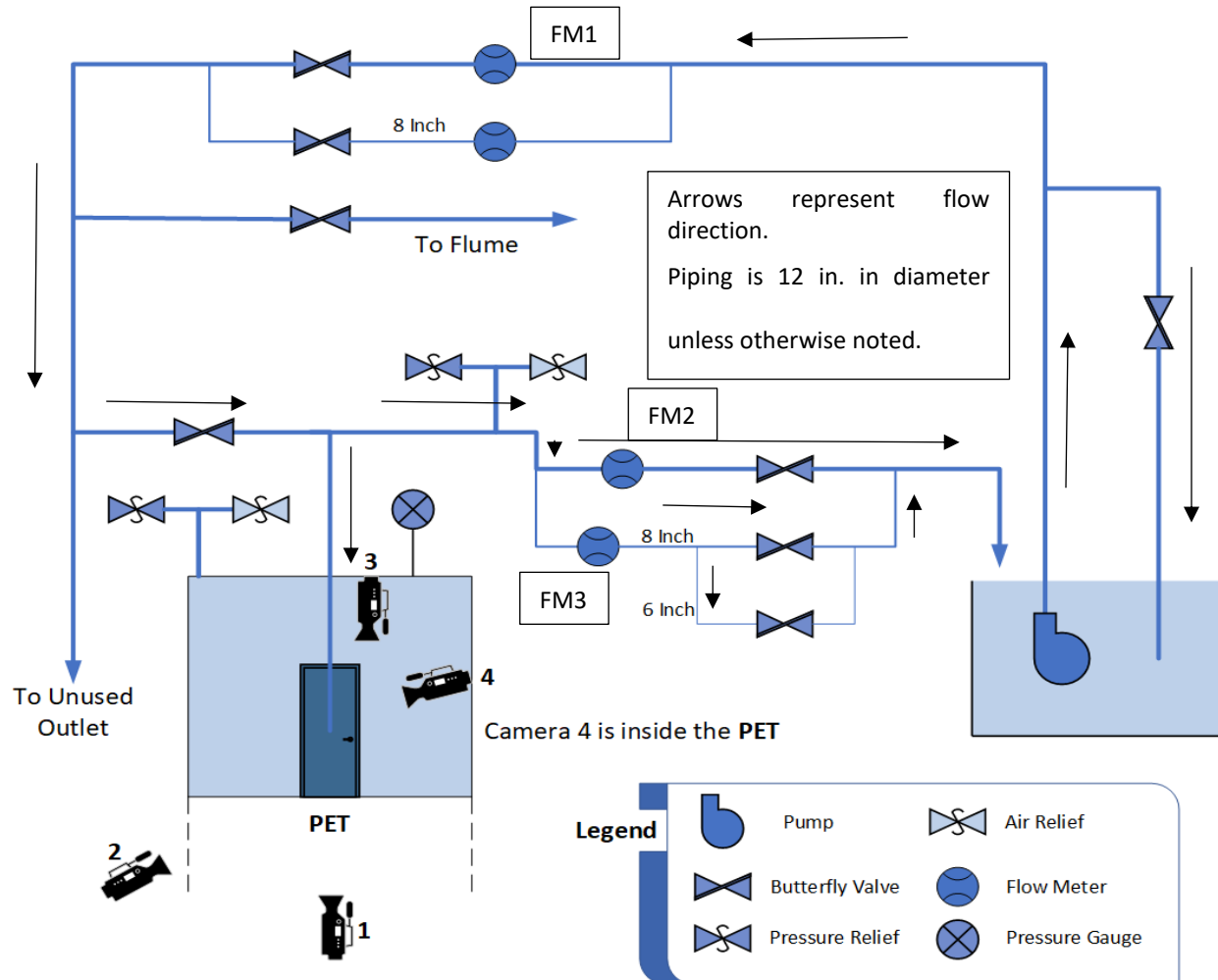


Figure 15. PET Post-Mods - Piping & Instrumentation Diagram

## Software

- 1) PACTware v5.0
- 2) ABB Asset Vision Basic
- 3) PC200W v4.5
- 4) ShortCut v3.2

- 5) Omega OM-CP-IFC200 Data Recorder Software for Windows
- 6) Additel Land Wireless v2.0.0
- 7) CodeWrights GMBH HART Communications DTM
- 8) ABB HART Communications Service Port Splitter
- 9) Microflex Generic HART DTM 6
- 10) ABB FEx 100 HART Watermaster DTM

## Connections

The flowmeters were connected to the computer in a similar manner as the previous setup. In this case all flowmeters were connected to the same HART Modem using what is called as a Multi-Drop Connection. In this type of setup, the flowmeters are connected in parallel to the same HART Modem, and a unique 'channel' different than '0' must be selected in each of the flowmeter's OS, which is achieved through their graphical display.

In the PACTware interface, the connection of all four flowmeters is similar to the one of a single one; however, special attention must be paid to the channel each flowmeter is using to transmit information, since the DTM assigned to each flowmeter must be changed to that specific channel.

The ABB Asset Vision Software can be used as a replacement for the PACTware interface, however, the Communications DTM CodeWrights GMBH, is not compatible with Asset Vision Basic, instead, the Service Port Splitter DTM is used. This setup was only used once, as semi-stable connection was only achieved one single time, the connection is described as semi-stable since it was lost after ~30 mins of uptime. More on this in the

## Pressure and Flowrate Behavior PredictionsPressure and Flowrate Behavior Predictions.

In this experiment the two depth sensors were connected to the CR1000; since the second pressure transducer is from Omega, and the datalogger is from Campbell Scientific, Campbell Scientific Software Shortcut does not show a special wiring diagram for connecting the sensor to the datalogger that would allow it to measure a wide array of properties; therefore, the sensor was connected in such a way, to allow the datalogger to measure the voltage signal coming from the sensor. An Omega provided current to depth formula shown below, was used to transform each measurement into a depth measurement. The voltage signal was created by pairing the sensor's current output through a 100 ohm resistor; these allowed the voltage signal to be converted back into a current signal. It was not possible to configure the CR1000 to correctly measure the current signal from the Omega sensor.

$$PSIG = 0.9340(mA - 3.945539)$$

*Equation 1. Omega - Current to Pressure Formula*

Where:

- PSIG is the gage pressure at the sensor's point in pounds per square inch.
- mA is the current output of the sensor in milliamperes.

## Experiments, Results and Analysis

Four different types of experiments have been realized so far in the PET; they can be described as the following:

- Hollow core door experiments, with the submersible Global pump.
- Hollow core door experiments, with the Flygt pump.
- Empty tank, flowrate behavior with the Flygt pump.
- Steel door experiments, with the Flygt pump.

### Pre-Mods Experiments, Results and Analysis

#### Frame Construction

The doors used for these experiments were 36 in. x 80 in. JELD-WEN flush primed, pre-hung, hollow core doors. For the door to fit inside the PET opening, a frame had to be built. The frame was built using 2 in. x 6 in. wood studs; this size was selected so the door frame would be narrower than the studs and could fit inside them.

The frame was divided in two sections so it could be placed inside the PET. Once, a frame with outer dimensions equal to the PET inner dimensions was built, Figure 16; however, it could not be placed in position due to the angles located at the PET opening. The two frame sections, called outer and inner sections, depending on their location with respect to the door, were built separately, using the aforementioned 2x6 studs.



*Figure 16. Mismatched Size Frame*

The outer frame sat against the PET walls, it was 3 in. thick, it was comprised of two studs nailed to each other; and each of the vertical and horizontal sections were screwed to the angles through the available holes. The decision to nail two contiguous studs for the outer frame was made so the opening produced by it, would be of the same size as the opening provided by the angles on the PET; by doing so, the inner frame could just 'slide' into position, without the need for any extra maneuvering.

The inner frame was constructed so its outer dimensions, would be the same as the inner dimensions of the outer frame, this would help position the inner frame, which was then nailed to the outer frame in several spots. The inner frame was erected with the pre-hung door in the



middle, with two 2x6 studs nailed at the sides, and at the top. Unlike the outer frame, which was two studs thick all around, the inner frame was enclosed by single studs at the top, at the bottom and on the sides; another single stud was added in the middle of the space between the door, and each outer stud, to add support for the walls. Figure 17 shows the end result.



*Figure 17. Inner-frame installed inside the PET*

As seen above, plywood panels 7/16 in. thick, were installed to the frame, to act as a wall. These plywood panels were first painted with water resistant stain to prevent mold, and then screwed to the studs of the wood frame, after the frame had been installed in its place inside the PET. After attaching the plywood panels, silicone was used to seal all the seams between the PET and the frame on the outside, between the PET and the plywood panels on the inside, and in any other place it was deemed necessary.

## Experiments

These experiments were the first ones that were performed. The Global submersible pump was connected to the PET through 3 in. diameter piping. An electromagnetic flowmeter measured the flowrate into the tank, and a series of valves was used to direct the water flow into the tank, or into the reservoir. A schematic of the experiment was shown in Figure 13 on page 16.

A total of five experiments of this kind have been conducted in the PET. They can be divided into two categories according to the direction the door opened; therefore, there are outward opening door experiments, in which the door opened towards the outside of the tank, and inward opening door experiments, in which the door opened towards the inside.

The first three experiments were outward opening ones. During the first experiment, the goal of physically failing the door was not achieved; as the results in Figure 18 show, once a water depth of ~23 in. was reached in the tank, a steady-state level was achieved. This steady state was caused by extreme bowing of the door.

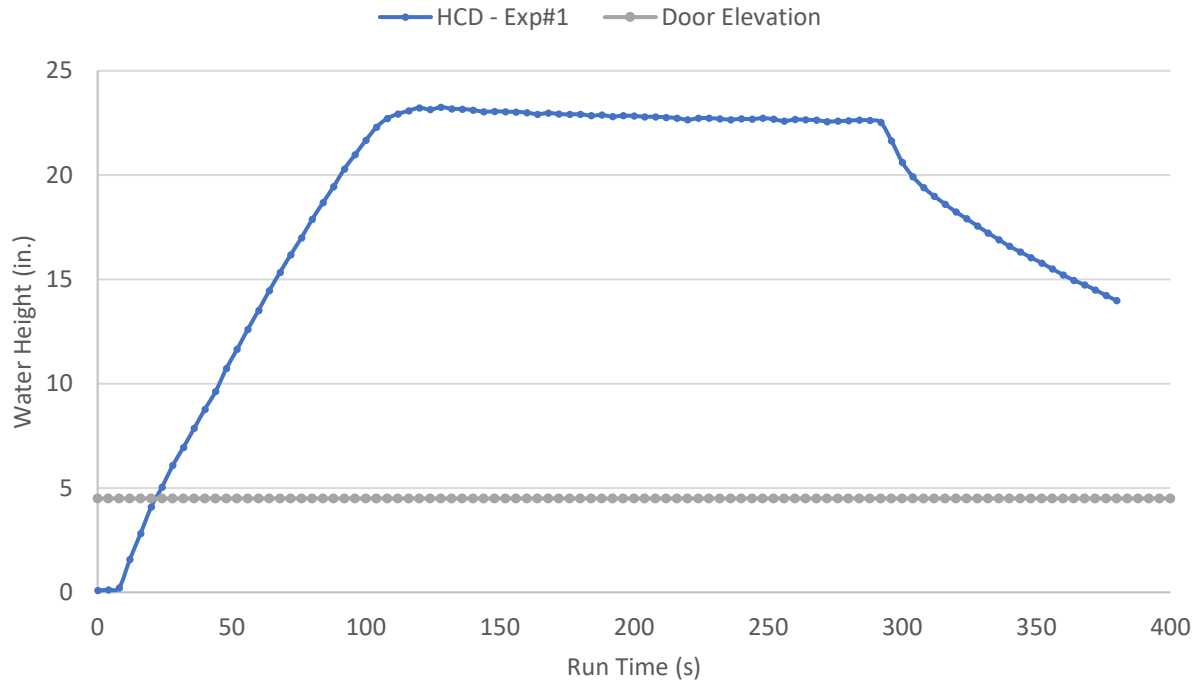


Figure 18. Hollow-Core Door Experiment #1 - Outward Opening Door, Depth Results

As shown in Figure 19, the lower end of the door (the one water was pushing against) started bending towards the outside, equalizing the flowrates into and out of the PET.



*Figure 19. Experiment #1 - Outward Opening Door Showing Leakage Underneath from Bowing Effect*

To address the bending issue of the doors, and induce catastrophic failures on them, a 4 in. plywood strip was screwed at the bottom end of the frame, see Figure 20. The two following experiments were performed with this modification.



*Figure 20. Plywood Strip Screwed to Bottom End of Frame*

The results showing the water depth achieved inside the PET for hollow-core door experiments #2 and #3 are displayed in Figure 21. It can be seen how in both experiments greater water depths were achieved than those obtained in experiment #1. The quick decrease in water depth at the end of both experiments points towards the rupture of the door, therefore the plywood strip screwed at the bottom of the frame, helped accomplish the objective of inducing the failure of the doors.

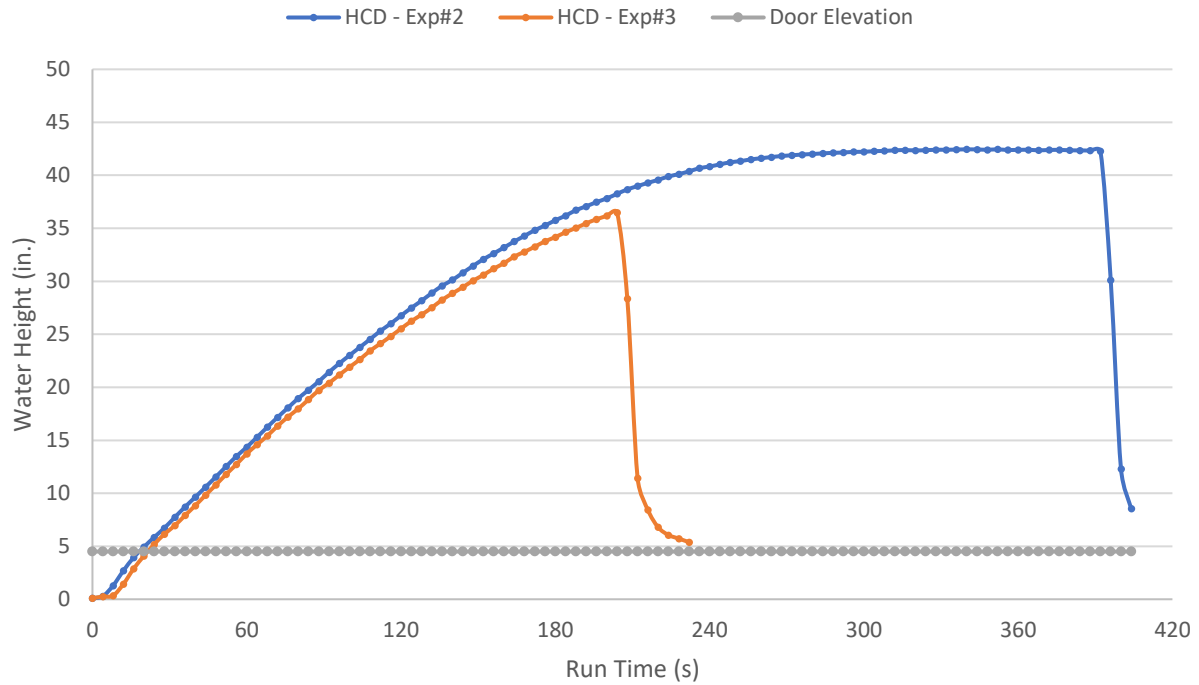


Figure 21. Hollow-Core Door Experiments #2 & #3 - Outward Opening Doors, Water Depth Results

Figure 22 and Figure 23 show the end result of experiments #2 and #3. Both experiments left the door completely broken when finalized, and in both experiments the break occurred around the latch area.



*Figure 22. Broken Door, Result of Experiment #2*



*Figure 23. Broken Door, Result of Experiment #2*

The two subsequent experiments were performed with the door opening inwards. In this configuration, the side and top edges of the door push against the door trim, the theory being that this effect would reduce leaking, and avoid the need of a plywood strip to keep the door from bending. Similarly, to the outward opening doors, vinyl weather stripping was located at the doors' threshold. The recorded water depths in the tank achieved during both experiments are shown in Figure 24.



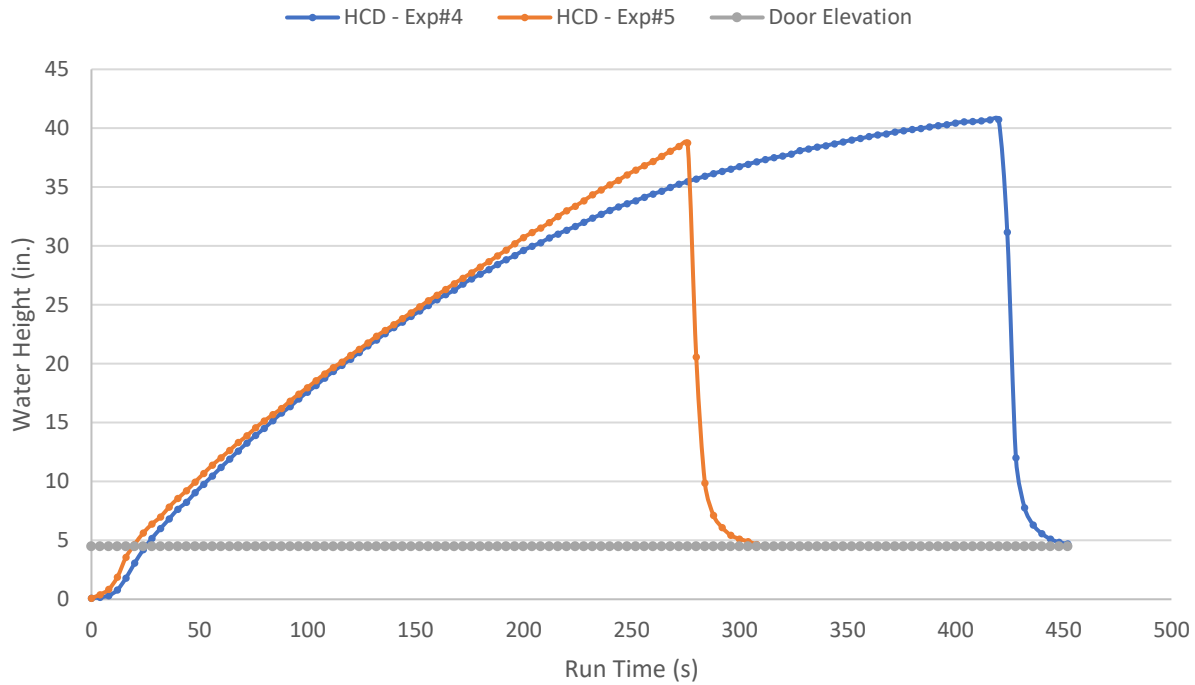


Figure 24. Hollow-Core Door Experiments #4 & #5 - Inward Opening Doors, Water Depth

The results proved that the door trim successfully kept the doors from bending, since similar results were obtained when compared to the previous two experiments. Both, experiment #4 and experiment #5 resulted in catastrophic failure of the doors used.

When comparing results shown in Figure 21 and Figure 24, it is possible to observe a discrepancy in the duration of the experiments and the depth of water achieved inside the PET. The experiments duration ranges from less than four minutes to more than seven minutes, while the maximum water depth reached varies between ~36in. and ~43 in. All these inconsistent results are attributed to variation in the quality of the doors. The used doors were cheap and with hollow cores, selected because they were believed to be the easiest ones to break, not because they would produce the most consistent results.

The data obtained from every experiment is analyzed to obtain the following elements:

- Water flowrate into the PET.
- Water flowrate out of the PET(Leakage).

In the experiments with the Global pump, the water flowrate into the PET was measured directly by the flowmeter. The water flowrate out of the PET was going to be measured by a combination of the ultrasonic transducer measurements and an equation relating the height of the column of water flowing through the v-notch weir, to the total water flowrate through the v-notch weir. Producing this measurement was not possible; the water leakage in this setup was much higher than what the V-weir allowed, so the water leaking from the system overflowed the entire bottom lip of the tank, rendering the ultrasonic measurements useless. On top of overflowing problem, in some experiments leakage occurred as small water jets that skipped the PET's antechamber and landed in the experiment area in front of the PET, completely bypassing measurement by the ultrasonic sensor.

To solve this issue, and still obtain the leakage rate from the PET, a mathematical method was designed. This method would use the data from the depth sensor and from the flowmeter to estimate the leakage rate.

As specified above, in these experiments, the flowmeter measured directly the water flow into the PET, and the depth sensor measured the depth of the water column inside the tank at a specific time interval. All that is needed to calculate the rate at which water is leaving the system is, calculate the rate at which water is accumulating in the system, and subtract it from the water entering the system (the system being the PET).

To calculate the water accumulating in the system, two consecutive water depth data points are subtracted, and that result is divided by the amount of time in between the data points. This will provide the average velocity at which the depth of the water column increased during that time interval, which then can be multiplied by the cross-sectional area of the inundated region to provide the average rate at which water is accumulating in the system for the specified time period. This average accumulation rate can then be subtracted from the average rate at which water has entered the system through the same time period, to obtain the average rate at which water has leaked from the system during the specified time interval.

The difficulty in analyzing the data from the experiments, arises from the fact that the time stamps at which the depth sensor and flowmeter collect the data are not the same. Therefore, it is not possible to just subtract the rate at which water is accumulating inside the PET from the rate at which water is entering the tank, because those rates are not linked to the same time interval. The second difficulty arises from the fact that the flowmeter did not collect data at consistent intervals. To solve both issues, a constant water flow into the PET was assumed. This 'Average Flowrate-In' is calculated as a weighted average from the flowmeter data points; each flowrate value was weighed by the duration of the time interval it was measured in.

The assumption of a constant flowrate into the PET was only possible because of the small variation in flowrates into the PET throughout the experiments; the difference between the flowrates at the highest and lowest PET water depths, was never more than 3%. It is also important to add that the calculated 'Average Flowrate-In' includes only the data points of the experiment that correspond to a stable flow, initial and final data points that indicate transient

conditions (water pump turning on, experiment door breaking) are not included to maximize the accuracy of the calculation.

Once the 'Average Flowrate-In' is known, it is assumed to be constant for the duration of the experiment, and then it becomes possible to estimate the water leaking the PET.

The analysis explained above was done to four of the first five experiments on hollow-core doors. The analysis could not be done to experiment #2 due to errors made at the time of recording the data. The first error consisted in incorrectly storing the timesteps of the CR1000 data; the time stamps at which data is recorded are recorded in the format 'hh:mm:ss', however, in experiment #2 the time stamps were stored as 'hh:mm', without the 'seconds' section. The second mistake consisted in not synchronizing the CR1000 internal clock with the computers' clock before collecting the depth data, causing the data of the flowmeter to be stored with an apparent delay of approximately two minutes, with respect to the data from the CR1000. The combination of the two errors made it impossible to relate the timing of the flowmeters' data with the timing of the CR1000 data, thus, impeding the analysis.

The following figures, Figure 25, Figure 26 and Figure 27 show the result of the analysis explained above on experiments #1 and #3.

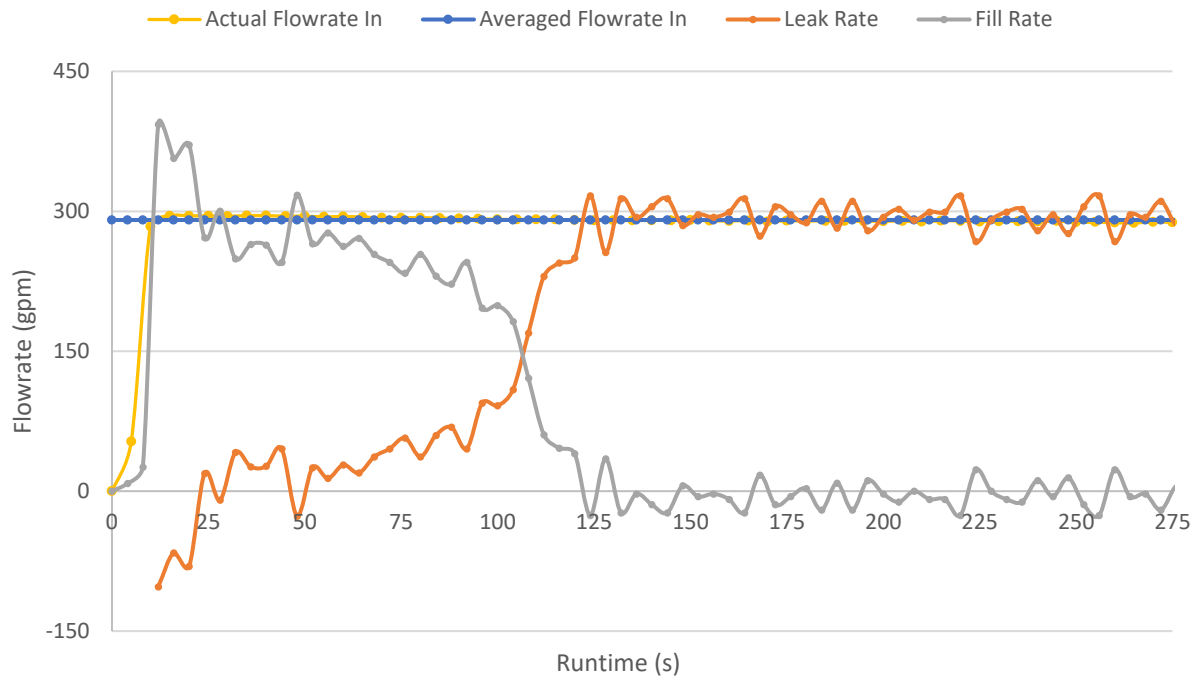


Figure 25. Hollow-Core Door Experiment #1 - Flow Information

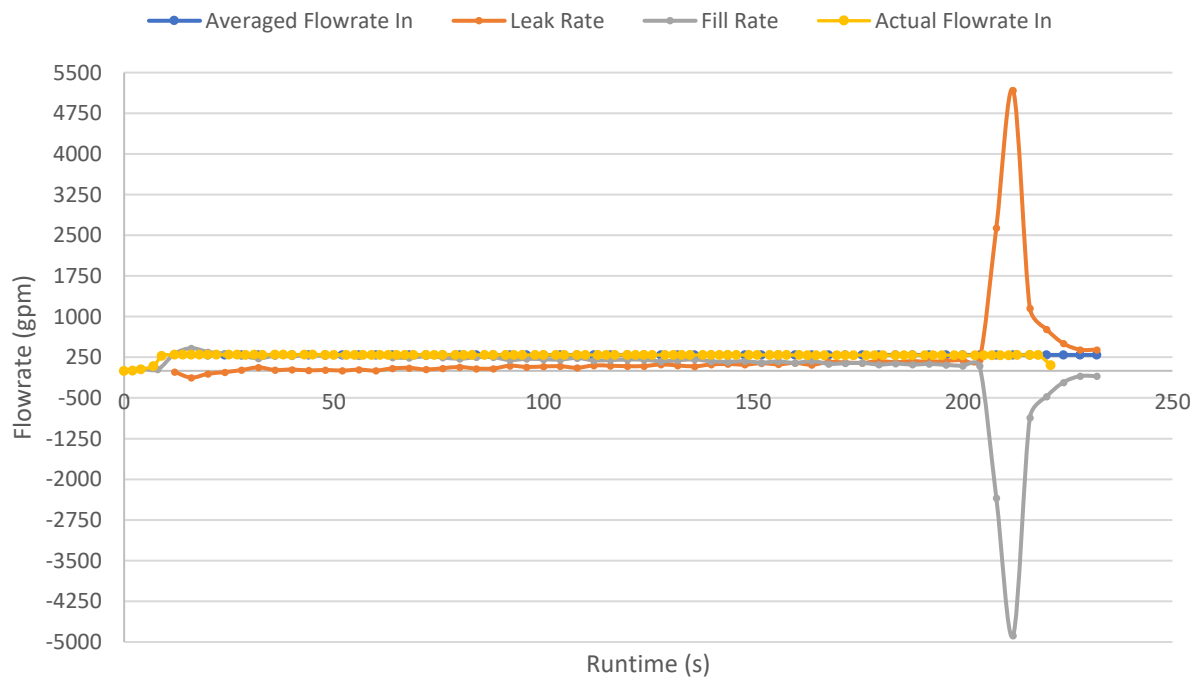


Figure 26. Hollow-Core Door Experiment #3 - Flow Information

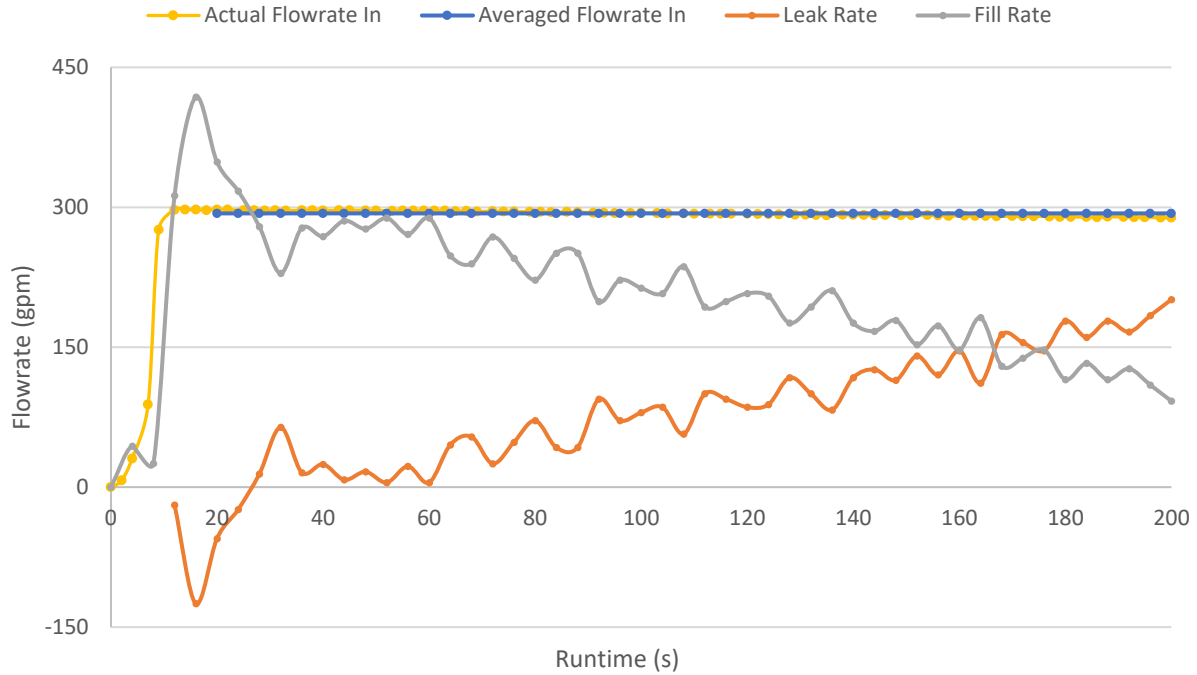


Figure 27. Hollow-Core Door Experiment #3 - Flow Information, Zoomed In

It is important to explain the difference between Figure 26 and Figure 27, since they portray the same data. The two flowrate spikes seen in Figure 26, represent the rupture of the door and leave all the other data-points out of sight, making it difficult to determine trends in the data. For Figure 27, the data was only plotted until the instant before the door ruptured, so that the trends of the flowrate into the PET, PET fill rate and leak rate can be appreciated. Better observation of the data, is also why unless otherwise noted, all the following 'Flow Information' figures are representative of the experiment until the moment right before the system fails.

Figure 25 and Figure 27 are the only figures in which the actual flowrate measurements have been plotted. This was done to show how little the flowrate varies during the experiment, and how well the 'Averaged Flowrate In' is able to represent it. Figure 28 and Figure 29 show the results of the flow analysis for hollow-core door experiment #4 and experiment #5.

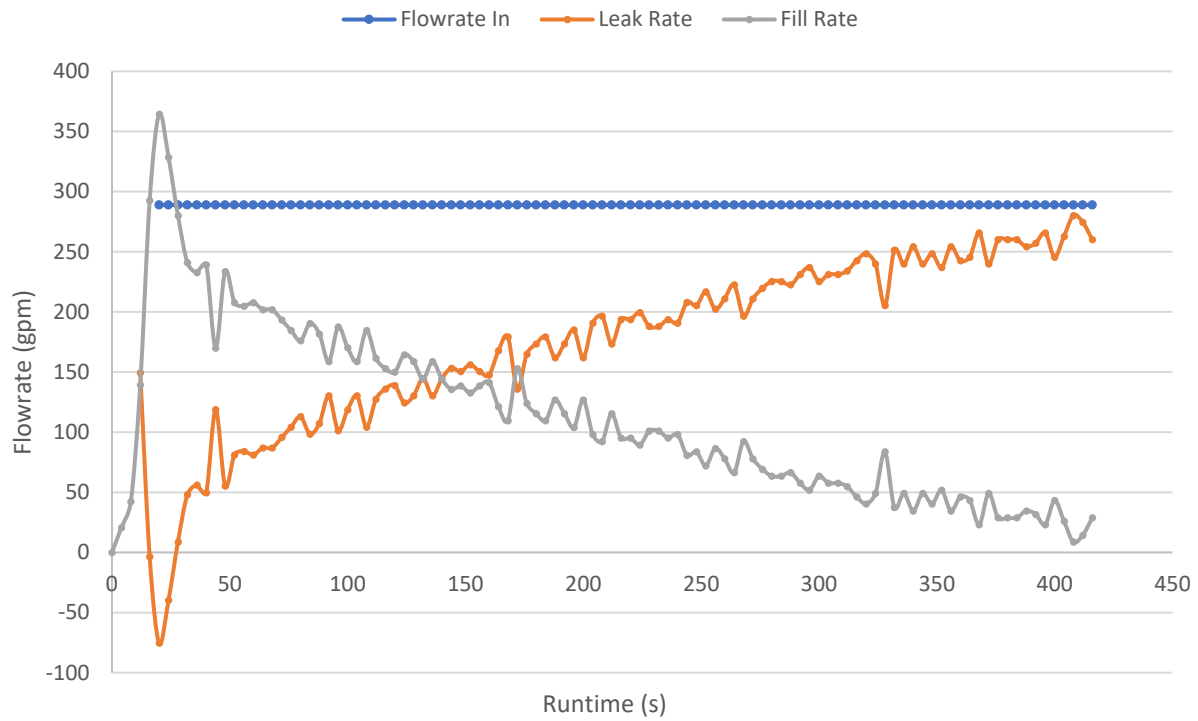


Figure 28. Hollow-Core Door Experiment 4 – Flow Information

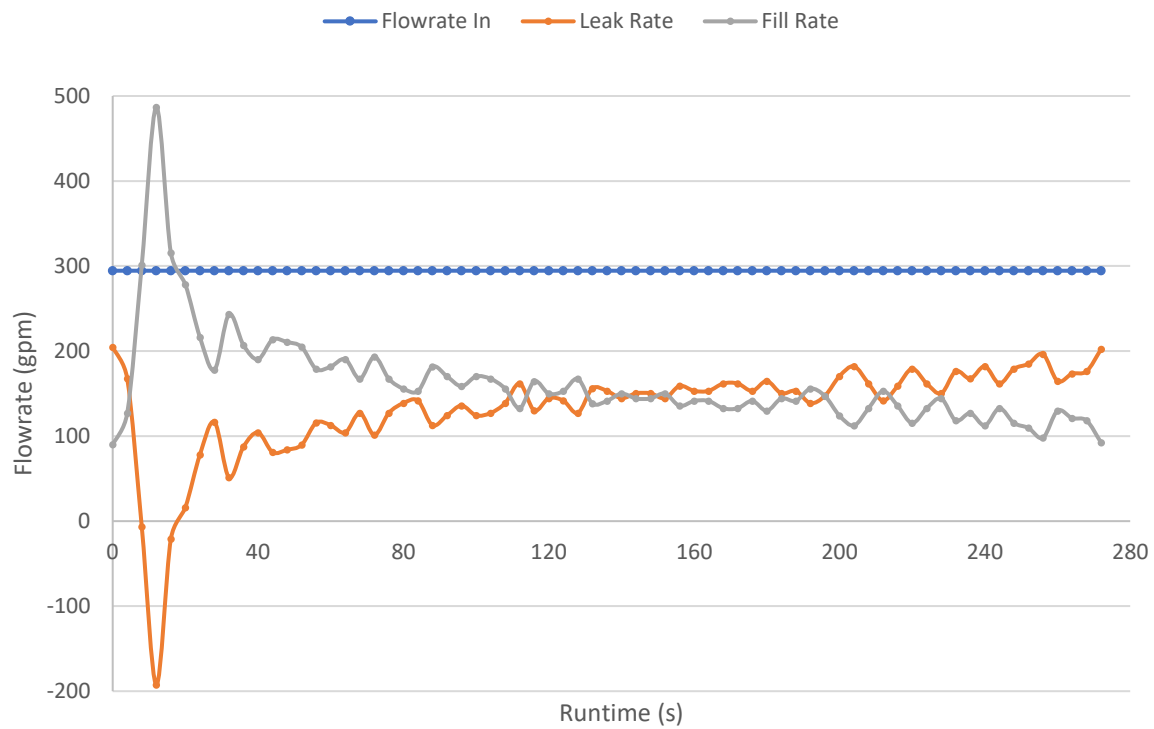


Figure 29. Hollow-Core Door Experiment 5 – Flow Information

In the plots of Figure 25 through Figure 29, it is possible to observe how the behavior of the systems is very similar. The noise section at the beginning of each experiment entails a PET filling rate higher than the actual rate of water entering the tank; this is physically impossible, however, this is attributed to two factors; the first one being rapid changes in the water level in the specific area around the depth sensors; at this points in time, water is beginning to accumulate inside the PET, and small waves can greatly affect the reading of the depth sensors; the second factor causing the initial miscalculations of the fill and leak rates, are the assumptions made to carry out the analysis, already explained in the previous section.

The second area of the figures shows a regular behavior, in which the filling rate of the PET decreases continuously, and the leakage rate increases. The increasing leakage rate is explained by an increase in the water level inside the PET; which not only causes the water to find more places by which to leak, but it also increases the pressure exerted on those points below the surface where there was already water leakage, and an augmented pressure causes an increase in the velocity the water leaks at.

With the assumed constant flowrate of water into the PET, the increasing leakage rate causes invariably a decrease in the filling rate of the tank.

Since Figure 26 is the only one where the complete experiment is plotted, it is the only one where the third and last section of the graphs is shown. This section contains a spike in the rate in the leak rate, and its corresponding negative spike in the PET fill rate. Both spikes are simply caused by the rupture of the door.



These experiments demonstrated a flaw in the setup of the system; the inability of the Global pump to completely fill the tank in systems where high amounts of leakage were encountered. The experiments also demonstrated the inability of the hollow core doors to sustain the pressure of a completely filled PET.

#### PET Improvements

To solve these problems, the PET was connected to a 60 HP pump. This pump was already in the same location as the PET, which facilitated the installation, and the pump would be able to provide a much higher flowrate into the tank; the pump curve is displayed in **Appendix #2: Global Pump, Performance Curve & Specs**, and it shows how at a system head of 0 ft. the pump would pump over 8,000 gpm of water, a much-needed improvement compared to the maximum 300 gpm of the Global submersible pump.

The pump is connected to piping lines 12 in. in diameter; the first flow split occurs at the return valve, which can force the flow back to the reservoir; the second occurs at the location of the upstream flowmeters; there is a 12 in. and an 8 in. flowmeter connected in parallel, however, since they cannot be used at the same time, only one of the two branches will be used, for this thesis purposes, the valve that regulates the flow through the upstream 8 in. line will remain closed.

After this bifurcation, the 8 in. line rejoins the 12 in. one until they hit the valve that directs the flow towards the flume. This valve remains closed so that the flow can be forced towards the PET, where it flows towards the top, where a T-joint splits the flow downwards towards the inside of the PET and horizontally along the top of the tank, where it goes back down towards the

downstream flowmeters. Once the flow of water reaches the bottom section, it encounters a bifurcation towards an 8 in. line; both 12 in. and 8 in. lines flow parallel to each other, and there are flowmeters in their middle sections. The 8 in. line further bifurcates into a 6 in. line; the butterfly valves located in each of the lines can be used to regulate the flow into and downstream of the PET; the two smaller lines then rejoin the 12 in. line which ends up discharging the water back into the original storage. A schematic of the piping diagram is shown in Figure 15.

## Pressure and Flowrate Behavior Predictions

Before performing experiments, two sets system simulations were performed in different software packages to understand how the system may behave in different conditions. The simulations were performed using two different software packages.

The first set of simulations were performed in Flow3D and had as objective the understanding of the system behavior in the event the tank filled completely with water. It is known that when a system is being filled with a fluid, the system fills and fluid is still being pumped into the system, a brief pressure spike may occur at the time the system reaches the filled status. It is necessary to understand the magnitude of the pressure spike to ensure all components within the system are able to handle it, and to install the necessary safety measures. At the time of this numerical simulations, the exact configuration of the piping system was not known, so three different scenarios were accounted for.

*Simulation #1: Pump flow directly into the PET*

In this simulation the full flow from the pump is discharged into the PET, Figure 30. It was devised as a worst-case scenario. The initial conditions are the following: fluid depth at  $t = 0$  s. is 7.5 ft; water flowrate( $Q$ ) is 4500 gpm; the pressure is measured at the bottom of the PET.

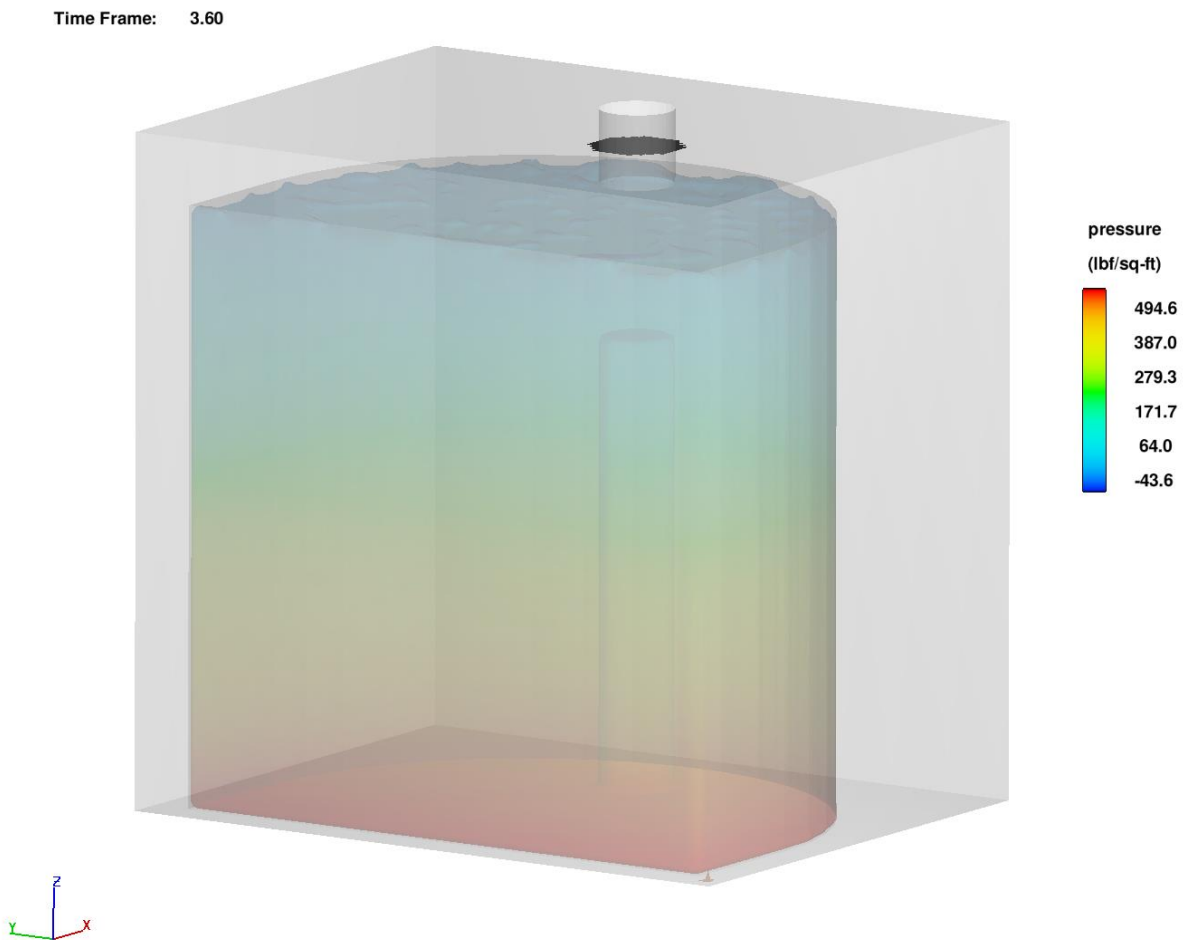


Figure 30. Flow3D Simulation #1 PET View

The results, Figure 31, show the pressure behavior at the moment the PET gets completely filled with water, and the pipe connecting the tee to the PET starts to get filled.

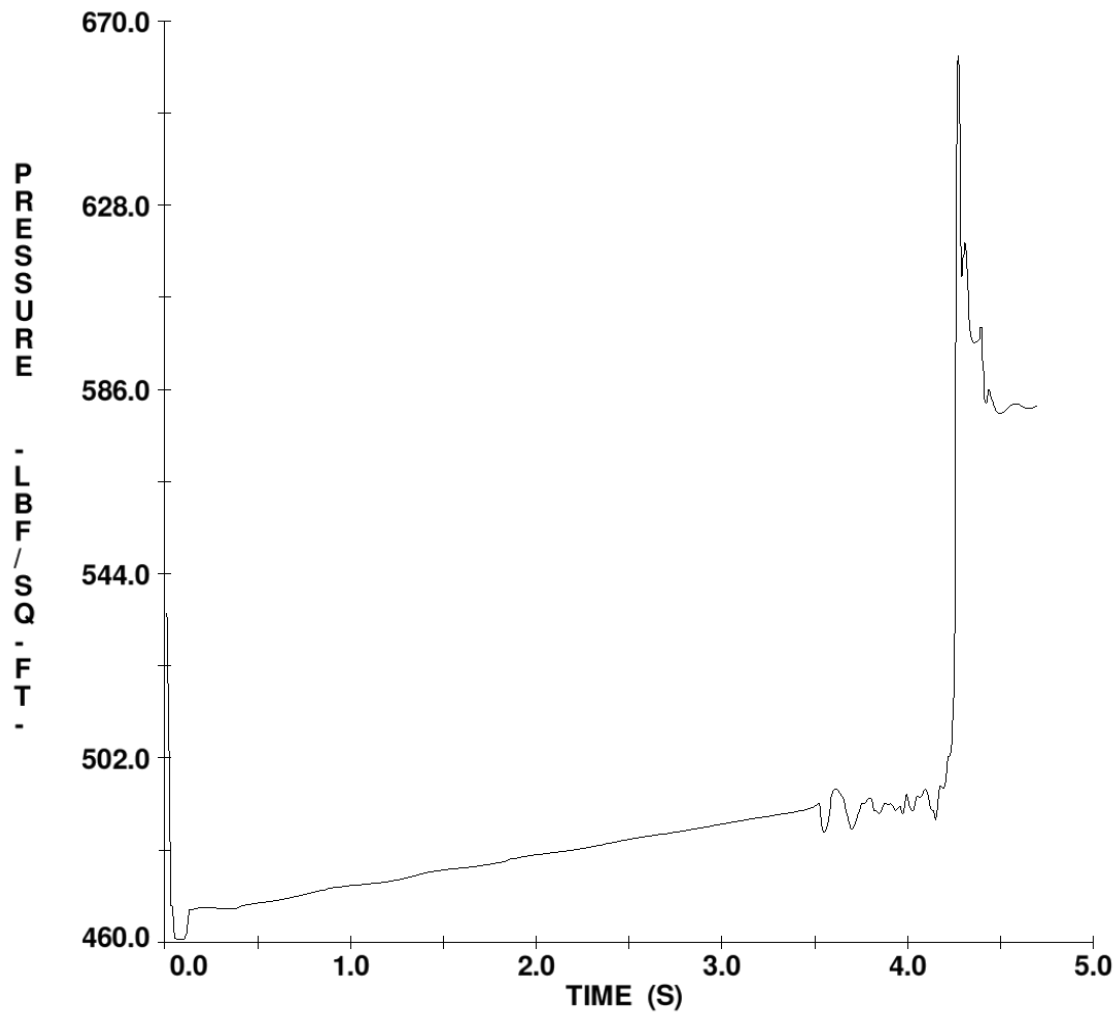


Figure 31. Flow3D Simulation #1 PET Pressure Prediction

As seen in Figure 31, the pressure raises almost linearly while the tank is filling with water, but at the exact moment the tank is filled, a pressure surge occurs, creating a maximum pressure of 662.09 psf. which translates to 4.60 psi. It is important to note that the pressure that would be achieved at the bottom of the tank by the column of water alone, without any pressure spikes is 499.2 psf. or 3.47 psi; therefore, the pressure surge has a magnitude of ~1 psi.

### *Simulation #2: Water Flow Dripping into the PET through a T-Joint*

In this simulation, flow from the pump flowed first through a tee located at the top of the PET. The tee would cause the water to split, some of it diverging down into the PET. The simulation initial conditions are as follow: fluid depth in the PET at  $t = 0$  seconds is 7.75 ft; water flow(Q) through the tee is 4,500 gpm and pressure is again being measured at the bottom of the PET. See Figure 32 for a graphical depiction of the model.

Time Frame: 3.80



Figure 32. Flow3D Simulation #2 PET View

The objective of this simulation was to find out the pressure in the PET at the moment it fills with water. Figure 33 shows small pressure variations occur during the tank's filling process, but a pressure spike, like the one in the previous simulation, is not present in this one. The reason is the lower water flowrate entering the tank. The gradual pressure increase at the end represents the filling of the pipe connecting the tee to the PET, which causes an increase of the pressure measured at the bottom of the PET. A simulation analyzing what would happen once that connecting pipe is filled with water is examined next.

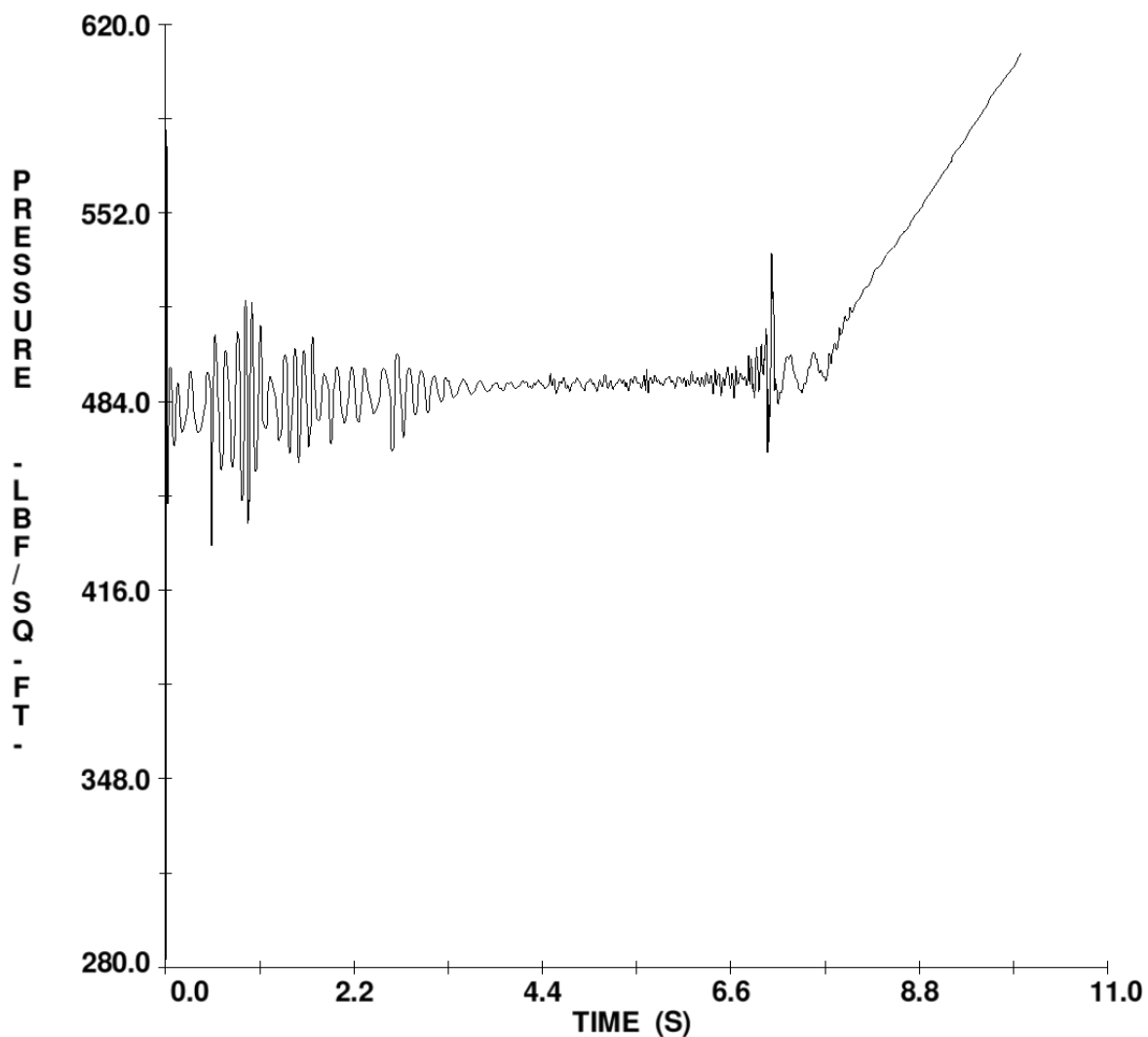


Figure 33. Flow3D Simulation #2 PET Pressure Behavior

### *Simulation #3: Water flow through the T-Joint*

This simulation has the same configuration as the previous one. The main difference is that instead of looking at the PET pressure while it fills with water, the objective is to look at the pressure behavior inside the tee while its lower section fills with water, see Figure 34. Initial conditions are: fluid depth at  $t = 0$  seconds is 8 ft; and water flow( $Q$ ) is 4,500 gpm and the pressure is measured at the tee itself.



Figure 34. Flow3D Simulation #3 PET View



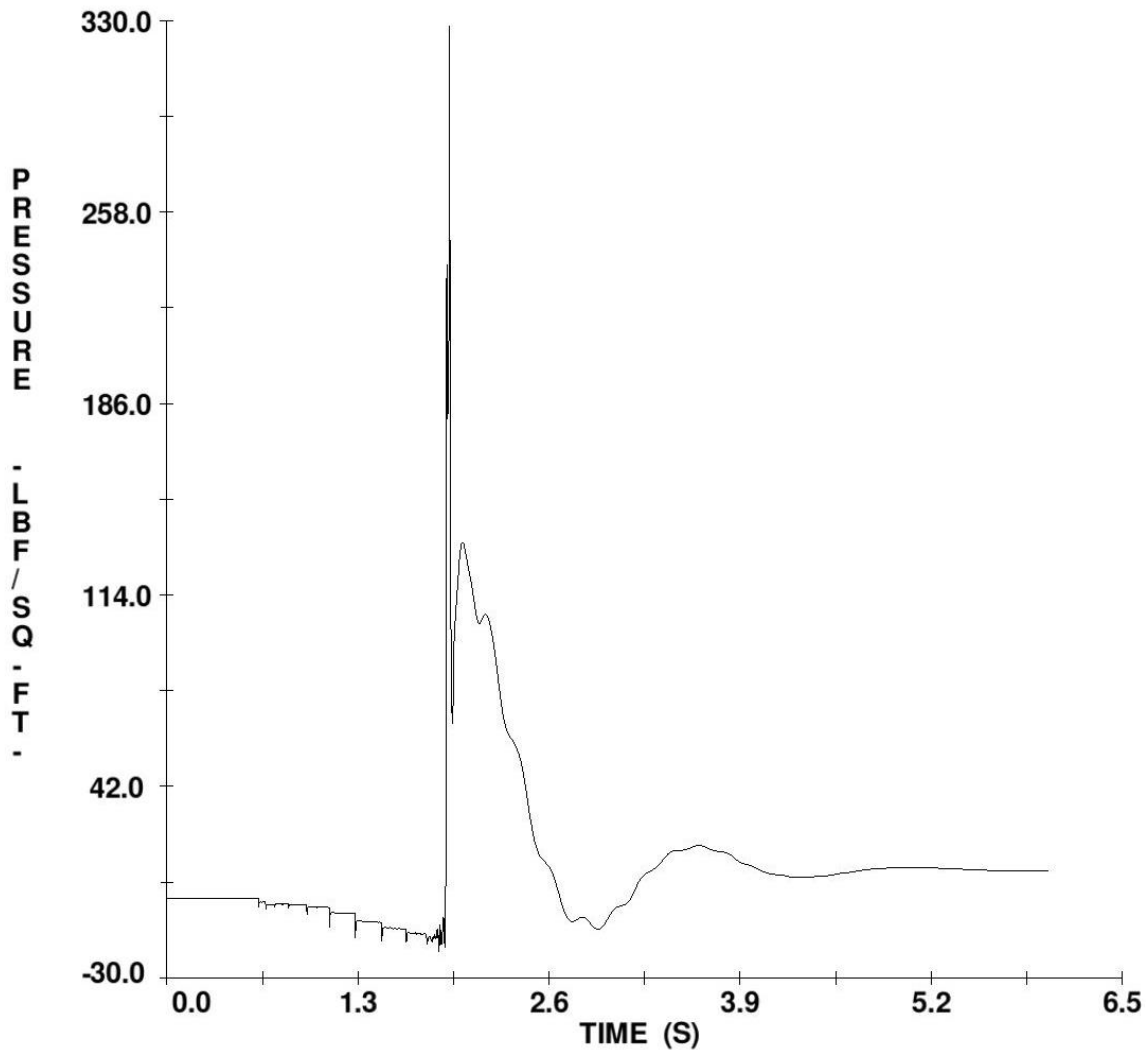


Figure 35. Flow3D Simulation #3 Piping System Pressure Behavior

As seen in Figure 35, the maximum pressure achieved by the pressure spike in the tee is 327.88 psf; which translates 2.28 psi at  $t = 1.92$  seconds. It is important to note that this pressure is substantially lower than the maximum operating pressure of Class 125 and SCH40 PVC pipes and fittings, which are the ones used throughout the PET.

From the simulations results, it is possible to conclude that the pressure spike that occurs at the moment the PET gets filled with water, will not be of any threat to the system, even if the PET was to be filled with the Flygt pump running at full capacity, the pressure spike would not

jeopardize the system. It has also been shown that, when the flow from the pump is diverted into the PET through a tee, and the pipe connecting the PET to such tee gets filled with water, the pressure spike that occurs at that moment will not jeopardize the system either.

The simulations made in SolidWorks had the objective of finding out the effect closing the downstream valves has on the pressure of the system once the PET has been filled with water. For these simulations, it was assumed the PET and all pipes were filled with water, since SolidWorks does not have the capability to deal with free-surface flows. Another assumption was the modeling of the valves. The system uses butterfly valves, however designing and simulating those in SolidWorks would be overly complicated, the solution was to simulate the valves as nozzles; closing the valves would be simulated as decreasing the outlet radius of the nozzles.

The system simulated in SolidWorks corresponded to a simplified version of the PET and the piping system around it. As shown in Figure 36, the PET has been simplified to its basic shape, an opening has been placed in the center of the front panel to included leakage in the simulations; the piping network has been simplified in length and shape; the valve locations have been moved to the top of the PET, and instead of having a double bifurcation(one in the 12 in. line and another in the 8 in. line), a single bifurcation was modeled.

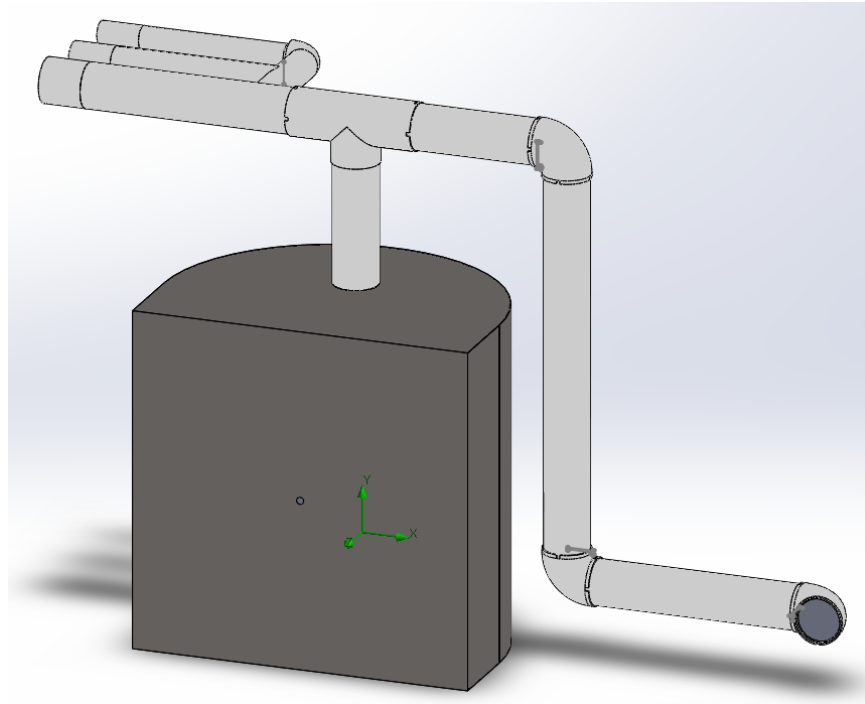


*Figure 36. SolidWorks PET Simulation Model*

Several configurations with different valve(nozzle) closings were simulated, however, in most cases they are not correct. The selected parametric study investigates the pressure behavior in the PET; the tank and the piping network, when the only downstream valve open is the 12 in. one; then, eleven extra cases are made, each one representing a slight closing of the valve; since the valves were modeled as nozzles, each case represents reducing the outlet diameter of the nozzle by one inch. The other input condition was a water flowrate of 4,500 gpm. The 'PET Average Total Pressure' results have been selected and plotted in Figure 37.

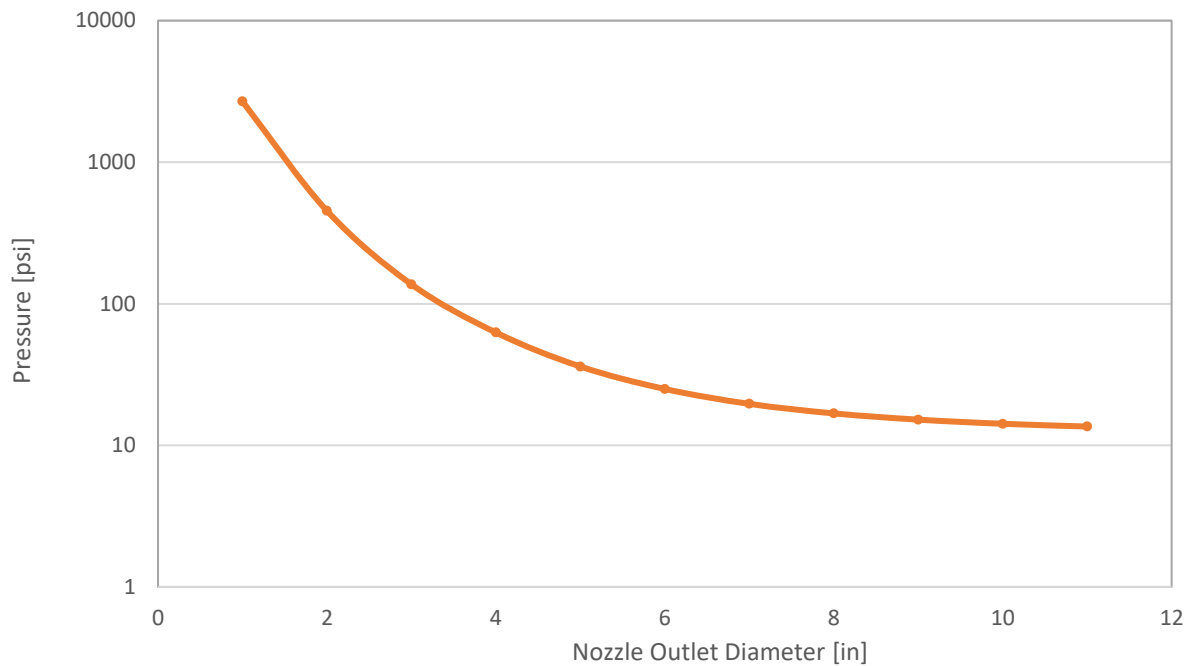


Figure 37. SolidWorks Simulation 'PET Average Total Pressure' Results

As seen in the figure above, the pressure in the system increases exponentially to a high point of 2684 psi when the diameter of the nozzle in the 12 in. line has been reduced to one inch; this was used to represent an almost total closing of the valve placed in this line.

This model results are inapplicable to the real system; the inclusion of a nozzle to increase in pressure in the system, causes the fluid to accelerate inside it; since the water flowrate in the simulation remains constant at 4,500 gpm, the final velocity of the water in the simulation grows as the squared ratio of the initial to final radii of the nozzle, and in turn will cause the total pressure in the system to follow the exponential growth. Since a way to insert the pump curve as a boundary condition in the simulation was not readily available, the exponential growth of the pressure in the system does not correspond to the pressure head provided by the pump.

The inability of SolidWorks to follow the pump curve is what makes the results of the simulation inapplicable to the real system. As mentioned above, the total pressure in the system for design point #1 is 2684 psi, which corresponds to a head of 6191 ft H<sub>2</sub>O; now, the pump cannot produce that much head (see **Appendix #1**: Flygt Pump, Performance Curve & Specs for the pump curve). There is an intrinsic relation between a systems' head and the fluid flowrate, the mistake is in assuming that the water flowrate will remain constant without regard of the total head of the system, which is exactly what was done in all of the simulations made in SolidWorks.

It was not possible to find a way to insert a flowrate or pressure constraint in SolidWorks that would allow for the simulation to mimic the pump curve of the real system, but if this can be overcome, then a comparison between the simulated and real systems could be performed.

## Flowrate-Behavior Experiment

The first experiment ran with the new setup was a control experiment. It was made to analyze the flow behavior with different setups of the 5 valves in the system (the return valve, the upstream 12 in. valve, and the downstream 12 in; 8 in. and 6 in. valves). Given the amount of data collected, Table 1 only contains a reduced data set of the all information recorded during the experiment.

Several deficiencies of the system were pinpointed from the data, and will be mentioned below:

1. The connection to the downstream 8" flowmeter was lost during the experiment. As mentioned before, the flowmeters can be connected to a computer using a different combination of DTM and User-Interface software. During the test run, the ABB Device DTM was paired to the ABB HART Protocol DTM with the PACTware User-Interface. These pairing was selected since using the ABB FEx 100 Device DTM allows the user to set a constant time interval for data recording.
2. The data-recording events do not happen at constant intervals. Even when the flowrates seen through the flowmeters screen, or at the PACTware interface is being updated at a user-selected constant time interval (1 second, 3 seconds or others), the data recorded by the flowmeters does not have a constant time interval between two subsequent time stamps. See the any of the 'Time Stamp' columns in Table 1, the time interval, which is the amount of time between two consequent time stamps, does not remain constant.

3. The interval between time stamps was much higher than those recorded in the experiments where the Global pump was used. In the previously performed experiments, the time interval between recorded data points ranged between two to three seconds; in this case however, the intervals can be as large as 12 seconds.
4. The time stamps at which data is recorded is not the same for all the connected flowmeters. As seen in Table 1, the time stamps at which data is recorded is mostly different for both flowmeters. This increases the difficulty of performing accurate analysis of the data.

Table 1. System Flowrate Behavior #1 – Fragment of the Entire Data Collected

Date	Upstream 12" Flowmeter				Downstream 12" Flowmeter			
	Time Stamp	Flowrate [gpm]	Velocity [ft/s]	Volume [gal]	Time Stamp	Flowrate [gpm]	Velocity [ft/s]	Volume [gal]
10-Nov-17	14:27:33	0.00	0.00	0	14:27:39	0.00	0.00	0
10-Nov-17	14:27:40	0.00	0.00	0	14:27:44	0.00	0.00	0
10-Nov-17	14:27:47	16.17	0.05	0	14:27:55	0.00	0.00	0
10-Nov-17	14:27:55	111.27	0.33	7	14:28:00	0.00	0.00	0
10-Nov-17	14:28:02	86.70	0.25	20	14:28:07	0.00	0.00	0
10-Nov-17	14:28:08	144.62	0.42	25	14:28:12	0.00	0.00	0
10-Nov-17	14:28:15	617.03	1.81	78	14:28:20	0.00	0.00	0
10-Nov-17	14:28:27	690.22	2.02	167	14:28:28	0.00	0.00	0
10-Nov-17	14:28:33	685.71	2.01	277	14:28:34	0.00	0.00	0
10-Nov-17	14:28:39	605.57	1.77	347	14:28:41	0.00	0.00	0
10-Nov-17	14:28:44	513.70	1.50	399	14:28:48	0.00	0.00	0
10-Nov-17	14:28:51	523.27	1.53	455	14:28:54	0.00	0.00	0
10-Nov-17	14:28:58	520.40	1.52	510	14:29:01	0.00	0.00	0
10-Nov-17	14:29:03	519.26	1.52	565	14:29:07	0.00	0.00	0
10-Nov-17	14:29:10	520.95	1.53	615	14:29:17	0.00	0.00	0
10-Nov-17	14:29:17	515.64	1.51	680	14:29:23	0.00	0.00	0
10-Nov-17	14:29:24	512.75	1.50	735	14:29:31	0.00	0.00	0
10-Nov-17	14:29:35	1266.96	3.71	890	14:29:39	212.05	0.62	16
10-Nov-17	14:29:42	1321.56	3.87	1071	14:29:44	326.71	0.96	48
10-Nov-17	14:29:49	1341.69	3.93	1226	14:29:51	394.93	1.16	85
10-Nov-17	14:29:54	1358.04	3.98	1357	14:29:58	365.42	1.07	127



## Post-Mods Experiments, Results and Analysis

### Post-Mods Hollow-Core Door Experiments

The two first experiments with the new system were performed on hollow-core doors for two reasons; the first was that these experiments would serve as trials, allowing the team to get acquainted with the equipment and new capabilities; the second reason was availability, the doors were remnants from previous experiments, and it was decided that it would be better to perform experiments on them than to try to return them.

#### *Frame Construction*

The wooden frame around these two doors was constructed as explained for the previous experiments. Nothing new to mention.

#### *Experiments*

The two experiments were run through the 12 in. lines; the recirculation valve was left open for experiment #6, while it was closed for the following experiment. The valves that directed the flow through the 12 in. lines were the only ones open, all the other valves were closed. The 12 in. upstream and both downstream flowmeters were connected to the computer using the multi-drop method to connect them through a single HART Modem, PACTware was used, together with the CodeWrights GMBH Hart Communication DTM for the modem, and Microflex Generic 6 DTM for the flowmeters. The two depth sensors were also connected, producing measurement reading every two seconds.

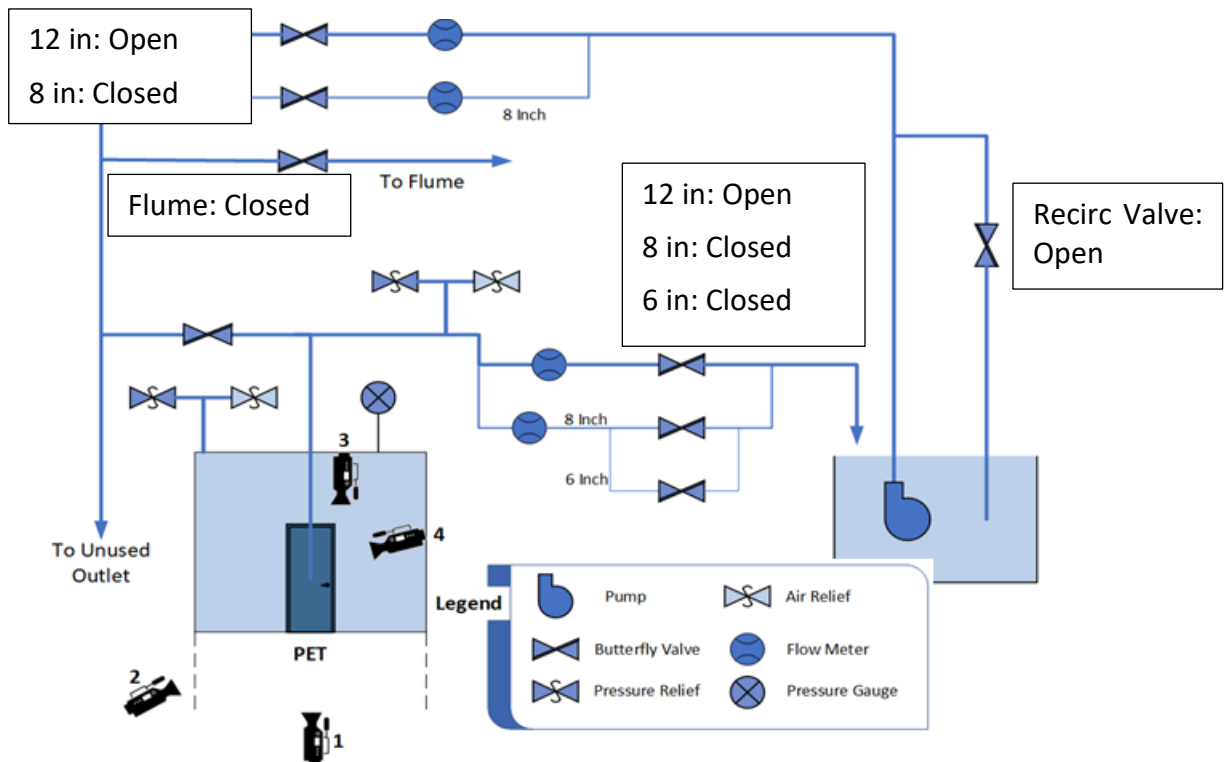


Figure 38. Hollow-Core Door - Experiment #6 - Initial Valve Configuration

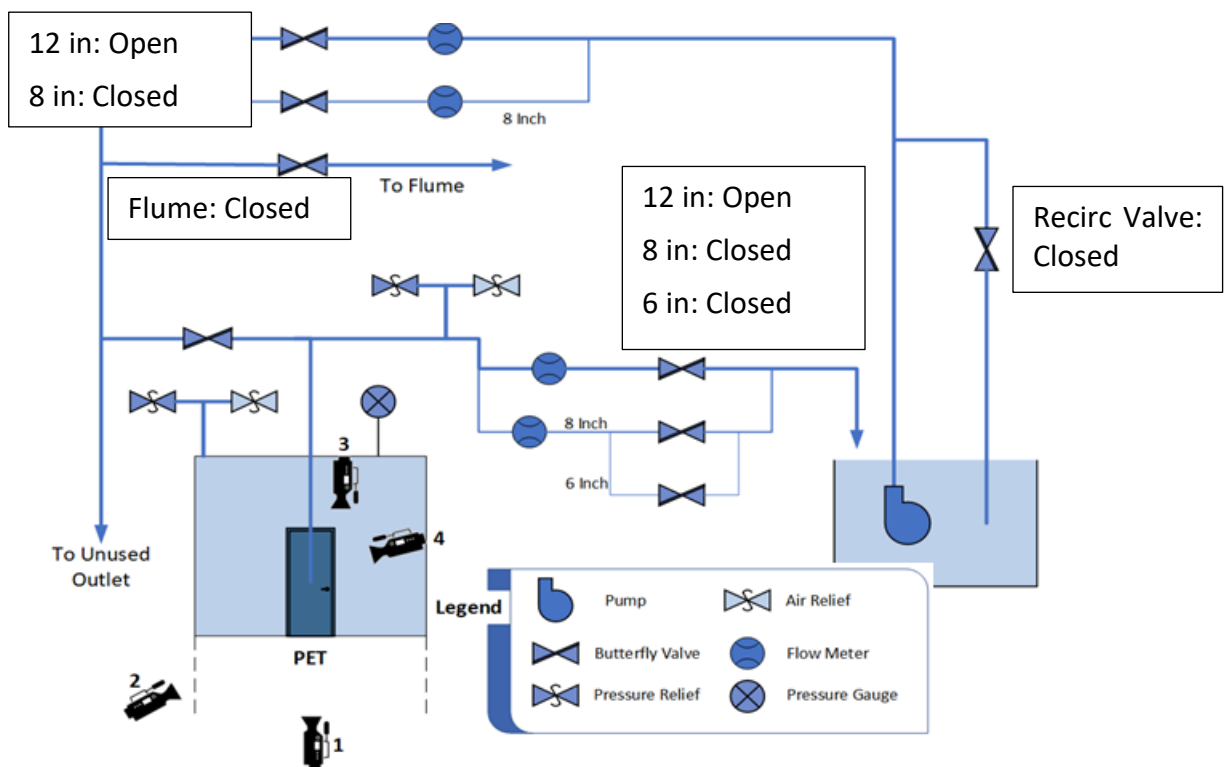


Figure 39. Hollow-Core Door - Experiment #7 - Initial Valve Configuration

In the previous experiments, the program uploaded to the CR1000 datalogger, sampled the CS451 depth sensor every second, and produced data every four seconds, recording the maximum and minimum depths achieved during the four second interval, an average of the four depth measurements, and a sample measurement on the 4<sup>th</sup> second. As mentioned above, the new program for the CR1000, only sampled and recorded depth measurements from the sensors every two seconds, therefore a new method to normalize the depth data had to be used.

This method consisted of a simple three-point running average, with different weights for each point. The central point was given a weight of 0.5, while both adjacent points, were given a 0.25 weight. This procedure was performed on the depth and voltage measurements of the Campbell Scientific and Omega depth sensors, respectively. After transforming the voltage measurements of the Omega sensor to inH<sub>2</sub>O using Equation 1, both measurements were averaged to come up with the normalized depth measurement.

The three-point running average was used in most of the data points collected from both sensors. However, four data-points were identified where this method was not appropriate. The first and last point of each experiment were two of the three data points with different processing, or in this case, no processing, as these two points were left without any changes from the raw measurements produced from the sensors. The first data point of the experiment was defined as the last depth recording before the water depth inside the PET started increasing.

Table 2 shows a fraction of the raw data collected for steel door experiment #11. The record with the first data point that signals an increase in the PET water depth has been pointed to with a red arrow, it can be seen how the record is the 60<sup>th</sup> raw measurement for that

experiment. Using the statement from the previous paragraph, it can be deduced that the data point considered to be as the first one for the steel door experiment #11, would be record #59, since it is the last depth recording before the water depth inside the PET started showing any obvious increase.

Table 2. CR1000 Raw Data - Fragment of Data Collected for SD - Experiment #11

CR1000				
Time Stamp	CS451		Volt	
	#	Lvl[in]	Tmp[F]	[mV]
13:53:22	45	-0.082	66.52	392.6
13:53:24	46	-0.093	66.52	392.6
13:53:26	47	0.348	66.52	392.6
13:53:28	48	0.026	66.52	393.3
13:53:30	49	0.006	66.52	393.3
13:53:32	50	0.036	66.52	392.9
13:53:34	51	-0.004	66.52	393.1
13:53:36	52	-0.004	66.52	392.9
13:53:38	53	-0.014	66.52	393.1
13:53:40	54	-0.015	66.52	392.9
13:53:42	55	-0.022	66.52	392.8
13:53:44	56	-0.018	66.52	392.8
13:53:46	57	-0.006	66.52	393.3
13:53:48	58	-0.026	66.52	392.6
13:53:50	59	-0.033	66.52	392.6
13:53:52	60	3.252	66.52	401.3
13:53:54	61	4.318	66.51	406.7

The last data point of the experiment, when possible, was defined as the second measurement with a recorded depth lower than 7 in; the 7 in. threshold was selected due to data availability, and the fact that most subsequent data points are not useful to this thesis. If the depth measurements were saved before the readings reached the 7in. threshold, the last data point, would be the last recorded data point.

The third point to which a different processing method was applied, was the one that contained the maximum depth measurement. If a three-point running average was applied to process this data point, it would be influenced by the depth measurement of the following data point, which usually corresponds to the first depth value after a system failure has been achieved. To avoid this, the data point containing the maximum depth achieved in the experiment, was only averaged with the previous data point, with weights of 0.75, and 0.25, respectively.

The last data point to receive a different data-processing method was the first data point to be recorded after the maximum water level in the PET was reached. The different data-processing method was applied to prevent the maximum depth measurement from skewing the leakage rate calculations. The first data point after the maximum water level in the tank was only average with the following data point, giving the former a weight of 0.75, and the latter a weight of 0.25.

The results of both experiments showing the water depths achieved inside the PET are shown in Figure 40.

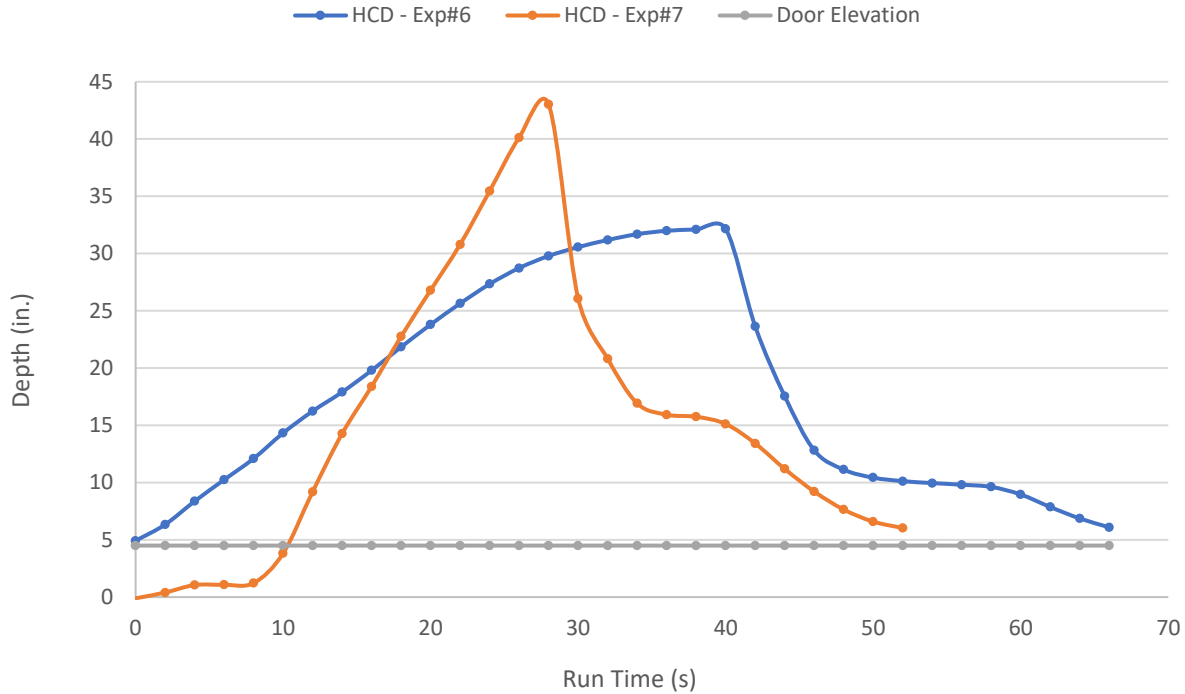


Figure 40. Hollow-Core Door Experiments #6 & #7 - PET Water Height

Comparing Figure 40 with other ‘PET Water Depth’ figures, such as Figure 24 in 33, it is possible to observe the longer time it takes the PET to drain. This plateau effect is caused by the pump itself. In experiment #6 the pump was left on for 16 seconds after the door broke, Figure 41 will show that the water flowrate into the PET at the time the door broke was ~ 1,000 gpm, and the results from the Flowrate-Behavior Experiment showed that when that amount of water is going into the PET, the depth of the water in it varies around 10 in; which corresponds to the depth values of the plateau observable in the previous figure. The same effect takes place after the rupture of the door in experiment #7; however, in this case the plateau stabilizes at ~16 in. because the full flow from the pump was directed into the PET.

The data collected in each experiment was analyzed to produce the following information:

- Water flowrate into the PET.
- Water flowrate out of the PET.
- PET fill-rate.

Unlike the hollow-core door experiments performed with the Global pump, in which the flowmeter measured directly the water flowrate into the PET; in these experiments, the water flow into the PET had to be calculated as the subtraction between the water flowrate upstream and water flowrate downstream of the PET. As already stated, the flowmeters do not produce readings at the same time stamps, most of the time; and the interval at which they record the data is not constant; so, to estimate the water flowrate into the PET, flowrate values at the flowmeters, had to be estimated for several time stamps.

The data was created in a new table with an interval of two seconds; the timesteps in which the flowmeters actually recorded data were simply duplicated in this new table, but the timesteps in-between those that had data, were filled in by linearly interpolating the existent records, see the table below.

*Table 3. Flowmeter Data - Recorded vs. Created*

Flowmeter (12 in. Upstream) [FM1]		Flowmeter (12 in. Downstream) [FM2]		FM	FM1	FM2
Time Stamp	Flowrate [gpm]	Time Stamp	Flowrate [gpm]	Time Stamp	Calculated Flowrate [gpm]	Calculated Flowrate [gpm]
15:31:37	0.00	15:31:38	0.00	15:31:36	N/D	N/D
15:31:47	1532.56	15:31:44	481.56	15:31:38	153.26	0.00
15:31:50	2005.87	15:31:50	309.07	15:31:40	459.77	160.52
15:31:59	1760.40	15:31:57	274.50	15:31:42	766.28	321.04
15:32:01	1724.83	15:32:04	367.60	15:31:44	1072.79	481.56

It can be seen in Table 3, how the flowmeters did not record data at timestamp 15:31:42, look under the 'Time Stamp' column, for each 'Flowmeter...' section. Flowrates values for 15:31:42; were linearly interpolated from data occurring between 15:31:37 and 15:31:47 for FM1, and from data occurring between 15:31:38 and 15:31:44 for FM2. This process was repeated for all timesteps of every experiment.

Having estimated the data for the water flowrate at the upstream and downstream locations of the PET for a constant interval of two seconds for the whole experiment duration, it was possible to calculate an estimate of the water flowrate into the PET. The calculation consisted on subtracting the data for the downstream section from the data of upstream section. The two second interval for the flowmeters created data, was selected so that the new calculated data-points would line up with the depth sensors data recordings.

Once the upstream and downstream water flowrates were calculated, and with them the water flowrate into the PET, it was proceeded to calculate the filling rate of the PET. This property was calculated in the same way as in the hollow-core door experiments. The rate at which the water depth increased in the PET was calculated using two consequent depth measurements, and then that rate was multiplied by the area of the tank to produce a volumetric flowrate. As mentioned before, the water depth measurements for these, and all following experiments consisted in a running average of the measurements recorded by the Campbell Scientific and Omega depth sensors.

Finally, having calculated the water flowrate into the PET, and the rate at which the PET filled with water, it was possible to estimate the leakage rate from the tank. As mentioned above,



the water flowrate into the PET was calculated for the same timesteps as the ones used by the depth sensors to record data, this meant that now both properties needed to calculate the leakage rate, were available at the same timesteps, which reduced the calculation to a simple subtraction of the PET fill rate, from the flowrate into the tank.

The graphed results of the flow measurements and calculations, for experiment #6 are shown below.

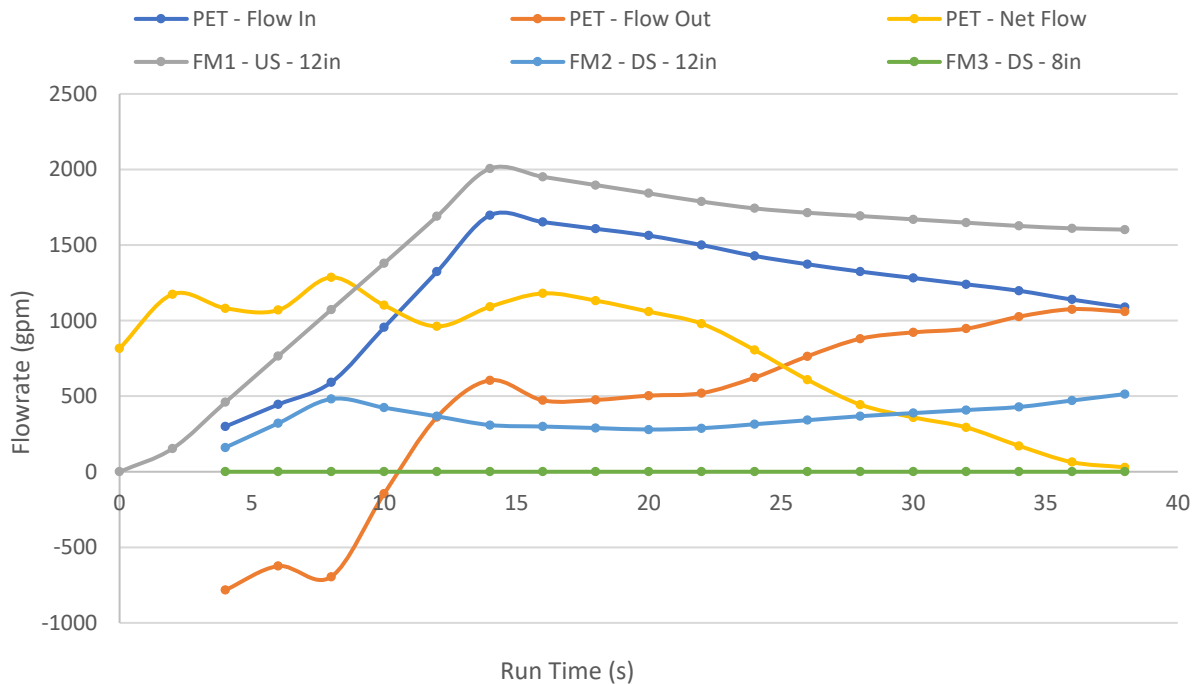


Figure 41. Hollow-Core Door Experiment #6 - Flow Information

It is possible to observe in the figure above, a similar behavior to the experiments with the previous pump configuration. Both flowmeters take several seconds to achieve steady-state readings. This does not cause trouble in longer experiments, but as seen in Figure 42, they can render much of the experiments data unusable. In Hollow Core Door experiment #6, the recirculation valve was open, and so were the valves located in the 12 in. upstream and

downstream valves, that is the reason the flowrate through the upstream 12 in. flowmeter remained constant around 1,600 gpm.

For Hollow-Core Door experiment #7, the experiment configuration was changed, the recirculation valve was closed, this caused the flow through the upstream section to achieve values upwards of 4,000 gpm; however, this experiment configuration also resulted in a very short experiment, in which the door ruptured before the flowmeters started reading steady state data.

It can be seen in Figure 42, how the data has no clear behavior. When compared to the data acquired for experiment #6 shown in Figure 41, it is possible to conclude that the analysis of this experiments' data has no meaning. The upstream 12 in. flowmeter achieves a steady-state behavior north of 30 seconds into the experiment, by this time the door had already ruptured. Neither of the flowmeters had a reading higher than 0 until second 13, and the upstream flowmeter did not produce a reading higher than 0 until second 17; by those times, the water depth readings inside the PET were ~13 in. and ~23 in. respectively.

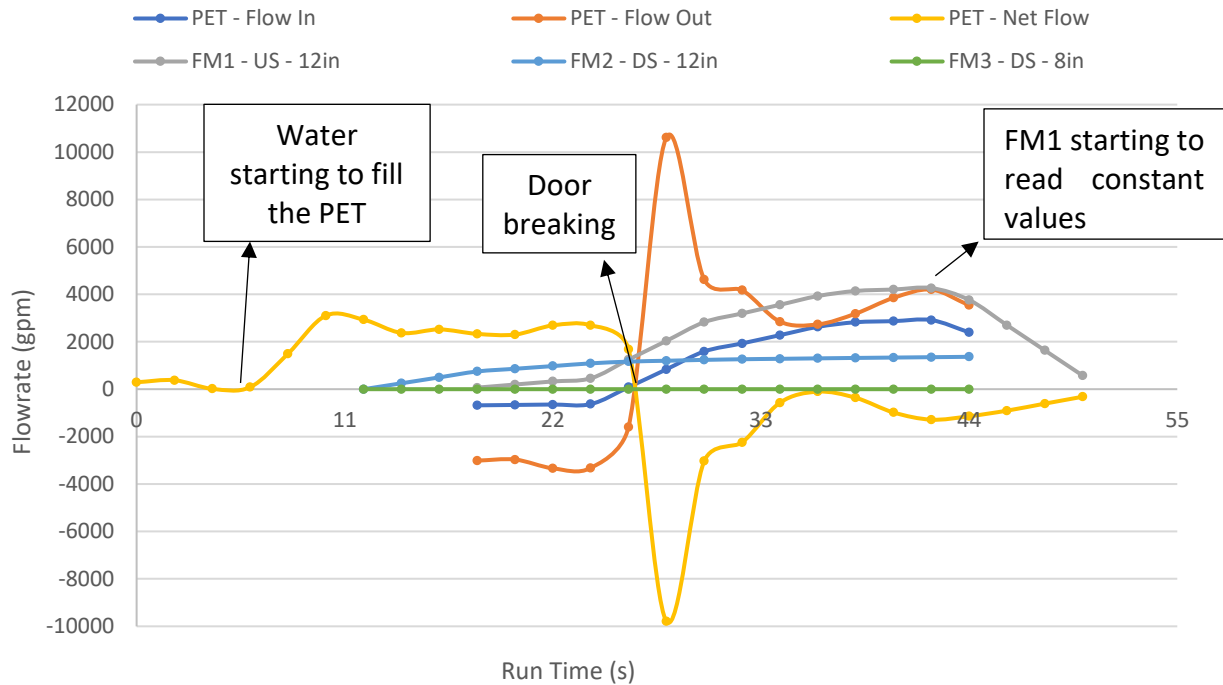


Figure 42. Hollow-Cor Door Experiment #7 - Flow Information

## Post-Mods Steel Door Experiments

### Frame Construction

The frame for the steel door was built in a similar manner to that of the hollow-core doors.

The frame was divided in two sections, an outer frame, and an inner frame.

The studs used for the outer frame were 2 in. x 8 in; but unlike the outer frame for the hollow-core doors, this outer frame was not 2 studs thick all around; the number of studs varied from two for the vertical sections to one for the horizontal sections. This was done to prevent the entire inner frame from bowing. In the pre-mods experiments, a slight bowing of the inner frame was observed for each experiment; reducing the number of studs used for the horizontal sections of the outer frame, meant that the lower and upper sections of the inner frame sat

against the angles of the PET, reducing any possible movement that the inner frame may have experienced before.

The inner frame was erected completely different from the one for the hollow-core doors. The first difference is the different stud sizes used for the frame; the upper, lower, side edges and door base used 2 in. x 8 in. studs, the same as the outer frame. But all the other studs (the ones around the door, and the vertical studs, placed in-between the ones around the door, and the ones at the edges) were 2 in. x 4 in. The two sizes were used for a simple reason, being a pre-hung steel door, the frame has to be joined to the wall it is being placed in, the recommended studs for attaching the frame to were 2 in. x 4 in. in size, besides, studs of the next available size (2 in. x 6 in.) did not fit inside the steel frame.

The steel frame was enclosed by studs of two sizes; at the bottom the frame was screwed to a 2 in. x 8 in. stud through the anchors present at the base of the frame; the base stud is 40 in. long and served at each end as a support for one of the vertical slabs that were screwed at each side of the frame. The frame came with masonry and steel stud wall anchors welded to its structure. The lack of wood stud anchors meant that they had to be installed separately, see Figure 43. The studs around the door had as before to be two, but in this case, the vertical studs had also to be screwed in place according to regulations, see Figure 44.



*Figure 43. Welded wood stud anchors, with holes for screws*



*Figure 44. Screwed Double Wood Studs into Anchors*

Unlike the hollow-core door frame, the only outer most vertical stud surrounding the door ran completely from the bottom to the top horizontal studs; the inner most slab ran from the base stud, to the lower of the two top studs, see Figure 45. As seen in the images below, there is an empty space in between the steel frame and the wood studs, generally this space is reserved for drywall, however, in this case plywood was used instead. Plywood sheets, similar to those used to create the wall for the hollow-core door frame were also used to create the wall for the steel door frame. To create a fire rated door, the plywood slid at least  $\frac{1}{2}$  in. into the steel frame.



Figure 45. (left) Top section of the stud inner frame. (right) Bottom section of the inner frame

To provide support points for the plywood sheets, 4 extra studs were nailed to the inner frame; two studs were placed against the right and left outermost 2x8 studs, and the other two

were placed in the middle of the space created by the door and the side studs. The finalized frame is shown below in Figure 46.



*Figure 46. Steel door frame and wall*

### *Experiments*

Unlike the experiments with hollow-core doors, these experiments were run using only two flowmeters, the 12 in. one in the upstream section, and mostly the 12 in. one in the downstream section. This was done to reduce the time intervals at which the flowmeters recorded data. It is important to note that some of the data recorded in these metal door experiments included pressure readings inside the PET, and water depth at the v-weir using the ultrasonic transducer; however, neither data will be shown for any experiment. The pressure gage measured 0 psi for all experiments, this was as expected since at no point was the

experiment filled with water. The ultrasonic transducer on the other hand, was producing readings, but its datalogger did not record the data properly, all it recorded was an output of 0 mA.

The first three experiments were run using the same configuration, hence, the grouping of the achieved PET water depth in the figure below. In the experiments, the recirculation valve was left fully open, as were the valves in the upstream and downstream section of the 12 in. line. The door was closed, but the dead bolt was not locked. The water depth results achieved for all these three experiments are shown Figure 48.

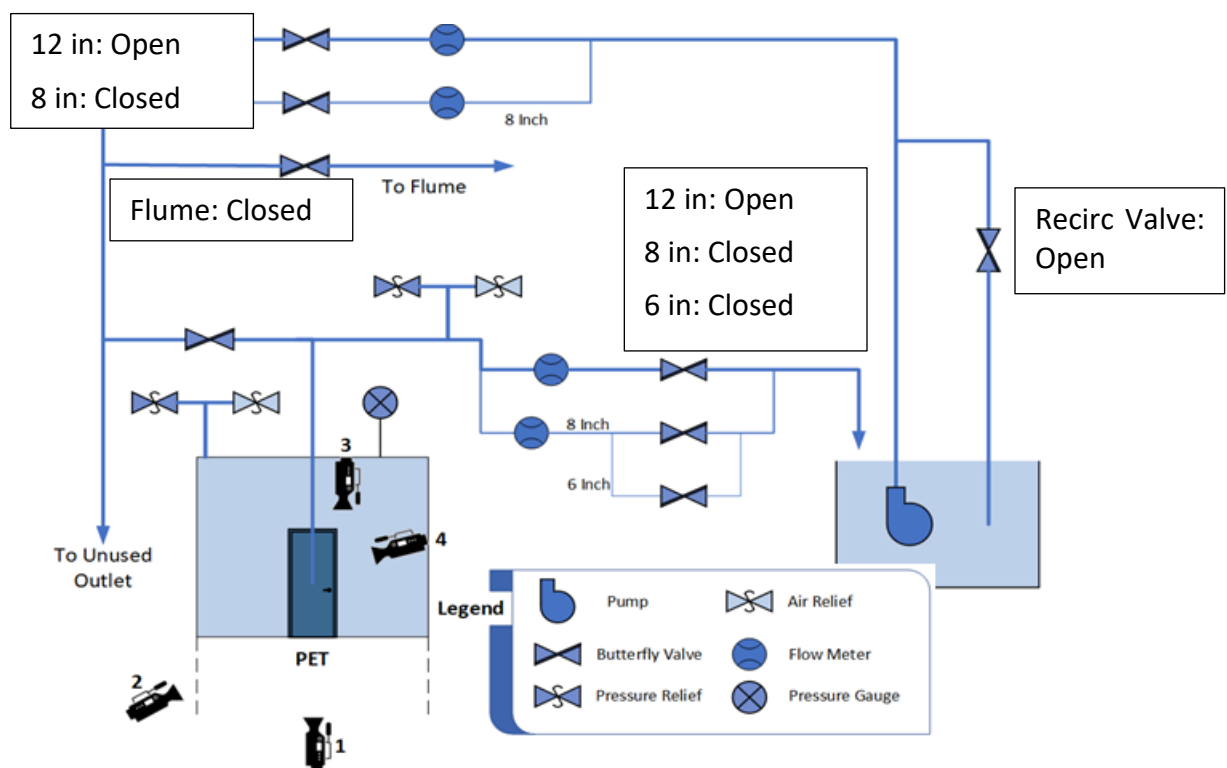


Figure 47. Steel Door Experiments #1, #2 & #3 - Initial Valve Configuration



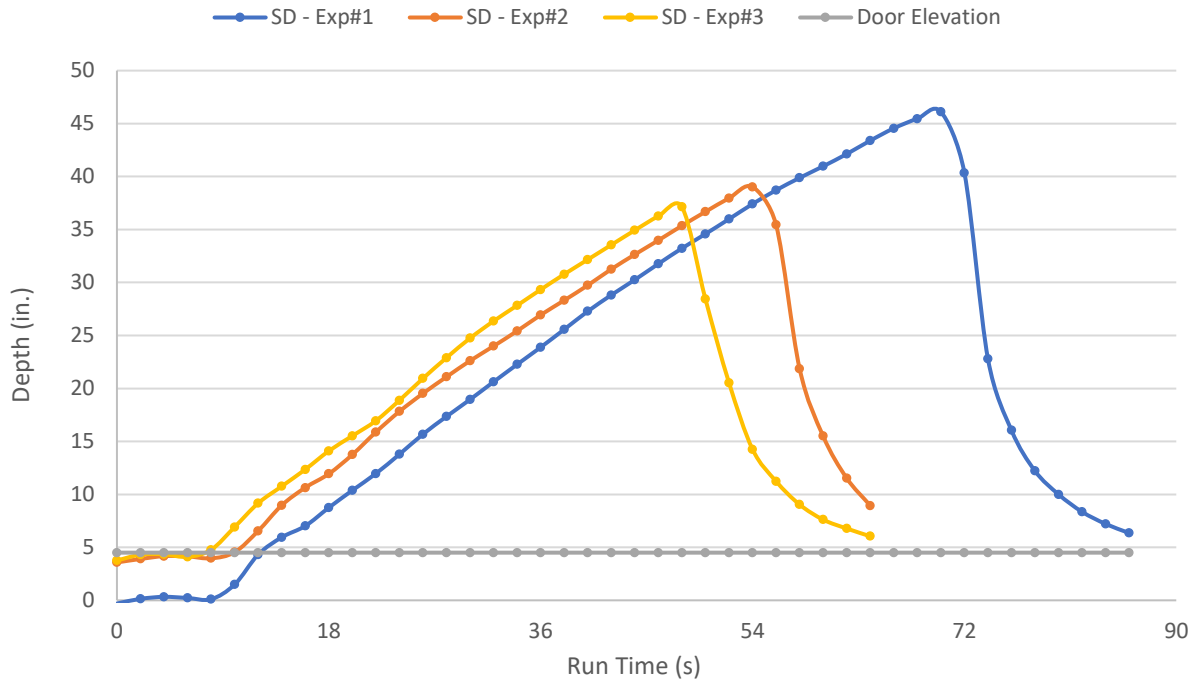


Figure 48. Steel Door Experiments #1, #2 & #3 - PET Water Height


The results were unexpected. In all of the experiments the door popped open after the maximum water height was reached. Experiment #1 produced the longer experiment, and the one in which the water reached the highest depth before popping the door open. In both experiments #2 and #3, the door popped open at a similar experiment time and water depth. It will be seen how in the following experiments also run with the deadbolt unlocked, that the door popped open at approximately the same water depth, regardless the water flowrates into and out of the PET.

In Figure 48 it is not possible to appreciate the plateau effect observable for the 'PET Water Depth' results of hollow-core door experiments #6 and #7 shown in Figure 40. This is because for the steel door experiments the pump was turned off as soon as possible after system failed was observed; this was done to try to prevent the formation of the plateaus.

In Figure 48 it is also possible to appreciate how the first depth measurement after the door pops open is not as steep as in previous experiments. This is a result from the averaging of the data between the Campbell Scientific and Omega depth sensors. Table 4 contains the results of the depth data analysis for both transducers. It can be seen between time stamps 14:56:00 and 14:56:02, that the analysis of the Campbell Scientific depth transducer data, shown under column 'Run. Ave.' yielded water depths of 46.43 in. and 36.34 in. respectively. At those same time stamps, the analysis on the Omega transducer data produced signals of 571.6 mV and 573.4 mV, which translate to 45.80 in. and 46.27 in. of water inside the PET, see columns 'Run. Av. Volt' and 'Volt to Depth', respectively. This means that while the Campbell Scientific transducer measures a decrease in the water depth inside the PET, the Omega transducer is recording a slight increase; the relatively high Omega transducer measurement is what drives the high depth of the first data point recorded after the system failure.

Table 4. Campbell Scientific vs Omega Depth Sensor Data Comparison

Dept Transducer				
Time Stamp	Run. Ave.	Run. Av Volt	Volt to Depth	Ave Depth
14:55:54	43.86	560.4	42.93	43.39
14:55:56	45.00	565.0	44.11	44.55
14:55:58	45.89	568.6	45.03	45.46
14:56:00	46.43	571.6	45.80	46.12
14:56:02	36.34	573.4	46.27	41.31
14:56:04	23.85	500.1	27.32	25.59
14:56:06	15.51	458.6	16.58	16.05
14:56:08	11.87	443.1	12.55	12.21
14:56:10	9.56	434.9	10.43	10.00
14:56:12	7.98	428.3	8.73	8.35



The problem is exclusive to the rapid change in water depth at the instant the system fails. The cause of the disparity is not known, unlike the data shown in Table 4, the analysis of the Campbell Scientific data does not always produce water depth slightly higher than the analysis of the Omega transducer data. Therefore, a difference in the sampling order of the transducer by the CR1000 datalogger can be ruled out. More on this problem in the section Summary and Conclusions; for the data presented and analyzed in this thesis, no fix has been applied to the issue.

The analysis made for the data of the metal door experiments is the same one as for the latter hollow-core doors experiments. Below are the 'Flow Information' graphs for the first three metal door experiments.

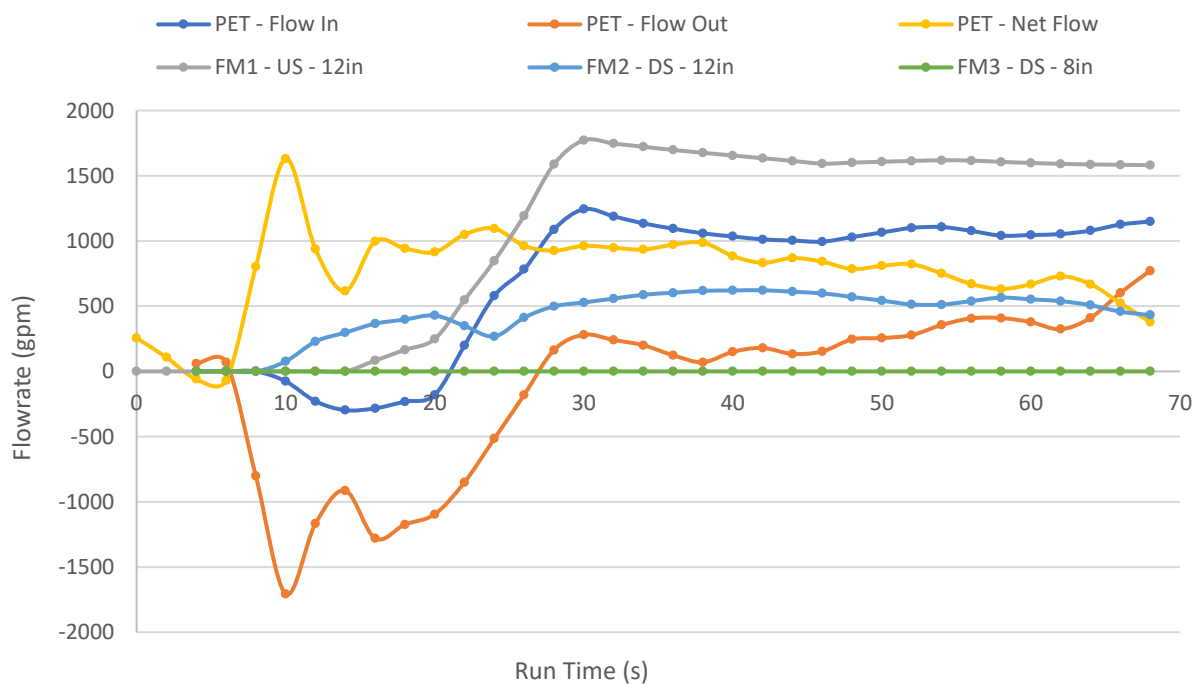


Figure 49. Steel Door Experiment #1 - Flow Information

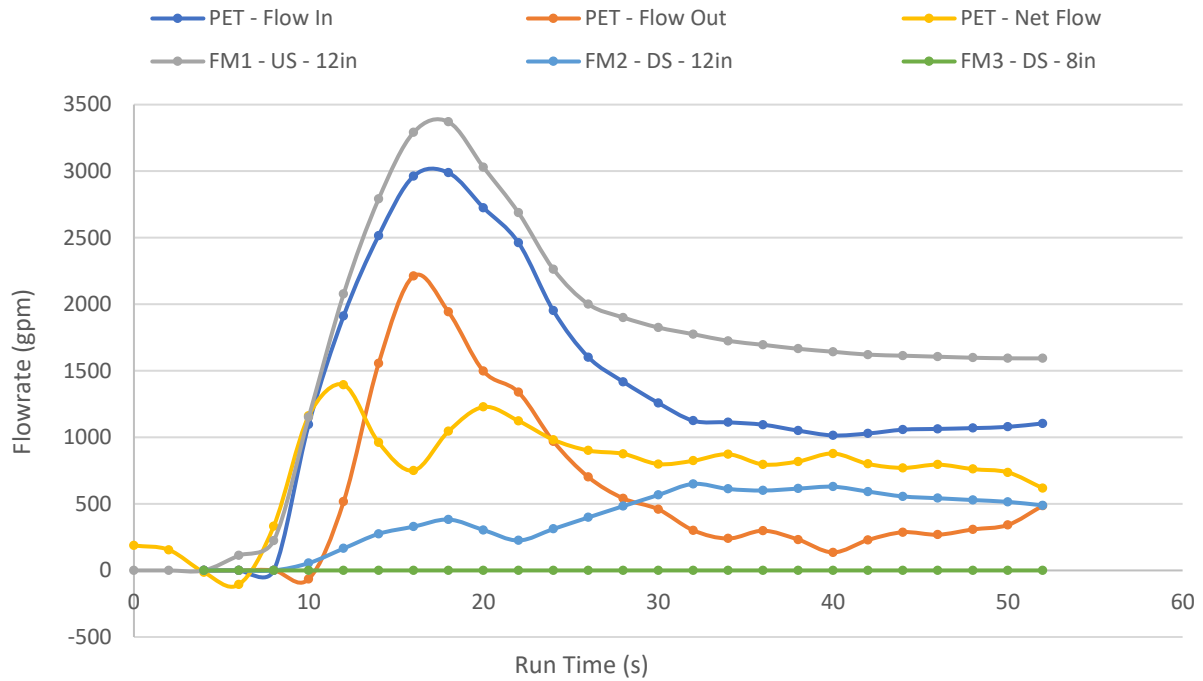


Figure 50. Steel Door Experiment #2 - Flow Information

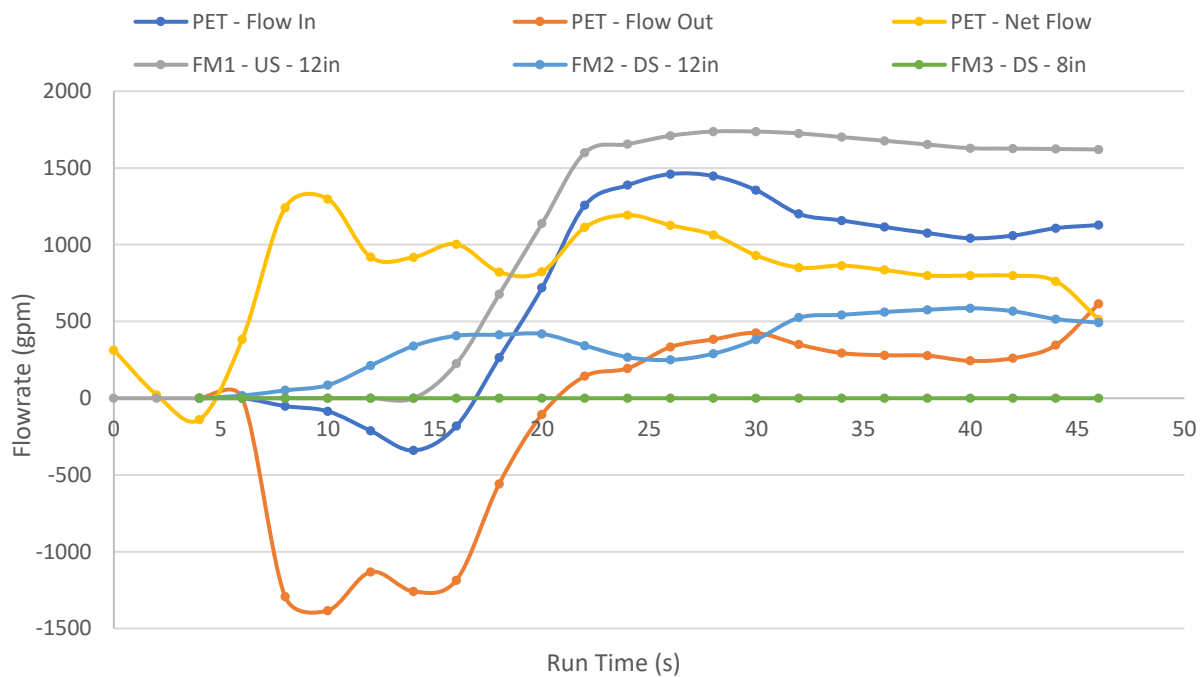


Figure 51. Steel Door Experiment #3 - Flow Information

It can be observed how the three graphs show a similar steady-state water flow behavior to each of the other experiments, and analogous to the ones from hollow-core door experiments.

The initial dead-time, ramp-up and steady-state behavior of the flowmeters is present in experiments #1 and #3, while experiment #2 presents a very abnormal behavior of FM1 at the beginning of the experiment. The lack of data from the flowmeters, while the depth sensors are recording the water depth inside the PET increasing, renders the data acquired during the first ~30 seconds of most experiments unusable.

All three experiments experienced the spikes in water flowrate out of the PET, and PET net water flow, that were also present in previous hollow-core door experiments. The difference is that instead of the door breaking, the door popping open is the cause of the spikes. However, as previously noted, the spikes are not shown in the graphs to allow viewing of the flowrates behavior during the tests.

The next two experiments were similar to the first three. The main difference was in the valve configuration. Experiment #4 was performed with the recirculation valve open, and the upstream 12 in. line half-open. Experiment #5 was performed with the recirculation valve also in the open position, but with the upstream 12 in. valve three quarters open; this experiment was actually going to be performed with the upstream 12 in. valve one-quarter open, but after performing the experiment, and comparing the flowmeter recordings with experiment #4, it was realized that the valve was in the three quarters open position.

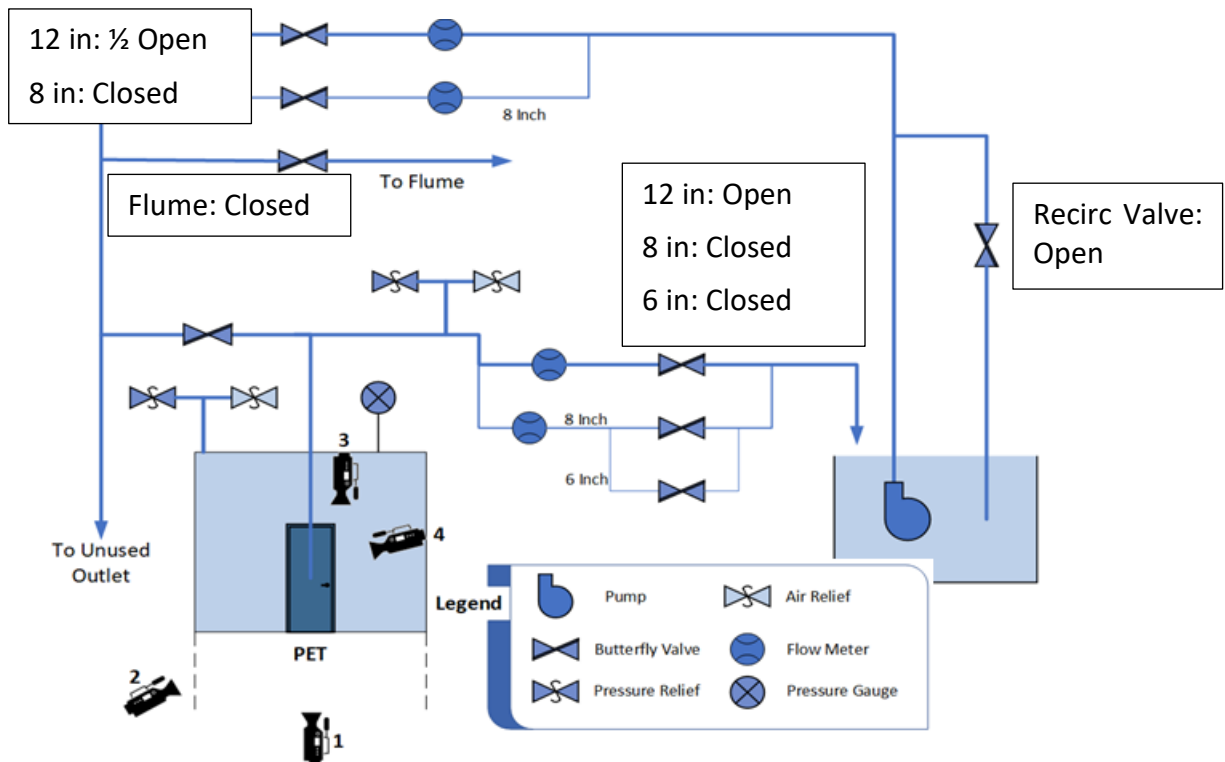


Figure 52. Steel Door Experiment #4 - Initial Valve Configuration

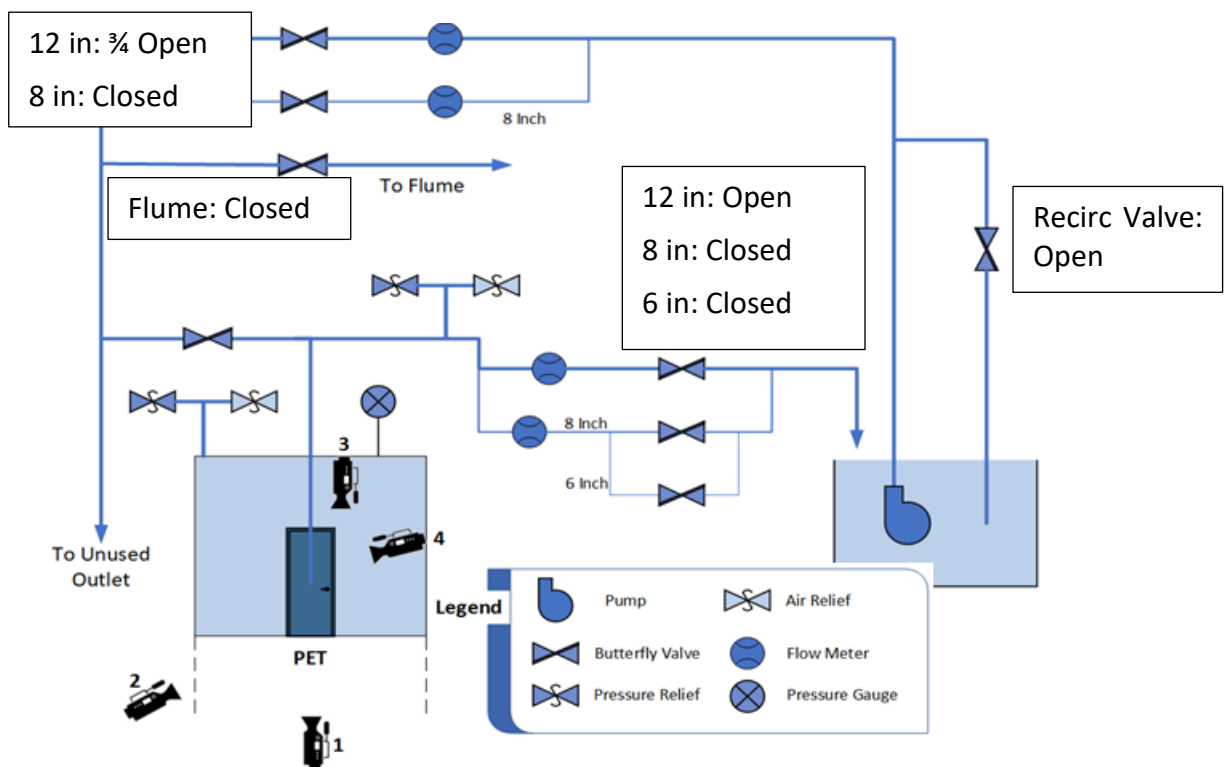


Figure 53. Steel Door Experiment #5 - Initial Valve Configuration

As mentioned in the results analysis for experiments #1 through #3, the PET water height achieved in both experiments was almost identical regardless of the difference in time of the experiments. The difference in time is a product of the lower water flowrate into the PET in experiment #4, which resulted in a longer time to achieve the water height that caused the door to pop open. The water depth results achieved for experiments #4 and #5 are shown below.

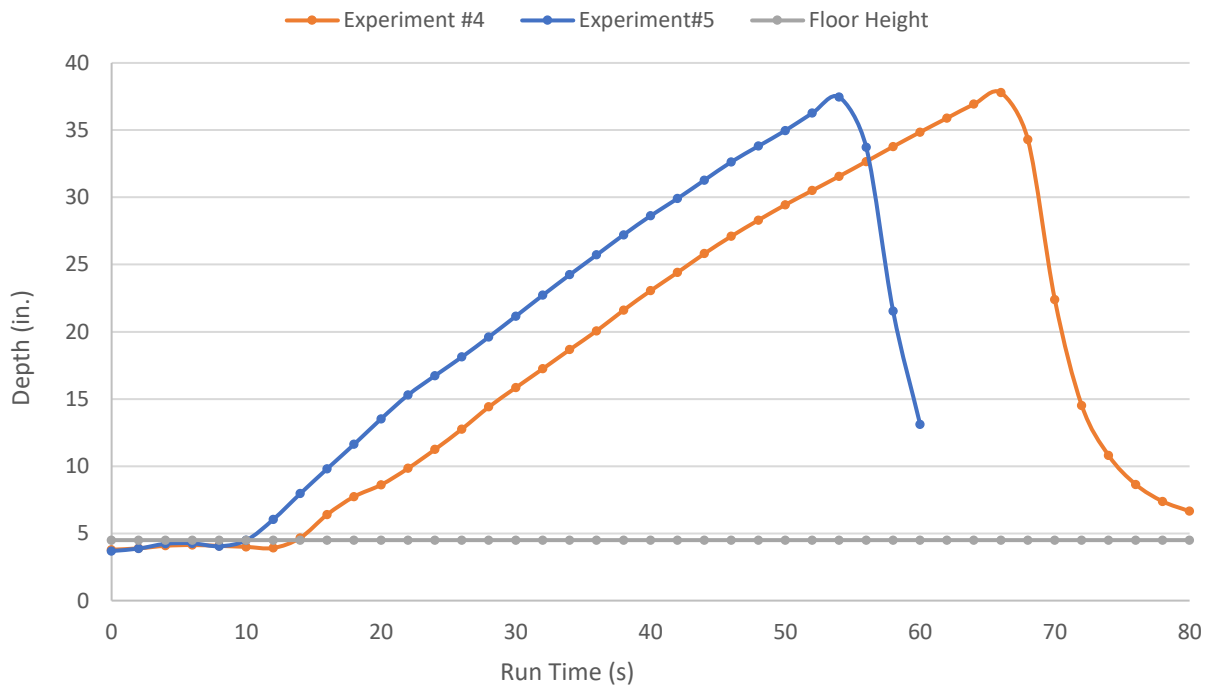


Figure 54. Steel Door Experiment #4 & #5 - PET Water Height

Below are the analysis results of the data from experiments #4 and #5. It is possible to observe how the restriction created by an upstream valve half open causes the flow in the upstream section to decrease. In experiment #5 in which the recirculation valve was also opened, the upstream water flowrate reached a steady-state value close to 1,700 gpm., while in experiment #3, the flowrate was always closer to the 1,400 gpm. mark. It is important to also note the changes in the water flowrate into the PET since this property dictates how fast will the PET fill with water. In experiment #4 the water flowrate into the PET varied between 600 and

900 gpm; while in experiment #5, with the higher upstream water flow, the flowrate into the PET was also higher, closer to the 1,000 gpm value.

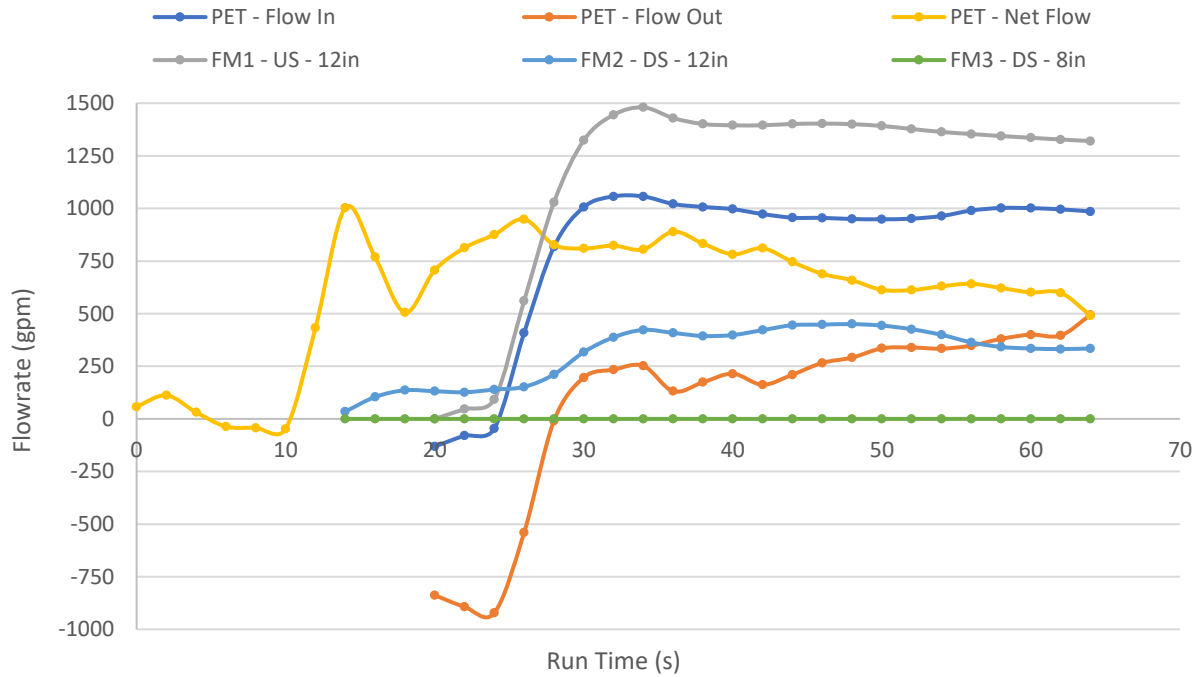


Figure 55. Steel Door Experiment #4 - Flow Information



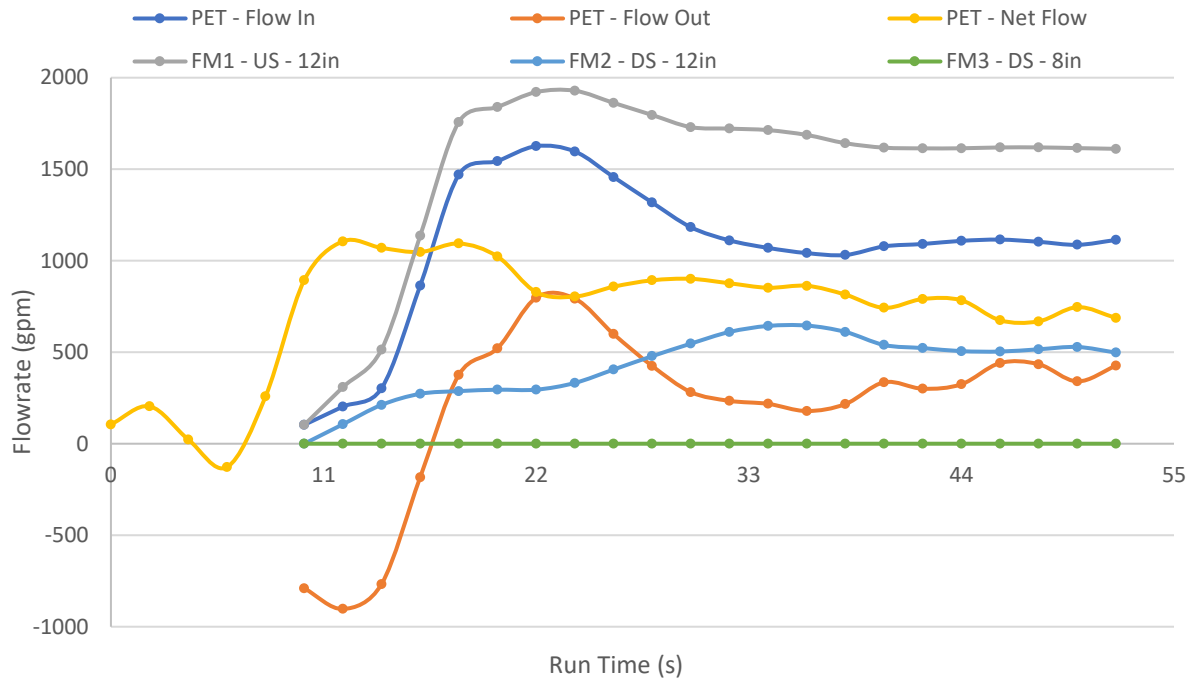


Figure 56. Steel Door Experiment #5 - Flow Information

The following three experiments are very important. They were also performed with the door closed, with an open dead bolt; the recirculation valve was open, as in the previous two experiments, but this time the upstream 12 in. valve was only open one quarter of the way. Figure 58 shows the PET water depths achieved during each of these experiments.

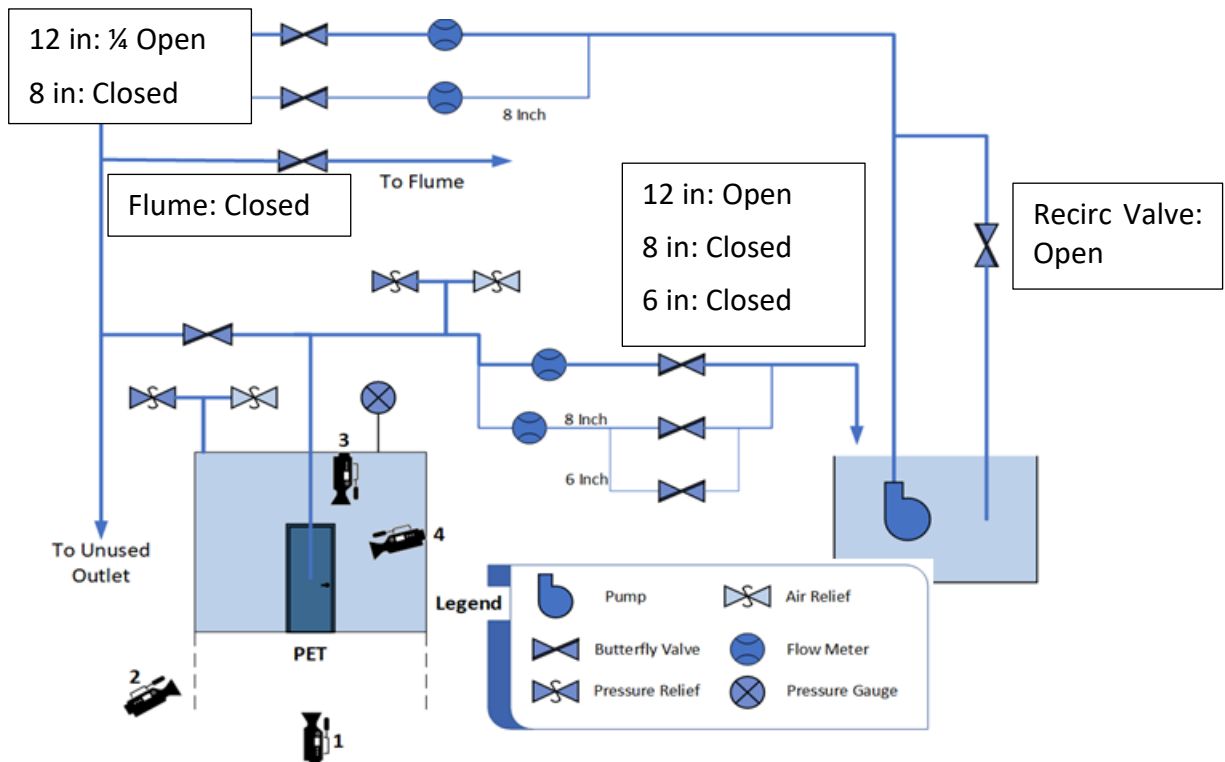


Figure 57. Steel Door Experiments #6, #7 & #8 - Initial Valve Configuration

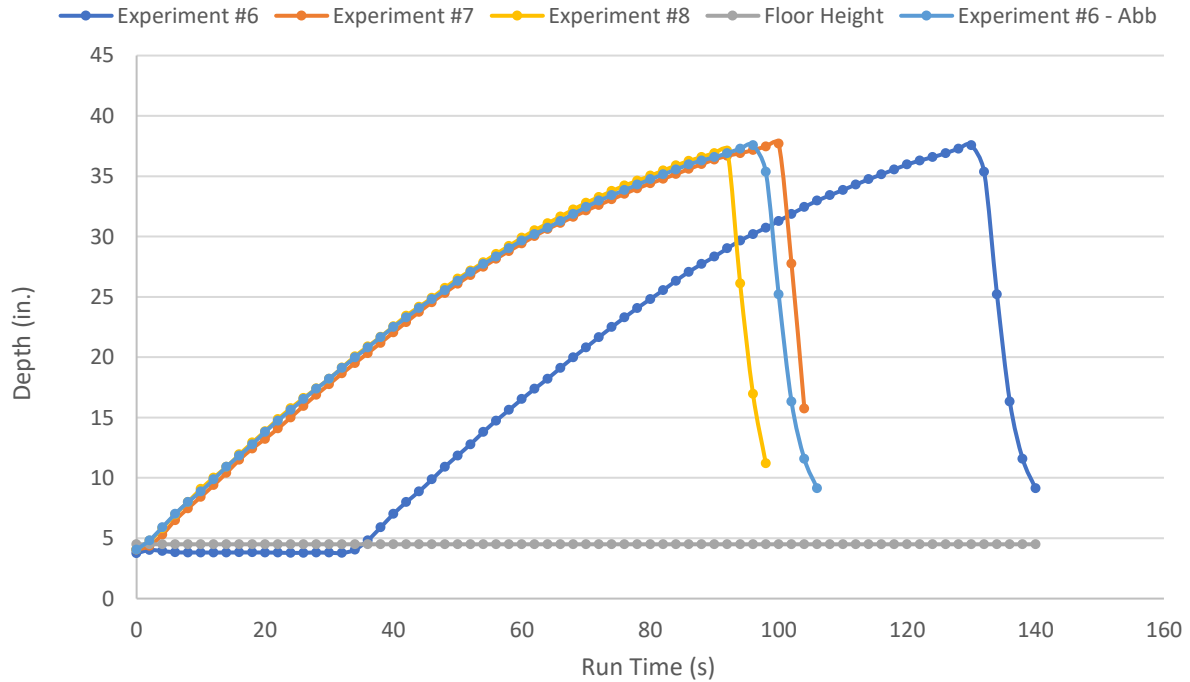


Figure 58. Steel Door Experiment #6, #7 & #8 - PET Water Height

By comparing the results from these three experiments, it is possible to conclude that the steel door has a very constant behavior. It can be observed how experiment #6 had a lead time of  $\sim 30$  seconds, once eliminated it can be seen how the time duration of all three experiments was very similar, and so was the water depth achieved before the door popped open.

Evaluating the results shown in Figure 58, together with those in Figure 59, Figure 60 and Figure 61, shown below, it is possible to appreciate two very important distinctions between these experiments and the previous ones. These three experiments are the first ones in which the flowmeters start producing data before or at the same time the depth sensors inside the PET start detecting an increase in the water depth. This is of importance, because this low flow configuration can be used at the beginning of all other experiments, to reduce the time it takes the flowmeters to achieve steady-state readings.

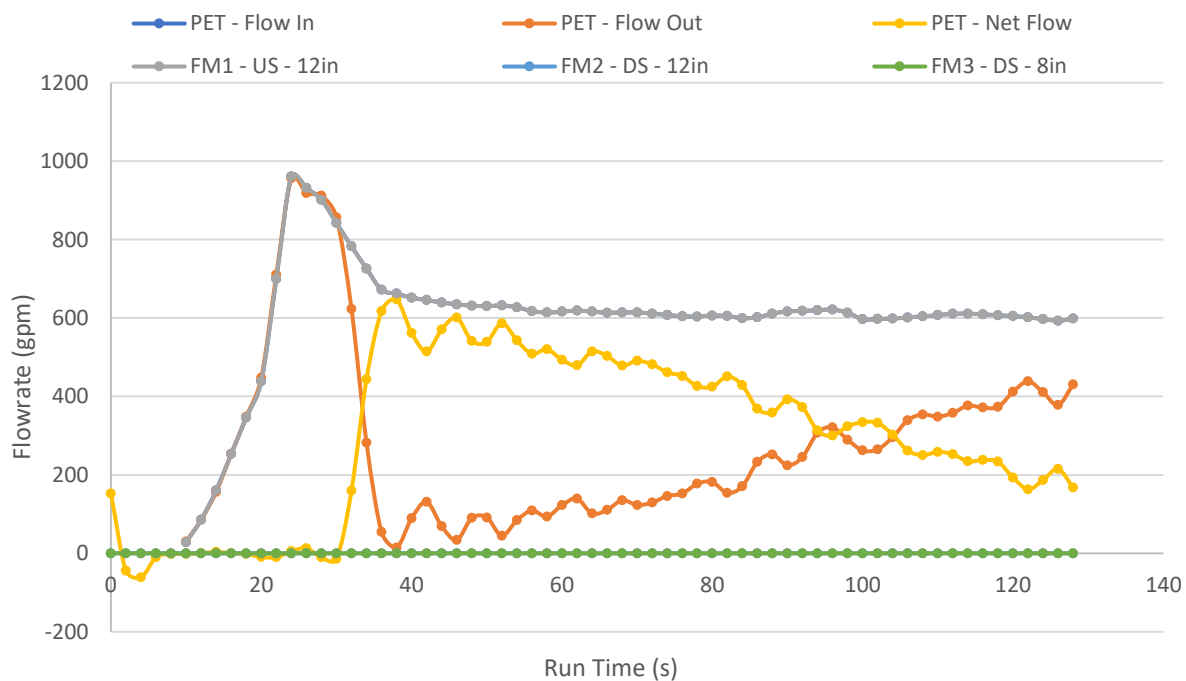


Figure 59. Steel Door Experiment #6 - Flow Information

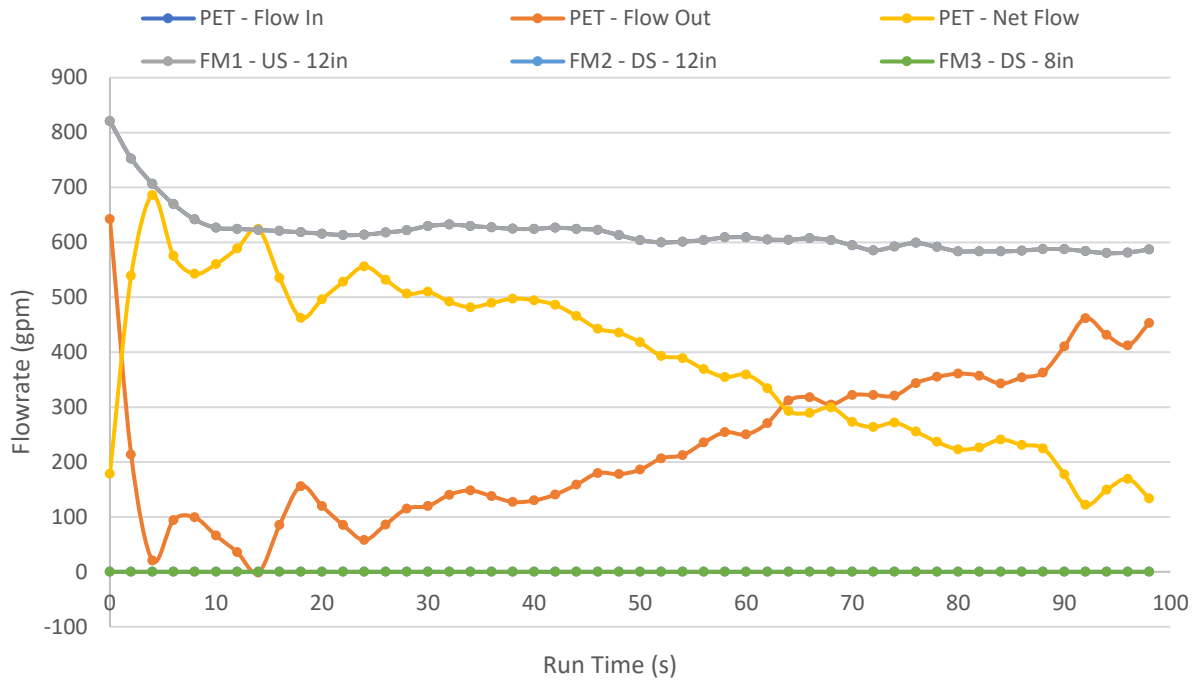


Figure 60. Steel Door Experiment #7 - Flow Information

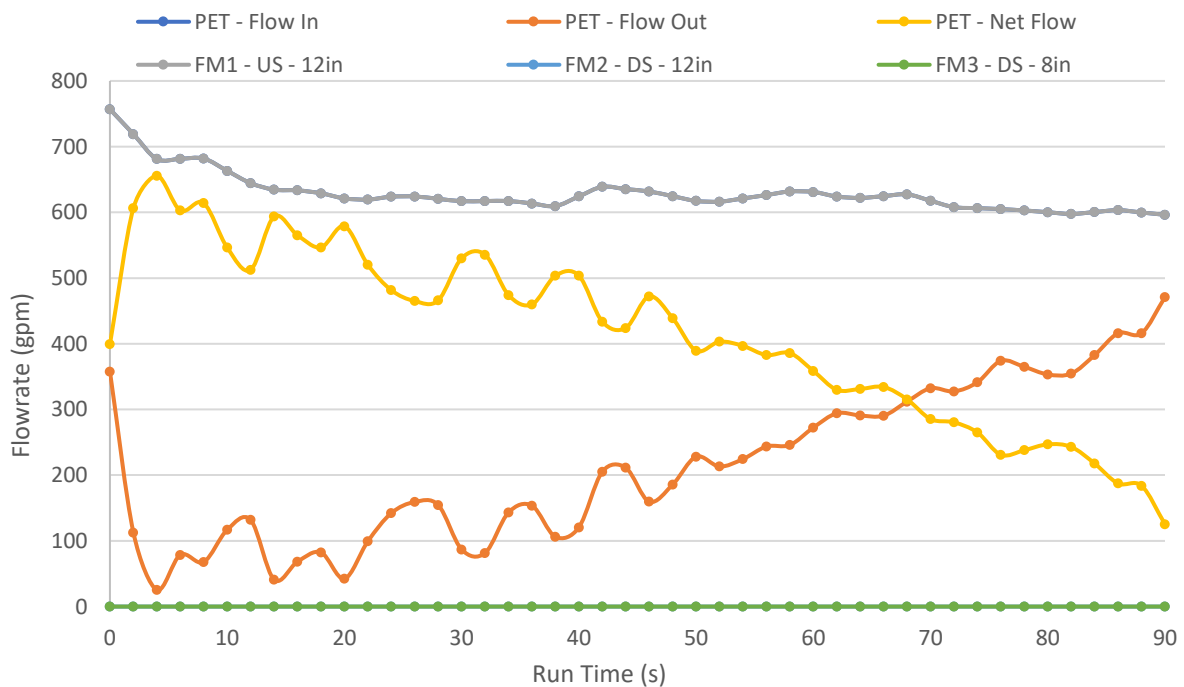


Figure 61. Steel Door Experiment #8 - Flow Information

The second important distinction is the 0 gpm reading of the downstream 12 in. flowmeter. This may be due one of two reasons; the first theory is that the water flow is so low

through the flowmeter, that it is below its low flowrate or low velocity threshold. The last theory is that the readings are right because there is simply no water flowing through the pipe, and all the water being pumped is going directly into the PET.

The following experiments, experiments #9, #10 and #11, were all performed with the deadbolt on. Experiment #9 was the first one performed with the door closed in this configuration; the recirculation valve was open, and the upstream 12 in. valve was only half open. As seen in the figure below, which also contains the water depth inside the PET for experiments #10 and #11, closing the dead-bolt in the door caused a slight increase in the maximum water depth achieved inside the PET, compared to the previous experiments.

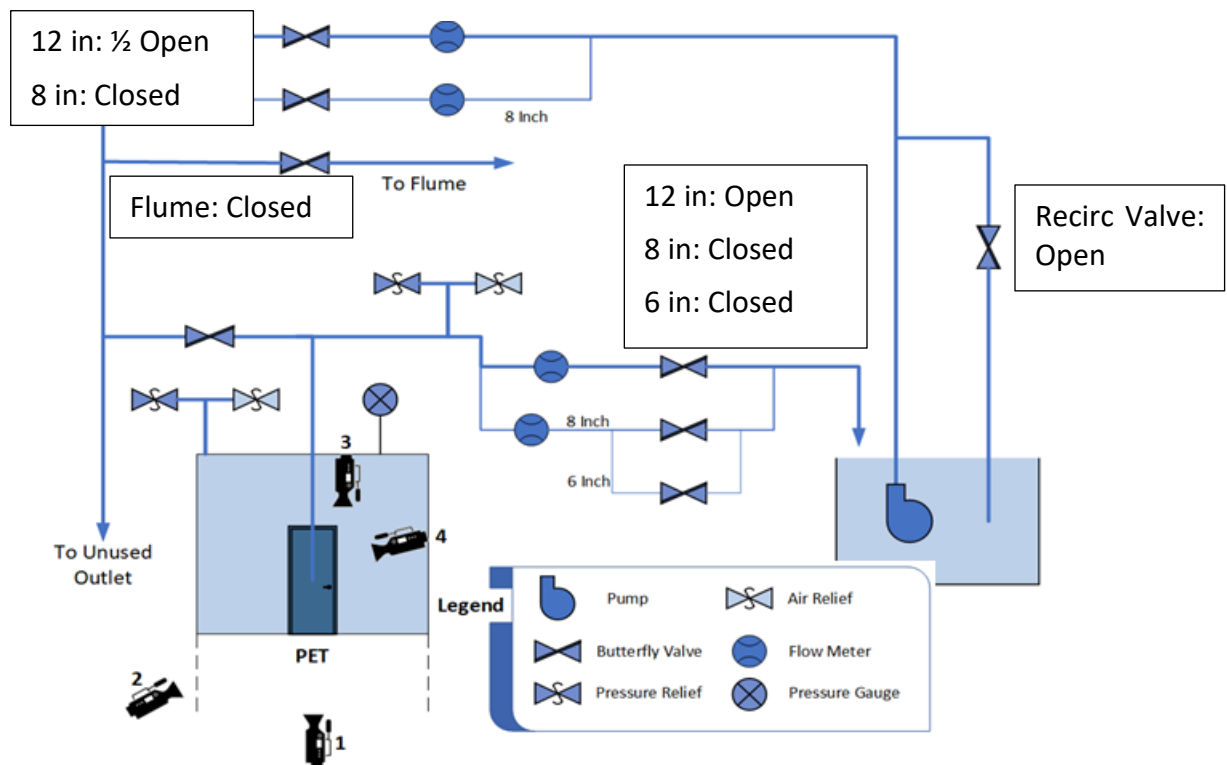


Figure 62. Steel Door Experiment #9 - Initial Valve Configuration

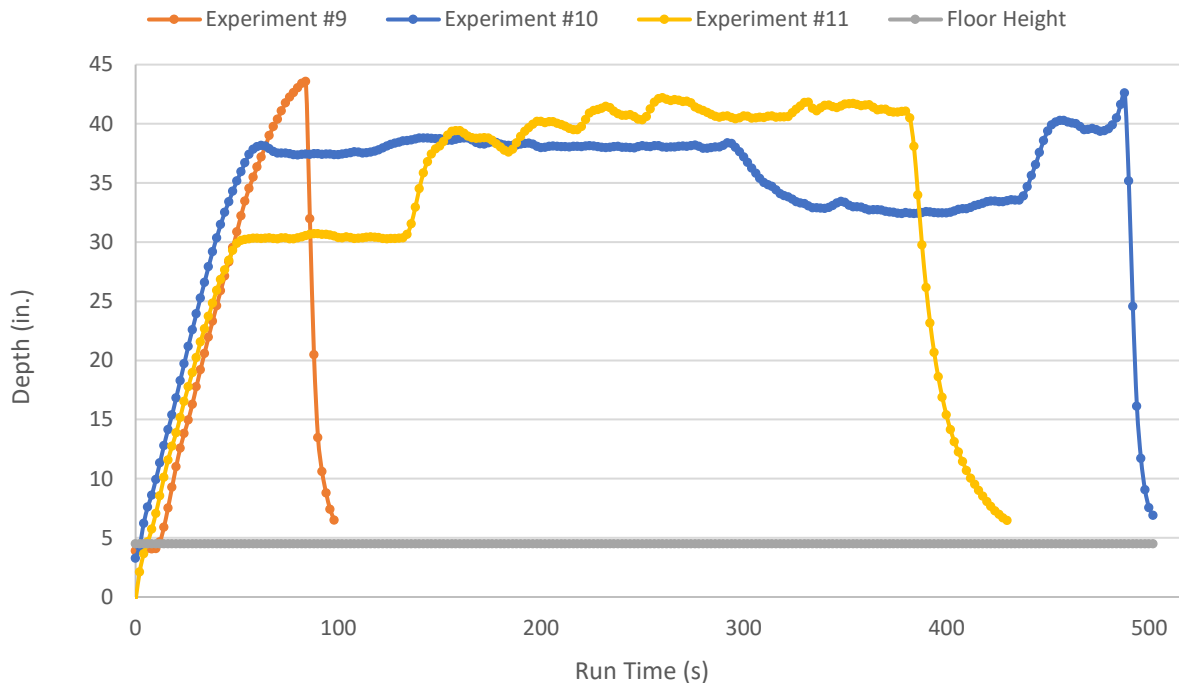


Figure 63. Steel Door Experiment #9, #10 & #11 - PET Water Height

The result of this experiment was also unexpected; the deadbolt bent when the water inside the PET reached its maximum depth, which cause the door to pop open. It is believed that the failure occurred in two stages, with each stage corresponding to the failure of a lock; this was concluded given the succession of sounds heard during the experiment; before the door popped open, two popping sounds were heard, leading to believe the first one meant the door latch failing, and the second one representing the door popping open because of the deadbolts' failure. This theory is confirmed in the following experiment, experiment #10.

Even though the door did not break or bend, the system after this experiment is considered to have failed. The locking mechanism, an integral part of any door failed, causing the door to pop open; and that is synonymous to a door rupture, in the way that both results cause the water contained in a room, to uncontrollably enter another.



Figure 64. Bent Deadbolt, Result of Experiment #9

The same analysis made to previous experiments was also made to this one; there is an almost constant water flow into the PET, and it is possible to appreciate the increase in leakage from the PET as a result of the lower net water flow into the PET.

Not mentioned before is the reason why the reading of FM1 become negative at the end of some experiments; this happens after turning down the pump; the column of water that is going up to the PET losses its forward momentum and goes back down into the reservoir through the 12 in. flowmeter. Since the flow is in the backwards direction, the flowmeter measures it as negative flow.

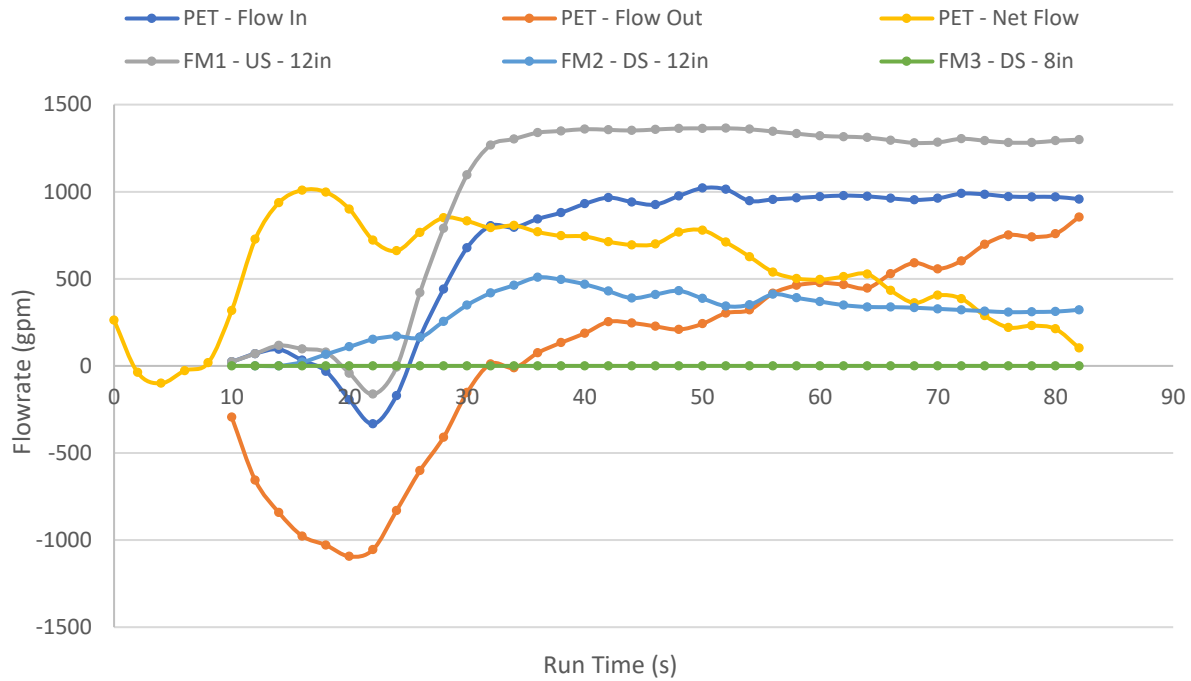


Figure 65. Steel door experiment #9 - Flow Information

The results for second experiment with the deadbolt locked are shown in Figure 63. It is possible to appreciate how much longer this experiment lasted when compared to all the previous ones. The final PET water depth achieved, on the other hand, is very close to the one obtained in experiment #9.



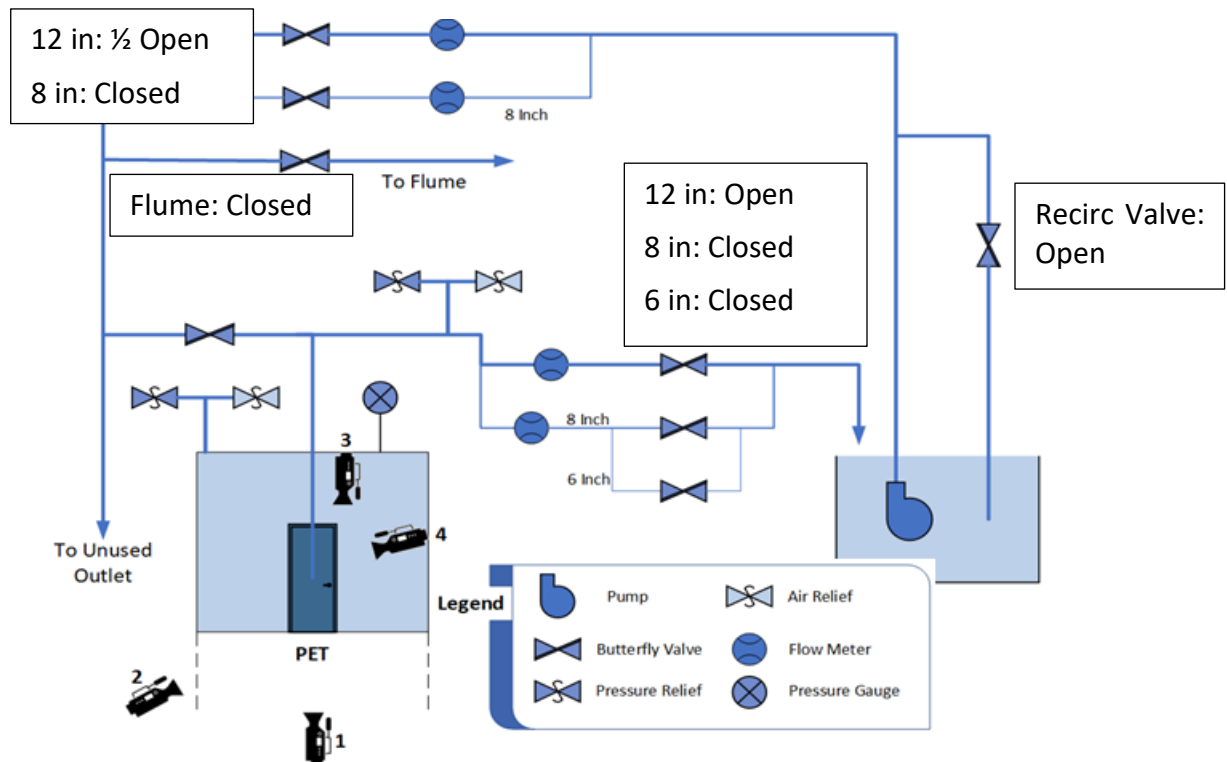


Figure 66. Steel Door Experiment #10 - Initial Valve Configuration

Unlike previous experiments, the valve configuration was not held constant throughout the experiment. The results of changing the valve configurations can be observed in Figure 63 above by the increase and decrease of the water depth inside the PET from constant spots; and in Figure 67, by the different flowrate sections in which the data can be split (observed easily in the data for FM1, which achieves a new steady-state behavior after the position of most valves is altered).

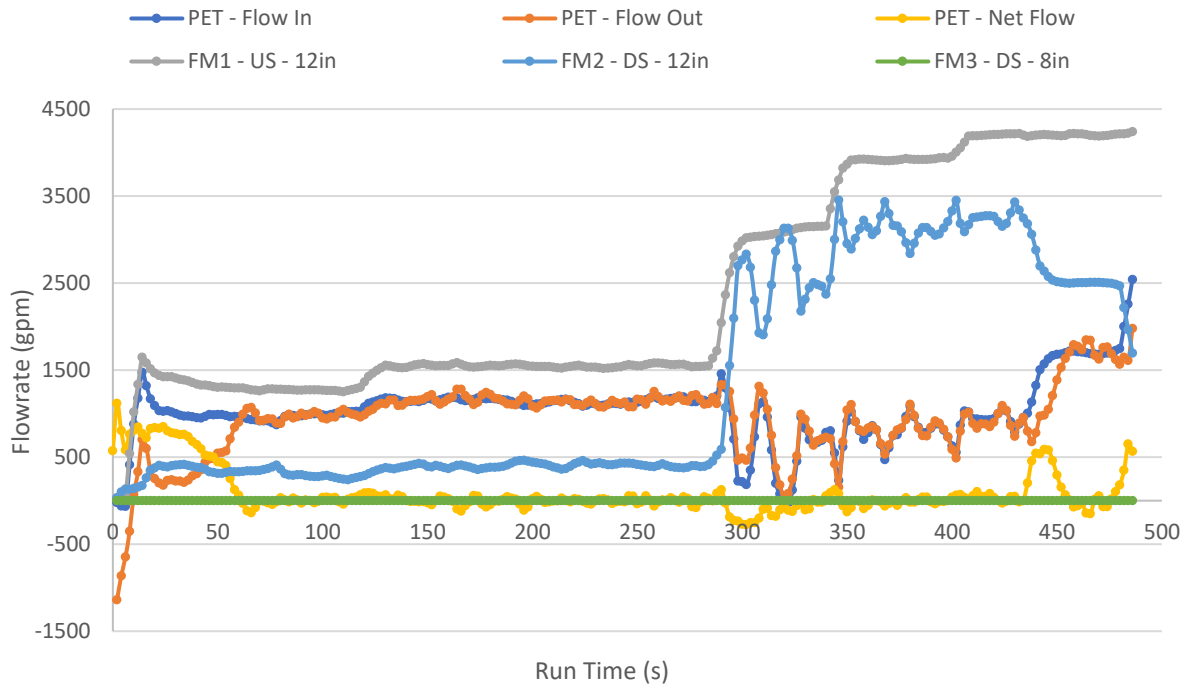


Figure 67. Steel Door Experiment #10 – Flow Information

The initial valve configuration for this experiment was the following: the recirculation valve was fully open, the upstream 12 in. valve was half-open and the downstream 12 in. valve was fully open. Because of experiment #9, it was expected that the deadbolt would bend and the door would pop open after a water depth of ~45 in. had been achieved inside the PET; however, before reaching the 40 in. mark, as seen in Figure 63, a different thing happened; the same popping noise heard in experiment #9 was also heard this time, the difference was that the deadbolt did not pop right after, instead, the bottom section of the steel door bent towards the outside, causing an increase in the water flow out of the PET, similar to what happened with the hollow-core doors, when they were tested opening outwardly.

After this unexpected event, the upstream 12 in. valve was fully opened to increase the flow towards the PET. Although the PET now had more water going in, the bending of the door meant there could also be more water going out, and the water depth inside the PET stabilized

again. The recirculation valve was then closed in three steps; it was first closed half way, then three quarters of the way, and the fully closed. Each of the effect of the steps on the upstream flow can be appreciated on the FM1 data in Figure 67 above, after run-time mark around second 300.

The increase of the upstream flow caused a decrease in the water depth inside the PET, this phenomenon was expected to occur; the increased upstream flow, also meant an increase in the upstream velocity of the water, at greater velocities, the water no longer has time to split into two separate flows when it encounters the T-joint at the top of the PET; at these high velocities, the horizontal flow entering T-joint skids through the downward pointing section of the joint, and continues to flow to the other horizontal end.

To solve this problem, and restore the flow going into the PET, the downstream 12 in. valve was closed in two steps, as seen by the FM2 data in Figure 67. First, the downstream valve was closed half way, but after the water depth inside the PET reached a level around 40 in. the flowrates into and out of the PET equalized again. The downstream 12 in. valve was then fully closed, directing the full flow of the pump towards the PET, in this case, ~4,200 gpm. This caused the water level in the PET to raise, and before it reached the 45 in. mark, just as in experiment #9, the dead bolt bent and the door popped open.



*Figure 68. Bent Deadbolt, Result of Experiment #10*

One of the main takeouts of this experiment is that it proved the versatility of the new PET piping configuration. All the improvements made to the PET were performed not only to increase the water flowrates in the system, but to have greater control over them. The execution of experiment #10 proves how the valve system can be used to direct the flow to where it is necessary.

Experiment #11 was the next one to be performed; for this experiment the door was locked in the same way as experiment#9 or experiment#10, this means both the door latch and deadbolt were locked; however, it is important to note that the deadbolt on this experiment was not the same as in the two previous ones, it was an aftermarket deadbolt acquired from a local

hardware store, and this fact may be the cause why the results of this experiment were different than the previous two.

The initial valve configuration for this experiment consisted in having the recirculation valve fully closed, the upstream 12 in. valve one-quarter-way open, and the downstream 8 in. valve fully open, note that in previous experiments the downstream 12 in. valve was open and the 8 in. one closed.

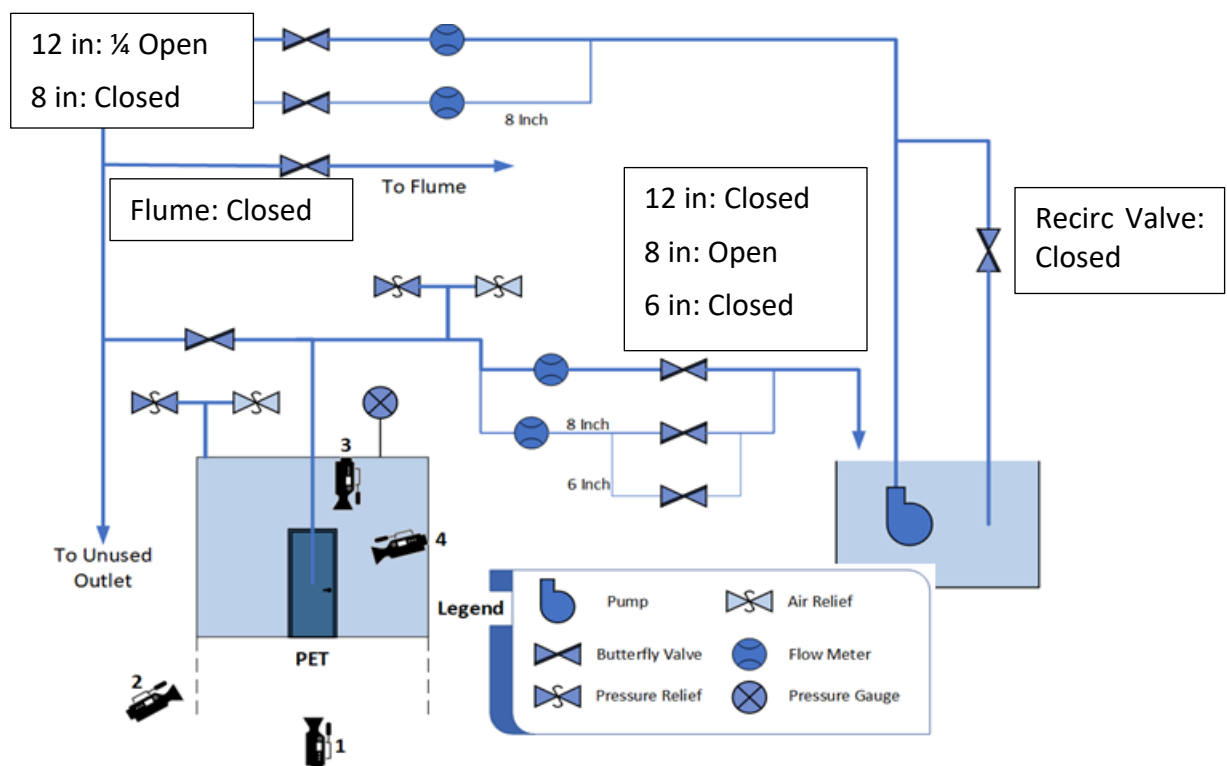


Figure 69. Steel Door Experiment #11 - Initial Valve Configuration

As in experiment #10, the configuration was not kept constant through the experiment, with the initial valve configuration, water depth inside the PET stabilized at ~30 in; see Figure 63. The upstream 12 in. valve was then fully open and the downstream 8 in. valve was progressively closed, the results in the flow conditions for the valve movements can be seen in Figure 70.

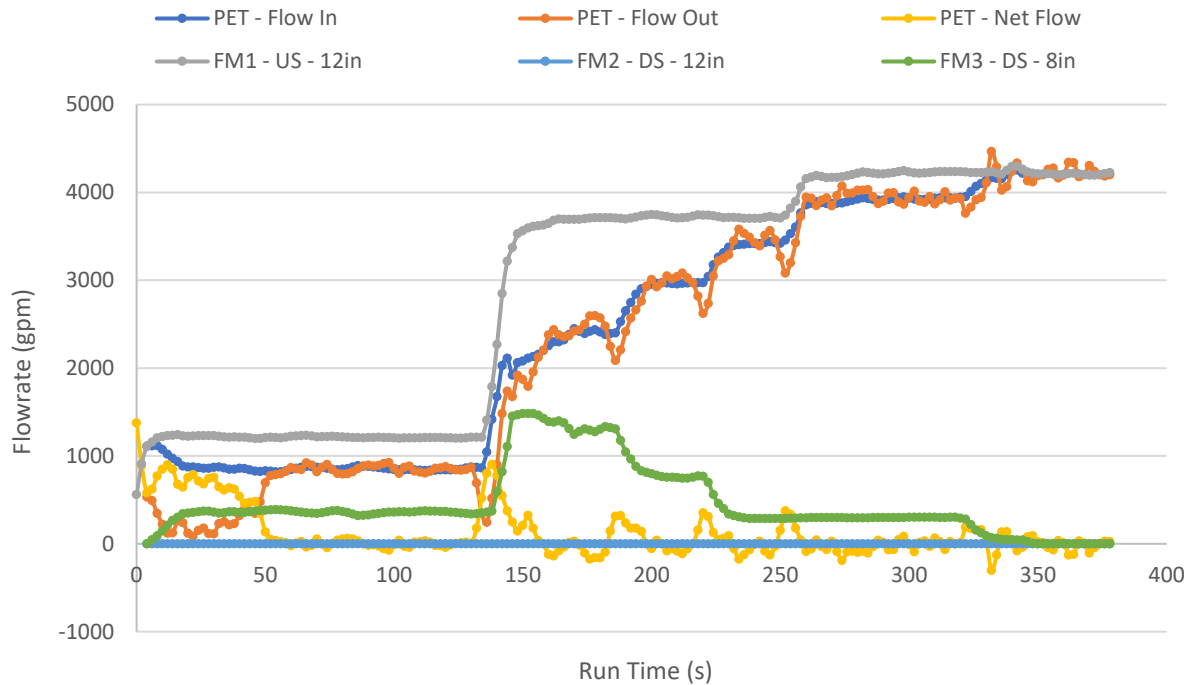


Figure 70. Steel Door Experiment #11 - Flow Information

After closing the downstream 8 in. valve though, the experiment conditions were the same ones as in experiment#10 after the downstream 12 in. valve was closed, the full flow from the pump was going into the PET; the results from experiment #11 were different than those from experiment#10. As seen in Figure 63, the tail end of the experiment#11 data is not as steep as those in the previous experiments, and the reason is that in this experiment the door did not pop open.

During experiment #11 the flow into and out of the PET reached a constant value, even when all the water from the pump was directed towards the PET. This happened because during this experiment the door suffered a permanent bend at the level of the lock. The bend is permanent because even after concluding the experiment, the curvature in the door could be easily seen, as in Figure 71.



*Figure 71. Experiment #11 - Post-Experiment Door State*

One of the causes of this unexpected results is the different dead-bolt used for the experiment, which can be seen in Figure 72. The bolt itself is longer than OEM ones, and the whole deadbolt system was assembled differently. Another possible attribute could be fatigue of the door itself, however this has not been tested and is only an assumption.



*Figure 72. Deadbolt Comparison - Experiments #9 #10 left, Experiment #11 right*

The importance of this experiment relies on two factors; it shows than steel door can be permanently bent, at water depths not much different than those that cause the bending of the hollow-core doors in the first experiments, and it also shows together with experiments #9 and #10, that it is a combination of the door material and its locking components, and not only the door material that will cause the biggest effects on the results.

Experiment #12 is the last one to have been performed thus far. It was performed with a similar initial valve configuration as experiments #4, #5 & #6. The recirculation valve was open, the upstream 12 in. valve was one quarter open, and the downstream 8 in. valve was also open. Note than in the previously mentioned experiments, the downstream 8 in. valve was closed, while the downstream 12 in. valve was left open.



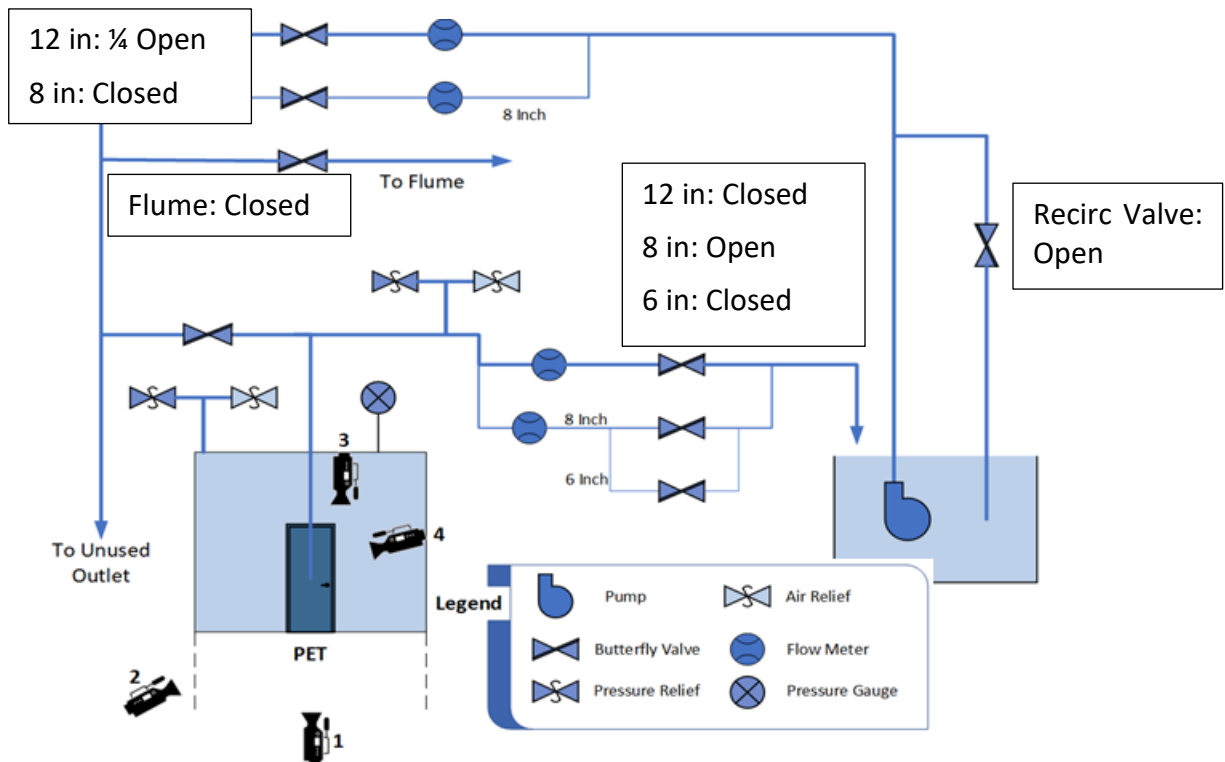


Figure 73. Steel Door Experiment #12 - Initial Valve Configuration

This experiment served two purposes. The first one was to determine whether the '0 gpm' reading of the downstream 12 in. flowmeter for experiments #4, #5 & #6 was due to extremely low flows, below the threshold of the 12 in. flowmeter; the experiment allowed this verification due to the same initial upstream valve configuration, while using the 8 in. downstream flowmeter which is capable of reading lower flowrates. The second objective of this experiment was to confirm whether the water depth achieved in experiment #1, which was higher than all other experiments performed with the open deadbolt, was either an anomaly or was caused because that test was the first one to be performed; this could be verified since the door and latch used for this test were brand new, and of the same model as in experiment #1.

The results showing the water depth achieved in this experiment are shown in Figure 74, and the flowrate analysis is shown in Figure 75. The spike at the end of both figures corresponds to the change of the upstream 12 in. valve to half-way open.

The deepest water level in experiment #12 corresponds to 44.5 in, which is 3.6% lower than that of experiment #1, 46.1 in; but ~19% higher than the depth achieved from experiment #2 through experiment #8. This leads to conclude that the water depth achieved in experiment #1 was related to it being the first experiment rather than an anomaly; although further testing with the same latch and door could be used to further prove this point.

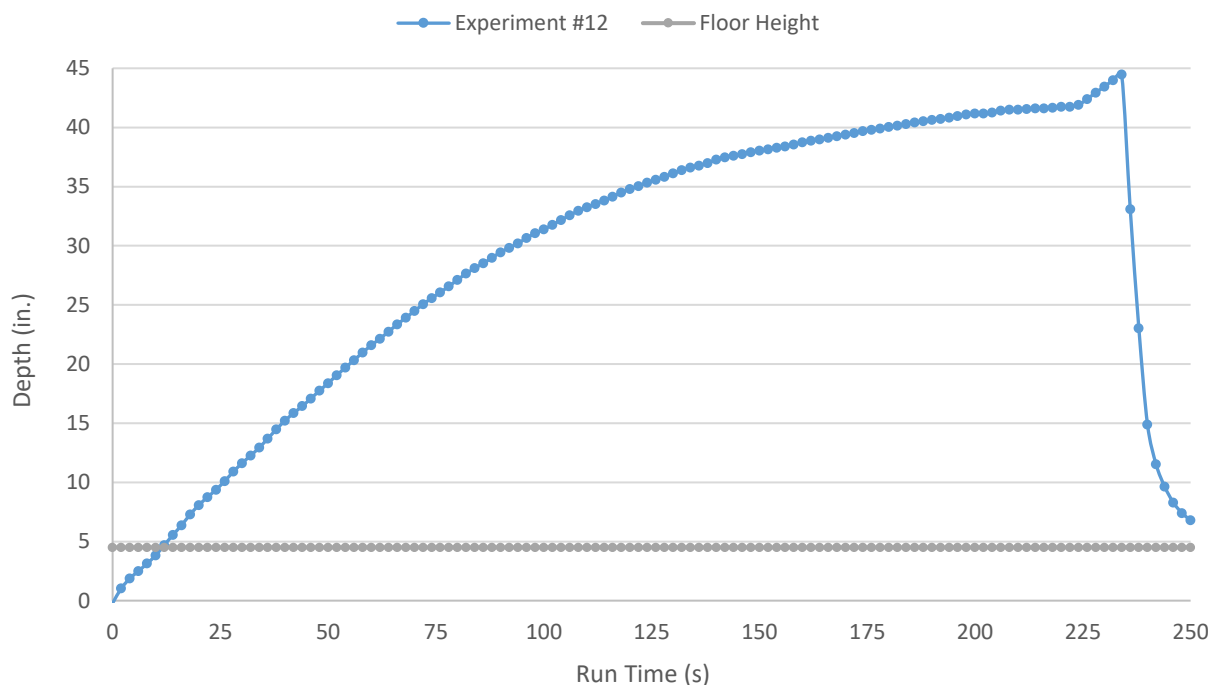


Figure 74. Experiment #12 - PET Water Height

One of the trendlines in Figure 75, shows the readings produced the 8 in. downstream flowmeter. It can be observed how the readings are '0 gpm' for duration of the experiment while the upstream 12 in. valve was open one quarter of the way. This can be used to assert than in

this configuration, there is either no water flowing through the downstream section of the PET or the flowrate through this section is below ~10 gpm, which is the cutoff flowrate for the 8 in. OIML Class 49 flowmeter (ABB, 2017).

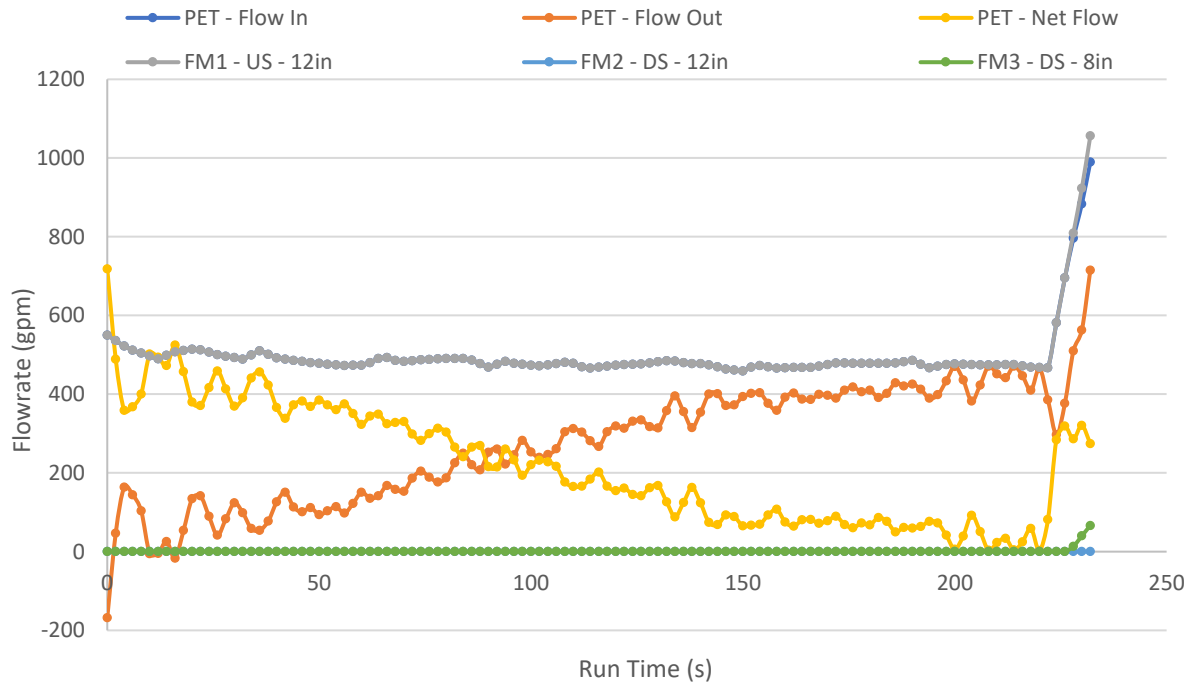


Figure 75. Steel Door Experiment #12 - Flow Information

## Data Processing Analysis

After performing all the experiments, the data processing method for the PET water depth measurements described in page 57, was compared against two other data processing methods. The two new methods consisted in first, using the raw depth data to calculate the Fill Rate and Leak Rate from the PET, and second, using a similar three point running average to the previously selected method, but this time using a uniform weight for all three points.

This analysis was performed on the results from steel doors experiments, specifically experiment #10, Figure 76 & Figure 77, and experiment #11, Figure 78 & Figure 79. That way the analysis would be performed in experiments that resulted in the door popping open right after the maximum water depth was achieved, and in an experiment in which the maximum water depth did not cause the door to pop open.

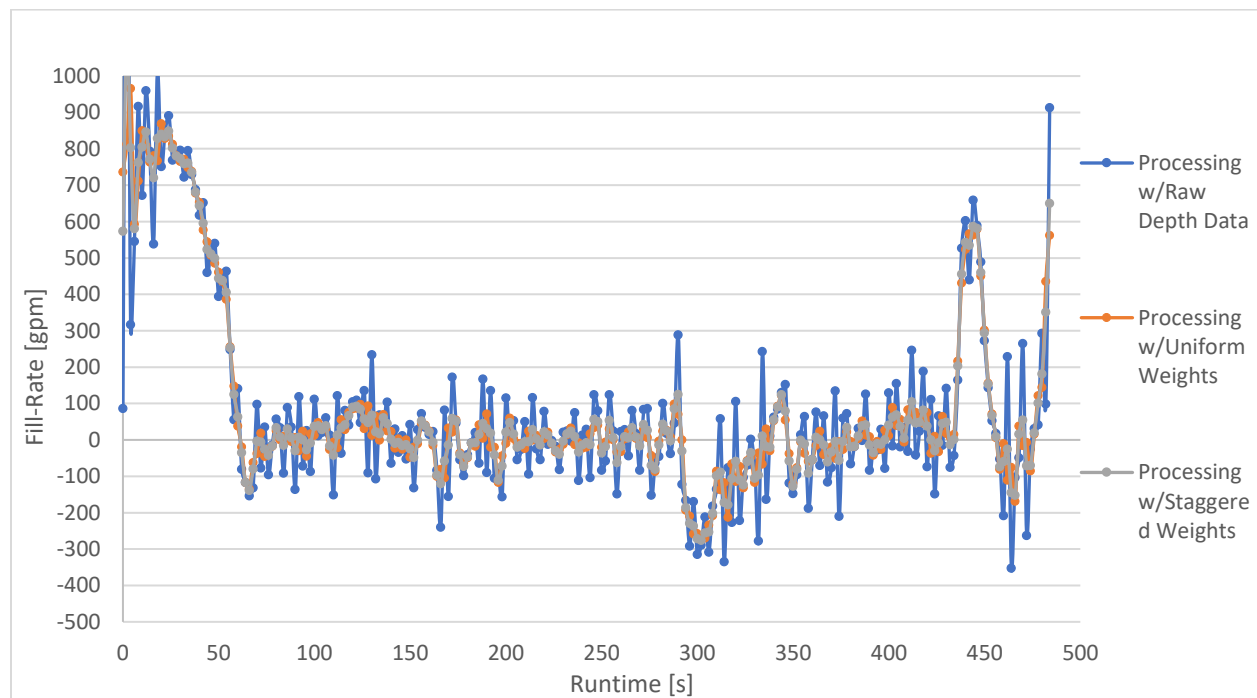


Figure 76. Steel Door Experiment #10 - Fill Rate Data-Processing Methods Comparison

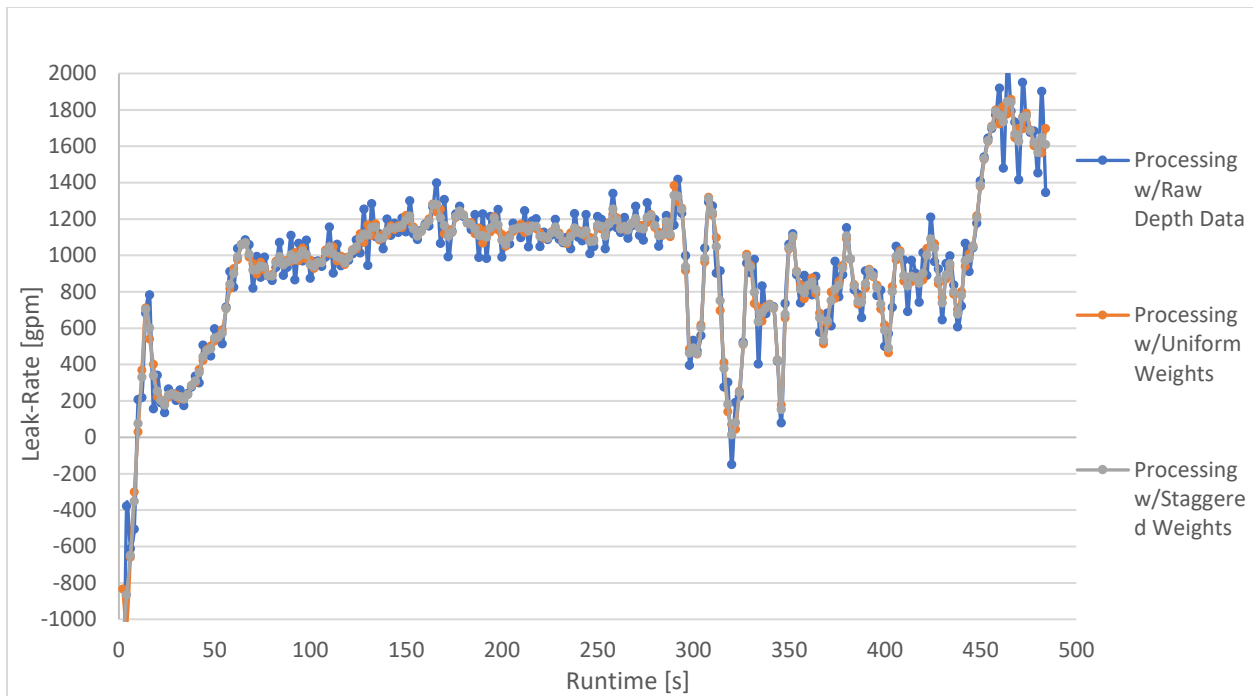


Figure 77. Steel Door Experiment #10 - Leak Rate Data-Processing Methods Comparison

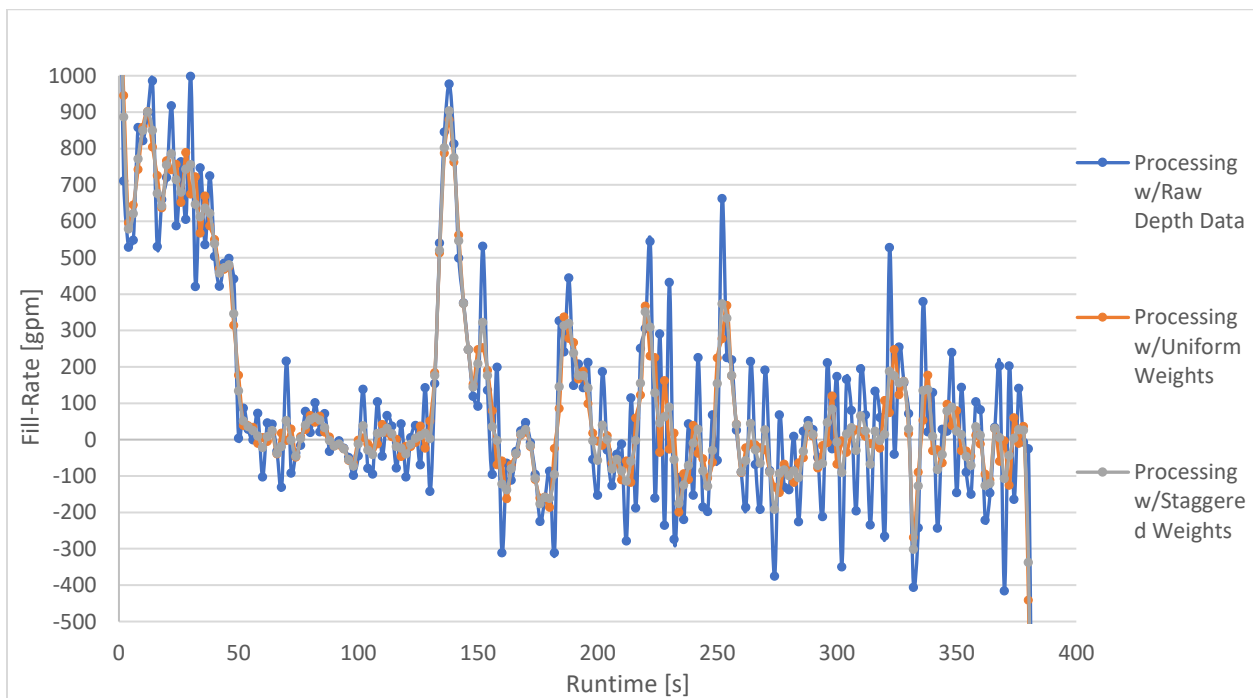


Figure 78. Steel Door Experiment #11 - Fill-Rate Data Processing Methods Comparison

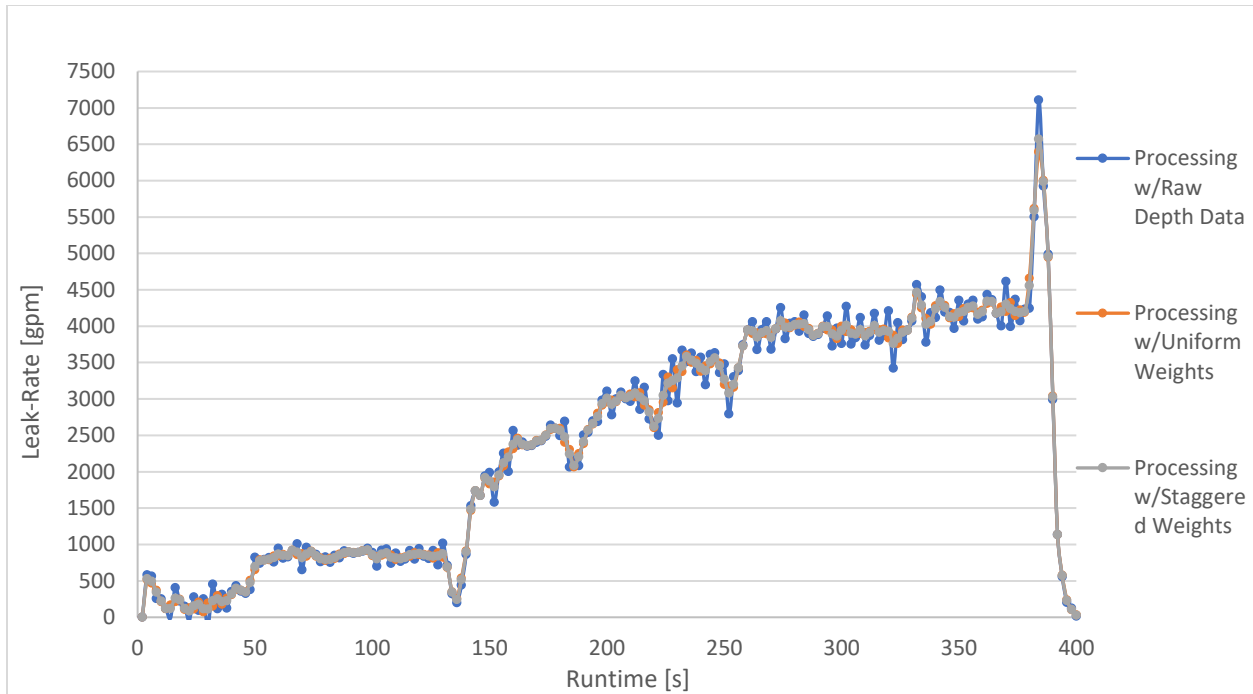


Figure 79. Steel Door Experiment #11 - Leak-Rate Data Processing Methods Comparison

As seen in the previous figures that show the comparison between results obtained for the different data processing methods, it is possible to observe how the two methods that use a three-point running average produce an observable smoothing of the data. The smoothing effect was quantified using an average and stand deviation of the data. The quantification was performed on the depth measurements, and leak rate and fill rate calculations.

The results of the quantifications are displayed on Table 5 and Table 6. The important results to note from the tables are the following:

- The average depth remains within 0.1 in. for all data processing methods, with a standard deviation with a difference of less than 1% between them all; this leads to conclude that the two data processing methods closely approximate the raw data behavior.

- All the standard deviation calculations for the three-point running average with uniform weights are always the lowest; this leads to the conclusion that this method is the one that smooths the data the most.
- The maximum and minimum data points, for the fill rate and leak rate calculations using the three-point running average with staggered weights, are closer to the maximum and minimum data points of those same calculations using the raw data, than the maximum and minimum data points of those calculations using the three-point running average with uniform weights; this leads to conclude that while the later methods smooths data the most, the first one is able to most closely approximate the behavior of the system quantified using the raw data.

Table 5. Steel Door Experiment #10 - Quantification of Results from Different Data Processing Methods

		<b>Raw Data</b>	<b>Uniform Weights</b>	<b>Staggered Weights</b>
<i>Depth</i>	Average	34.38	34.39	34.38
	Standard Dev.	7.34	7.29	7.30
	Max.	42.90	42.61	42.61
	Time of Max	488	488	488
<i>Fill Rate</i>	Average	8.33	8.33	8.33
	Standard Dev.	724.94	645.28	650.06
	Max.	2036.13	965.87	1118.70
	Time of Max.	2	4	2
<i>Leak Rate</i>	Min	-8441.71	-5071.39	-5345.73
	Time of Min.	490	488	490
	Average	1034.49	1053.45	1036.09
	Standard Dev.	938.72	862.34	869.51
	Max.	11426.31	8001.82	8330.33
	Time of Max.	490	490	490
	Min	-2056.56	-1027.16	-1139.13
	Time of Min.	2	4	2

Table 6. Steel Door Experiment #11 - Quantification of Results from Different Data Processing Methods

		<b>Raw Data</b>	<b>Uniform Weights</b>	<b>Staggered Weights</b>
<i>Depth</i>	Average	32.68	32.67	32.67
	Standard Dev.	10.94	10.93	10.93
	Max.	42.25	42.20	42.20
	Time of Max	260	260	260
<i>Fill Rate</i>	Average	18.09	18.09	18.09
	Standard Dev.	495.48	459.01	462.93
	Max.	1596.95	1301.49	1375.35
	Time of Max.	0	0	0
<i>Leak Rate</i>	Min	-2903.06	-2463.41	-2443.14
	Time of Min.	384	386	386
	Average	2420.40	2450.45	2420.02
	Standard Dev.	1574.29	1561.70	1563.14
	Max.	7105.77	6395.36	6572.96
	Time of Max.	384	384	384
	Min	-129.06	31.01	26.85
	Time of Min.	30	400	400



Having performed the previous analysis, it is possible to conclude that selecting a three-point running average with staggered weights for the center and adjacent points to process the raw depth data was a good decision. Not only does the selected method is able to retain the behavior of the real system, but it also produces a smoothing effect of the data produced by the depth transducers, which then translates in a smoothing effect of the data calculated using those measurements.

## Leak Rate and Water Depth Dependency

From the experiments performed it was concluded that the main element in causing a failure of the door or its locking mechanism was the water depth achieved inside the PET. However, it is important to determine the relationship between the depth of the water column in the PET and the rate at which water is entering and leaving the tanks through the door and its frame.

Figure 80 shows the leakage rate in the hollow-core door experiments as it varies with PET water depth. It is important to note that for this figure the y-axis limits have been modified to include only the data from experiments #3 through #6 (as mentioned before the data collected in Hollow-Core Door experiment #7 was not useful). The figure shows how for experiments #3 through #5 the leakage rate increases steadily with water depth, however, the data for experiment #6 show much higher leakage rates for the same water depths as for the other experiments plotted, which points to the leakage rate depending on variables more than just the water depth.

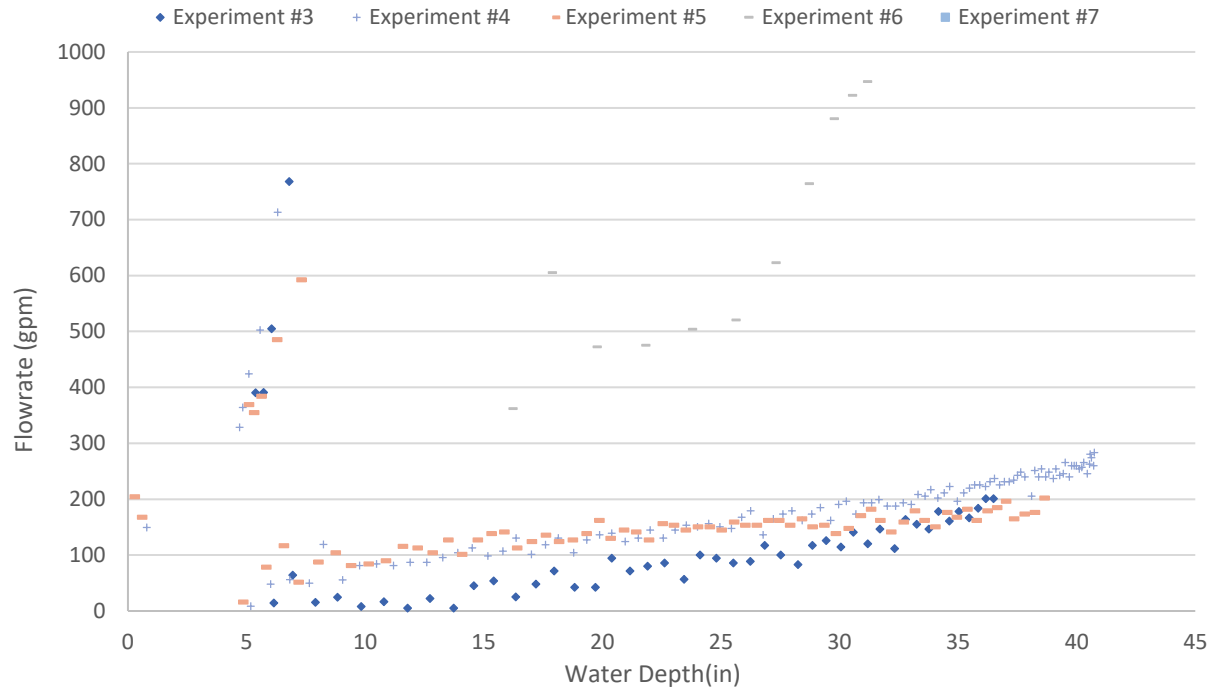


Figure 80. Hollow-Core Door Experiments - Leak Rate vs. PET Water Depth

A similar analysis was performed on the steel door experiments, however, to ease their understanding, several constraints have been placed on the results shown in Figure 81. The first constraint was to only show the values once the water depth had reached 20 in. inside the PET, this would eliminate some of the leak rate calculations categorized as noise, that happen at the beginning of most experiments. The second constraint was placed on the data itself, as the data shown only represents the leakage rate as a function of depth, until the latch from the steel door gives out, this was made as to not compare flowrates for different states of the door or its locking mechanism between themselves. Lastly, the flowrate produced by the Global Pump was included in the figure show where it stood in comparison to the leakage rates observed in the steel door experiments.

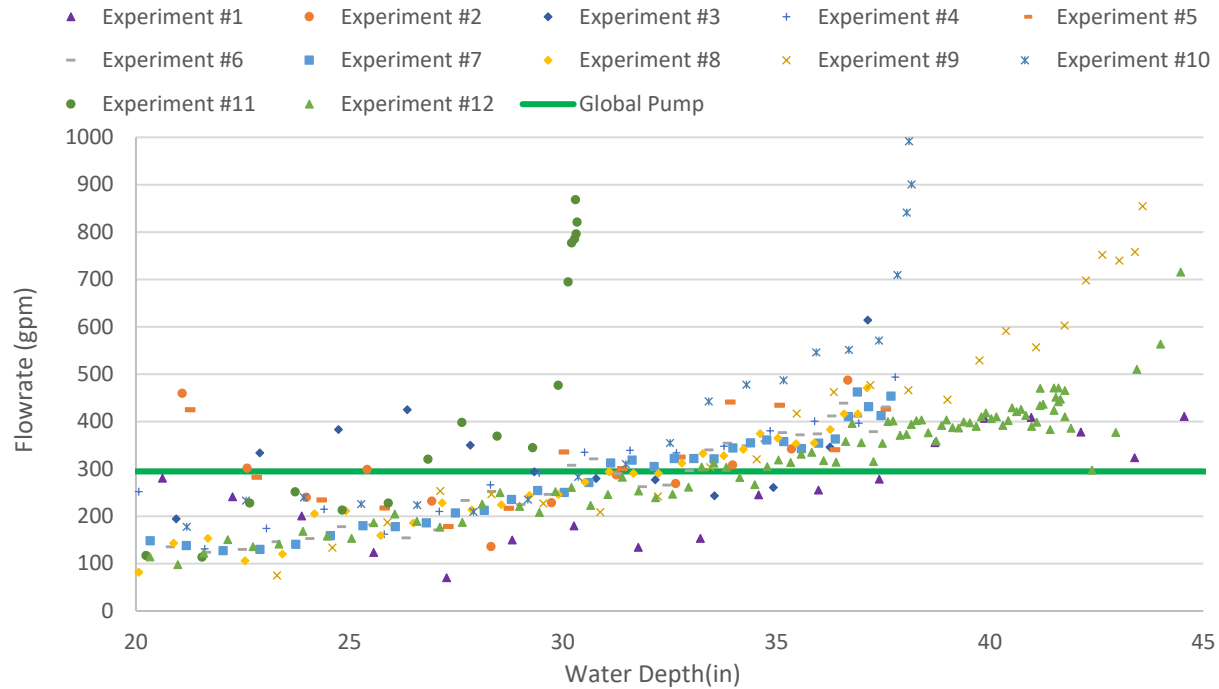


Figure 81. Steel Door Experiments - Zoomed Leak Rate vs. PET Water Depth, Global Pump Incl.

Figure 81 shows a similar behavior to that of Figure 80, the bulk of the experiments have a similar trend, with the leakage rate increasing as the water depth inside the PET does, but the data from experiment #10 and experiment #11 show at water depths of 30 in. and 37 in. respectively, much higher leakage rates than in any of the other experiments; experiment #9 shows the same trend when its results are compared to those from experiment #1 and experiment #12. The data from these three experiments supports the previous statement, the leakage rate from the system does not depend only on the water depth inside the PET.

Finally, from the inclusion of the Global Pump maximum flowrate, it can be inferred that if the Global Pump was the one used to feed water to the PET in these experiments, no type of failure would be achieved in any of them. Figure 81 shows how after a water depth of 35 in. has been reached, the leakage rate in most of the experiments, was above the maximum possible

flowrate of the pump. This strengthens the idea that failure of a system will be mostly dependent on the depth of the water column than in any other variable.

The last analysis to be made corresponds to the effect the smoothing effects have on the depth measurements and leakage calculations once the system has failed. The systems to be compared are again those from experiment #10 and experiment #11. Those experiments are selected given their end results; experiment #10 ended with an abrupt opening of the door due to the failure of the latch and deadbolt; while experiment #11 ended with door still locked in place due to the deadbolt, but permanently bent, which caused a slower leakage rate.

Figure 82 and Figure 83 show the different water depths, measured directly from the depth sensors, and calculated by the data-processing methods described at the beginning of this section, available from steel door experiments #10 and #11, right after the water depth inside the PET achieved its maximum value, and caused the failure of the system. The CS451 data corresponds only to the data from the Campbell Scientific depth pressure transducer, and the OLVU 800 data corresponds only to the data from the Omega depth pressure transducer. The data labeled as 'Final', corresponds to the averaged data of the two sensors, whether it is the average of their raw measurements, or the average after the measurements have been processed.

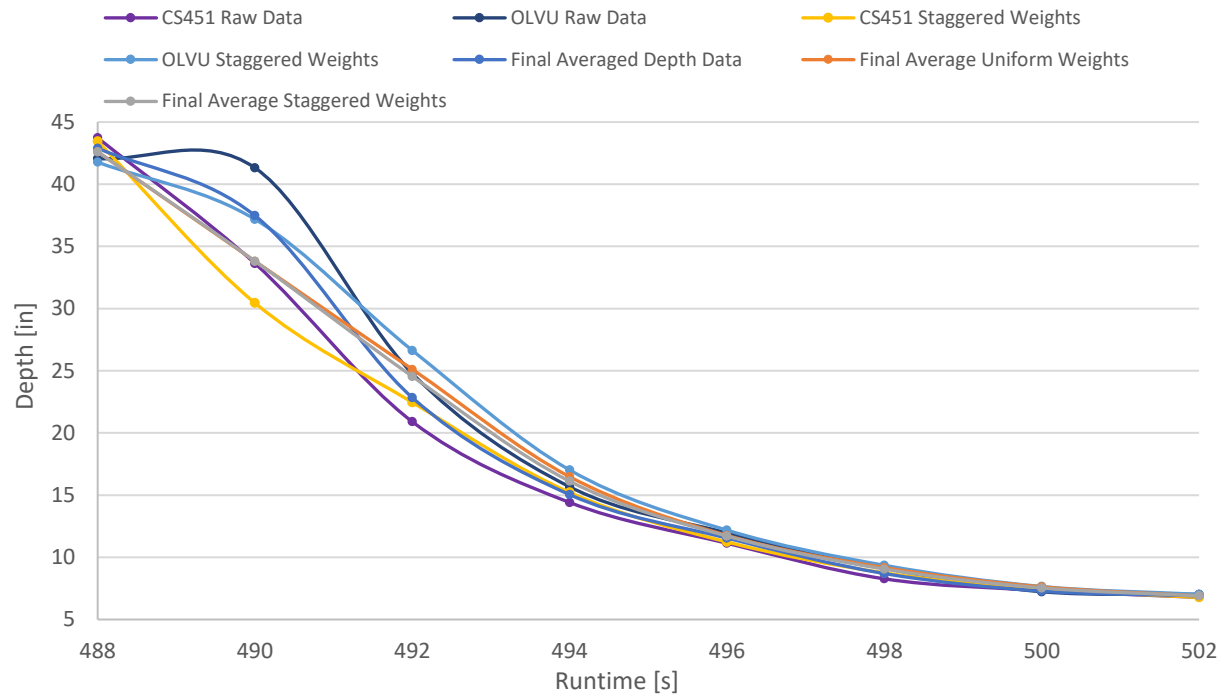


Figure 82. Steel Door Experiment #10 - Depth Data Comparison

In Figure 82 it is possible to observe how the second reading of the Omega sensor does not match the one from the CampBell Scientific one. The disparity already has been explained, but in this case, it is possible to observe how much it affects the calculation of the final depth measurements. Taking the raw CS451 measurements as the reference, since that sensor is the one with the highest accuracy, it is also possible to observe how the trendline 'Final Average Staggered Weights', which represents the selected method for data-processing, is the one that closes replicates the raw data behavior.

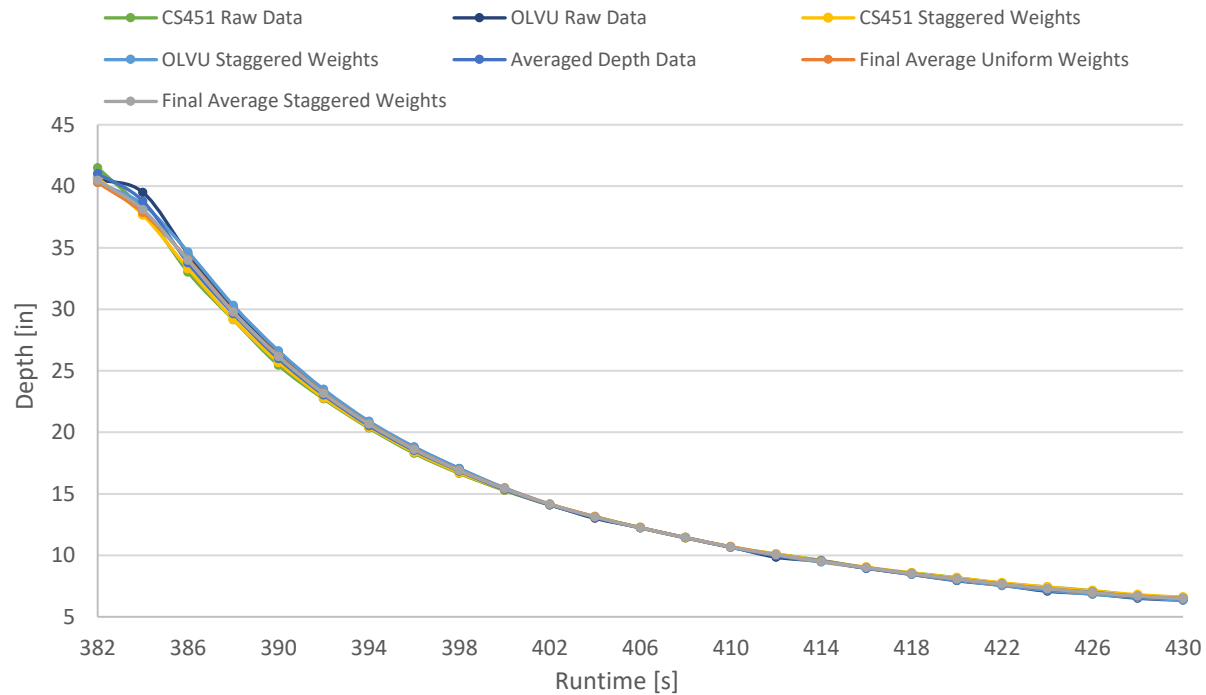


Figure 83. Steel Door Experiment #11 - Depth Data Comparison

Taking a look at Figure 83, it is possible to observe how the difference between the readings from the Campbell Scientific sensor and the Omega sensor are much smaller in experiment #11. In this experiment, the leakage rate did not increase rapidly when the system failed because the door did not pop open, which caused the water in the PET to drain at a slower pace. The fact in the slow depth changing conditions the disparity between the measurements from both sensors is acceptable, leads to the Omega sensor is mostly affected in rapid changing conditions.

A quantification of the difference between each of the depth measurements and the selected method is available in Table 7 and

Table 8 for the results from experiment #10 and #11, respectively.

Table 7. Steel Door Experiment #10 - Depth Data Analysis Comparison

Depth Data Analysis															
Time St.	Sel. Depth	Raw Data						3-Point Average							
								Staggered Weights						Uniform Weights	
		CS 451	% Diff.	OLVU 800	% Diff.	Fin. Av. Depth	% Diff.	CS 451	% Diff.	OLVU 800	% Diff.	Fin. Depth	% Diff.	Fin. Depth	% Diff.
488	42.61	43.73	2.64	42.1	-1.27	42.90	0.69	43.44	1.97	41.77	-1.97	42.61	0.00	42.61	0.00
490	35.17	33.63	-4.38	41.3	17.47	37.47	6.55	30.45	-9.96	37.18	9.96	33.81	0.00	33.81	-2.18
492	24.55	20.90	-14.86	24.8	0.94	22.84	-6.96	22.46	-8.50	26.63	8.50	24.55	0.00	25.12	2.32
494	16.12	14.41	-10.59	15.7	-2.78	15.04	-6.68	15.21	-5.61	17.02	5.61	16.12	0.00	16.48	2.23
496	11.71	11.13	-4.94	12.0	2.22	11.55	-1.36	11.24	-4.04	12.18	4.04	11.71	0.00	11.76	0.45
498	9.06	8.27	-8.68	9.1	0.72	8.70	-3.98	8.75	-3.36	9.36	3.36	9.06	0.00	9.18	1.33
500	7.54	7.34	-2.73	7.2	-4.10	7.28	-3.42	7.43	-1.48	7.65	1.48	7.54	0.00	7.63	1.14
502	6.90	6.78	-1.78	7.0	1.78	6.90	0.00	6.78	-1.78	7.03	1.78	6.90	0.00	6.90	0.00



Table 8. Steel Door Experiment #11 - Depth Data Analysis Comparison

Depth Data Analysis															
Time St.	Time St.	Time St.						Time St.							
								Stagg. Weights						Stagg. Weights	
		CS 451	% Diff.	OLVU 800	% Diff.	Fin. Av. Depth	% Diff.	CS 451	% Diff.	OLVU 800	% Diff.	Final Depth	% Diff.	Final Depth	% Diff.
382	40.48	41.50	2.51	40.6	0.20	41.03	1.36	40.66	0.44	40.31	-0.44	40.48	0.00	40.30	-0.45
384	38.09	38.08	-0.04	39.5	3.70	38.79	1.83	37.67	-1.12	38.52	1.12	38.09	0.00	37.86	-0.61
386	33.98	33.01	-2.87	34.5	1.54	33.76	-0.66	33.31	-1.98	34.66	1.98	33.98	0.00	34.06	0.22
388	29.75	29.15	-2.02	30.1	1.21	29.63	-0.40	29.19	-1.88	30.31	1.88	29.75	0.00	29.79	0.13
390	26.16	25.45	-2.70	26.5	1.36	25.98	-0.67	25.69	-1.78	26.62	1.78	26.16	0.00	26.21	0.22
392	23.15	22.71	-1.89	23.4	0.90	23.03	-0.49	22.80	-1.49	23.49	1.49	23.15	0.00	23.18	0.16
394	20.66	20.34	-1.54	20.7	0.40	20.54	-0.57	20.42	-1.15	20.90	1.15	20.66	0.00	20.70	0.19
396	18.61	18.29	-1.70	18.7	0.76	18.52	-0.47	18.39	-1.15	18.82	1.15	18.61	0.00	18.63	0.16
398	16.88	16.65	-1.39	17.0	0.92	16.85	-0.23	16.72	-1.00	17.05	1.00	16.88	0.00	16.90	0.08
400	15.40	15.27	-0.84	15.4	-0.10	15.33	-0.47	15.32	-0.53	15.48	0.53	15.40	0.00	15.42	0.16
402	14.15	14.08	-0.49	14.1	-0.23	14.10	-0.36	14.14	-0.04	14.15	0.04	14.15	0.00	14.17	0.12
404	13.12	13.14	0.16	13.0	-0.89	13.07	-0.36	13.15	0.20	13.09	-0.20	13.12	0.00	13.14	0.12
406	12.24	12.22	-0.19	12.3	0.08	12.24	-0.05	12.25	0.08	12.23	-0.08	12.24	0.00	12.25	0.02
408	11.44	11.43	-0.07	11.4	-0.12	11.43	-0.10	11.43	-0.05	11.44	0.05	11.44	0.00	11.44	0.03
410	10.68	10.65	-0.29	10.7	-0.07	10.66	-0.18	10.71	0.25	10.65	-0.25	10.68	0.00	10.69	0.06
412	10.04	10.10	0.60	9.8	-1.93	9.97	-0.66	10.11	0.70	9.97	-0.70	10.04	0.00	10.06	0.22
414	9.51	9.59	0.86	9.5	0.01	9.55	0.44	9.57	0.60	9.45	-0.60	9.51	0.00	9.49	-0.15
416	8.99	8.98	-0.16	8.9	-0.61	8.96	-0.39	9.03	0.39	8.96	-0.39	8.99	0.00	9.01	0.13
418	8.51	8.57	0.72	8.4	-0.71	8.51	0.01	8.58	0.78	8.44	-0.78	8.51	0.00	8.51	0.00
420	8.07	8.18	1.40	7.9	-1.69	8.06	-0.15	8.16	1.21	7.97	-1.21	8.07	0.00	8.07	0.05
422	7.65	7.73	1.02	7.6	-1.08	7.65	-0.03	7.77	1.50	7.54	-1.50	7.65	0.00	7.65	0.01
424	7.29	7.42	1.88	7.1	-2.89	7.25	-0.50	7.43	1.91	7.15	-1.91	7.29	0.00	7.30	0.17
426	6.97	7.13	2.31	6.9	-1.40	7.00	0.45	7.10	1.96	6.83	-1.96	6.97	0.00	6.96	-0.15
428	6.68	6.74	0.84	6.5	-2.56	6.62	-0.86	6.80	1.79	6.56	-1.79	6.68	0.00	6.70	0.29
430	6.47	6.60	1.87	6.4	-1.87	6.47	0.00	6.60	1.87	6.35	-1.87	6.47	0.00	6.47	0.00

Although the three-point running average method used to smooth the data is able to closely replicate the behavior of the water depth inside the PET, even after a system fails; the data-processing method is not able to properly match the behavior of the leakage rate.

As seen in Figure 84 and to a lesser degree in Figure 85, the data analysis methods fall short in calculating the leakage rates, the instant after the water depth in the PET starts

decreasing. As explained above, steel door experiment #10 is one of the experiments affected by the disparity in the depth sensors recording of the water level inside the PET, once the system fails; Figure 84 shows how that disparity affects the leakage rate calculation during the initial seconds after the system fails.

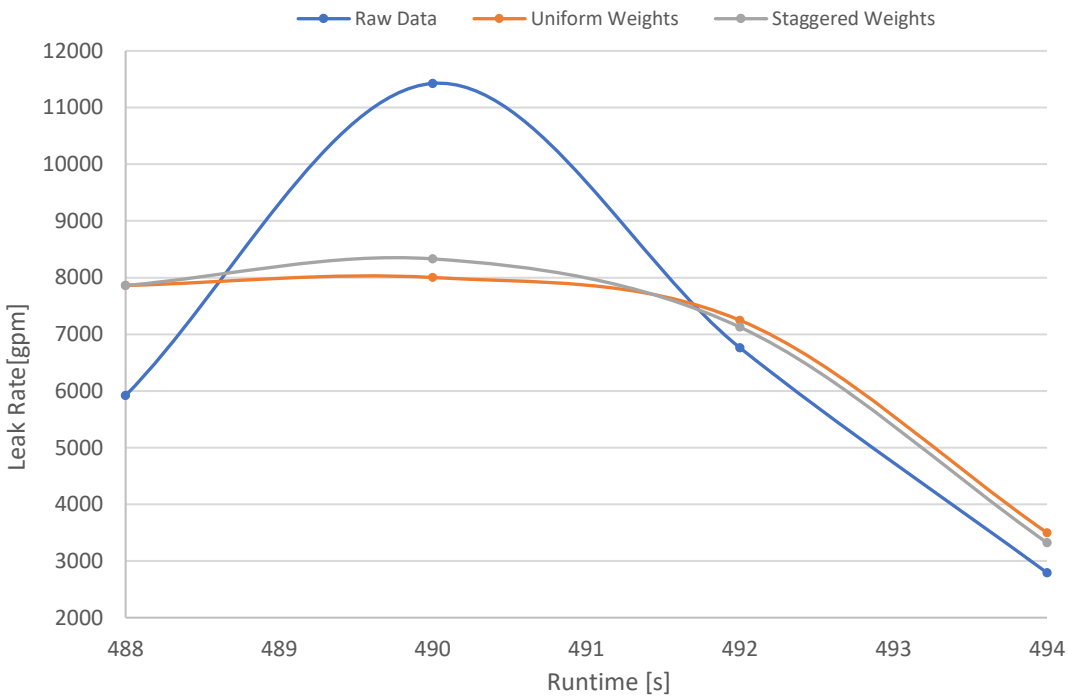


Figure 84. Steel Door Experiment #10 - Leak Rate Analysis Comparison

In experiment #11, as already mentioned, the disparity in depth measurements at the instant the water level in the PET starts decreasing is not as high in magnitude, as the one in experiment #10, this leads to a smaller difference between the leakage rate calculated using the raw depth measurements, and the leakage rate calculated using the three-point running average method, see Figure 85. It is also important to note how for experiment #11, even after the initial difference between the leakage rate different calculation methods; all three methods quickly converge to the same values for the remaining time steps.

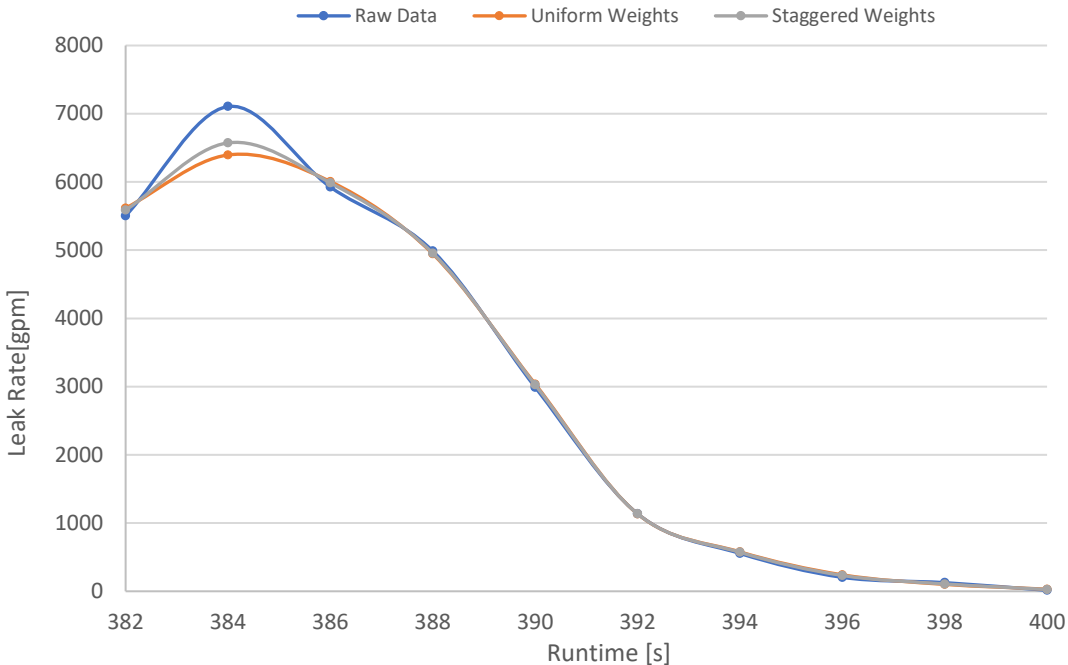


Figure 85. Steel Door Experiment #11 - Leak Rate Analysis Comparison

From all the analysis made, it can be said that further processing data of the data is still needed. The current data-processing method successfully follows the system real depth behavior while also smoothing the data, but more work needs to be done to be avoid the depth disparity present between both sensors in moments where the depth of the tank is susceptible to quick changes; since those moments appear to be the ones that greatly affect the measurements done by the Omega depth sensor, and that ultimately translate to the leakage rate calculations.

It must be noted that the difference between leakage rates may also be exacerbated by the 'Fill-Rate' measurements. As explained in the section Experiments starting on page 57, the depth data is used to calculate the PET filling rate, which in turn is used to calculate the leakage rate. The leakage rate is being indirectly affected by the disparity in the depth measurements.

## Summary and Conclusions

Table 9 and Table 10 show a summary of all the flooding experiments performed in the PET so far. It can be seen how the water levels achieved inside the PET, which are the main cause of failure of the system being tested remain similar across all experiments, including the tests on hollow-core doors. The two main differences are as already mentioned the failure states and the water flowrates into the PET.

In the steel door experiments, flowrates at least twice of those achieved with the Global pump were necessary to achieve failure of the locking mechanism in metal doors, although this shows the dependability of steel doors, it also shows how they will allow greater leakage amounts than hollow-core doors, in events with higher water flowrates. It will depend on the experimenters, whether failure of a system will be based only on the final state of the door and its locking mechanism, or if leakage rates will also be considered.

Table 9. Summary of Results from PET Steel Door Experiments

	Experiment Number											
	Steel Door											
	Opening Out											
	1	2	3	4	5	6	7	8	9	10	11	12
Max. Depth [in]	46.1	39.0	37.1	37.8	37.5	37.6	37.7	37.1	43.6	42.6	42.2	44.5
Max. Ave [in]	38.74								42.80			
Std. Dev [in]	2.84								0.58			
Flow into PET [gpm]	1148	1130	1120	979	1133	604	593	598	949	2790	3858	975
Result	Door Popped Open								Deadbolt Bent. Door Popped Open		Dead-bolt & Door Bent	Door Popped Open
Notes	Deadbolt Unlocked, Varying Valve Configurations								Deadbolt Locked, Varying Valve Configuration			
Recirc Valve	Open	Open	Open	Open	Open	Open	Open	Open	Open	Open - Closed	Closed	Open
Up 12 in. Valve	Open	Open	Open	½ Open	¾ Open	¼ Open	¼ Open	¼ Open	½ Open	½ Open - Open	¼ Open - Open	¼ Open - ½ Open
Do 12 in. Valve	Open	Open	Open	Open	Open	Open	Open	Open	Open	Open - Closed	Closed	Closed
Do 8 in. Valve	Closed	Closed	Closed	Closed	Closed	Closed	Closed	Closed	Closed	Closed	Open - Closed	Open

Table 10. Summary of Results from PET Hollow Core Door Experiments

	<b>Experiment Number</b>						
	<b>Hollow-Core Door</b>						
	<b>Opening Out</b>			<b>Opening In</b>			
	<b>1</b>	<b>2</b>	<b>3</b>	<b>4</b>	<b>5</b>	<b>6</b>	<b>7</b>
<b>Max. Depth[in]</b>	23.3	42.5	36.5	40.7	38.8	32.2	43.0
<b>Max. Ave[in]</b>		39.47		39.76		37.59	
<b>Std. Dev[in]</b>		2.98		0.98		5.44	
<b>Flow into PET[gpm]</b>	290	287	293	290	294	1038	837
<b>Result</b>	Door not failed	Broken Door					
<b>Notes</b>		Plywood Plate				Flygt Pump	

From the experiments performed, several conclusions can be determined:

The capabilities of the PET have been successfully upgraded; the PET was successfully connected to a bigger more powerful pump, capable of providing flowrates up to 14 times higher than in the previous configuration. The piping network around the PET can also be utilized to modify the water flowrate directed towards the PET at will of the experimenters.

The experiments show that improvements can be made in the instrumentation area, specifically the flowmeters. As already discussed the flowmeters are connected in a multi-drop configuration, which has been shown to increase the time interval at which sampling for data

occurs. New HART modems have already been acquired to have each flowmeter connect to the computer through a point-to-point connection, however, this method has not been applied yet, but once it is, data should be collected to find out if the solution was successful.

The depth sensors were shown to produce inconsistent results in steel door experiments, at the moment the system failed. The Omega sensor records a water depth inside the PET noticeably higher than the Campbell Scientific sensor. The cause of the disparity in measurements is not yet known but should be found and fixed; if the cause is not found, then a solution must be studied to prevent the current skewing that the first data point recorded after the system failure is currently occurring.

A way to directly measure the leakage from the system or the water flowrate into the PET is also necessary. A way to directly measure the leakage rate from the PET would provide the necessary validation of the leakage rate estimates currently done.

Testing of several elements of the PET must still be performed, the water collection system, as well as the method used to seal the wiring pass-through of the PET were not tested during any of the performed experiments, since the water level inside the PET only reached a maximum of 45 in. It is believed that performing experiments while having the metal door open towards the inside of the tank, will produce the necessary conditions for both systems to be tested; therefore, when these experiments are performed it is recommended to proceed with extreme caution due to the lack of knowledge on how the system will behave.

The results of the experiments with the metal door, show that the failure mode is very dependent on the method used to close the door; when only the door latch was locked, all

experiments resulted in the door popping open, however, when both the latch and deadbolt were locked, the outcome was either failure of the deadbolt itself, or permanent bending of the door.

The experiments performed also demonstrated how the metal doors are able to withstand higher depths and flows than hollow-core doors, just as expected. Even when the failure of the metal doors occurred at similar water depths than those needed for the hollow-core doors to fail, the needed water flowrate into the PET to achieve those depths was higher for the metal doors.

The point made above brings the question, as to at what point does leakage of fluid from a system, becomes the factor that is used to consider the system as failed. If the doors are used as a barrier to prevent a room from flooding, it is necessary to not only test the door for how much fluid it need to break, but to also establish limits on how much leakage is allowable before qualifying the system as a success or failure state.

The current data processing method used for the water depth measurements has proved to be good mix between smoothing factor while also representing the real behavior of the system. The linear interpolation method, used to estimate the flowmeter flowrates in-between the actual readings has yet to be compared against other models to establish whether it is the correct method to be used or not, and if it is not, what other method should be used instead.

To finalize, the experiments performed with the hollow-core and metal doors with the new system were successful; they allowed the collection of new data, that will be used to establish the fragility models of NPP components, which is the ultimate objective of CFEL, but



also pinpointed new flaws or improvements that could be made to the PET to better achieve that objective.

## Future Work

There are two different aspects to this section, the first one explores the several areas where the PET can receive upgrades, and the second one explores what type of experiments should be performed in the future.

The first area of the PET that needs to be improved, is the measurement of water leakage from the inside of the tank. In all of the experiments so far, water leakage has overflowed the method initially devised to measure the phenomenon (the v-weir); however, information has been found, that water flowing through a rectangular weir can also be accurately measured. Obtaining precise measurements of water leakage, in the systems that presents water flows that overflow the V-weir are especially important now that a direct measurement of the water flowing into the PET cannot be obtained. A precise measurement of the water flowing out of the PET can also be used as a validation tool, for the some of the calculations made to analyze the experiment data.

Another area that needs further work is the analysis of the data produced by the depth sensors. The Omega depth sensor consistently recorded a higher depth measurement than the Campbell Scientific sensor at the moment the system failed; the higher measurement caused that first data point to be slightly skewed when compared to other experiments. If it is not possible to determine the cause of the disparity, a possible solution could be to give weights to each data set, that way the average depth data will be more dependent on the data from sensor with the most accurate readings. Another solution could be to take into account the readings of

only one sensor, for the data points in and around a disparity between the readings; this, however, should only be done, if it is known which sensor is doing the accurate measurements.

An element of the PET that needs to be tested is the water collection system. The system was built to collect the water ejected by the relief valves and reroute it to the test area in front of the PET, to avoid water splashing into the electrical systems of the laboratory. The system, will only work in an experiment that is able to completely fill the PET, however, this has not been achieved yet; none of the experiments have filled the PET with water, and so the workings of the relief valves and the water collection system have not been tested.

The uneven timing and long interval between data-points for the flowmeters is another problem that should be solved. A solution is in progress, and that is to connect each flowmeter in a point-to-point manner, instead of using a multi-drop connection. A couple of HART modems have been ordered, and the result of this fix will be documented soon. In the case the solution above does not work, another method must be employed; and there are a few possible ones:

- Stated in the section Flowrate-Behavior Experiment, when connecting the flowmeters to the computer while using ABB DTMs, there is an option to have all the flowmeters record data with a constant time interval of 5 seconds. Getting this method to work could be a solution.
- Another solution could be to perform a long-term experiment to find out the steady-state flow through each flowmeter at different valve openings. This has been partially done, and some of the data collected during the Flowrate-Behavior Experiment could be reused for this purpose. The steady-state information could then be used in place

of the data recorded for each experiment, since the steady state flows for the operated configurations were already known.

- The last solution could be to simply film the displays of each flowmeter. It is known that the data refresh rate at the flowmeters display is one second. Therefore, by filming the displays, more data could be generated for each experiment, which would then facilitate the analysis produced for each experiment.

Experiments showed that flowmeters, specially the upstream 12 in. one, takes around ~30 seconds to start producing data, an already mentioned solution would be to start every experiment with the same upstream valve configuration as steel door experiments #6, #7 or #8. The initial upstream valve configuration was the following: recirculation valve open, upstream 12 in. valve  $\frac{1}{4}$  open and upstream 8 in. valve closed. This configuration allowed the flowmeter to start producing data before water entered the PET.

Having tested the first metal door opening towards the outside of the PET, it is easy to determine that the next set of experiments should involve the metal door to open towards the inside of the PET. When opening this way, the door will push against the doorstops of the frame. Turning the door around will help in two ways: the first one is that the bowing observed in the last experiment will not be repeated, there is no place for the door to bend to; and the second way, is that the stresses on the door lock and on the deadbolt will be greatly reduced, so the failure of the door because of a bent deadbolt, or because the water pressure just forced the lock open will not be possible.

A future experiment will be the use of air-lock doors. This will create a completely water-tight environment in the PET that will closely mimic the conditions of several areas within NPPs and will be the ultimate experiment in terms of door systems.

It is recommended that by the time a system as complex as an air-tight door is tested, that the team has meetings with professional contractors to correctly install these and any other types of doors; several difficulties were encountered during the frame construction of normal steel doors, that could have been mitigated by learning from someone with direct experience in the area. Having a professional contractor help install the doors in place, and build the corresponding frame, will also serve as a boost for the validity of all experiments.

## Bibliography

ABB. (2017, 09 14). *Data Sheet - WaterMaster Electromagnetic Flowmeter*. Retrieved from ABB:

<https://search-ext.abb.com/library/Download.aspx?DocumentID=DS%2fWM-EN&LanguageCode=en&DocumentPartId=&Action=Launch>

ANSI. (2012). *American National Standard: Recommended Erection Instructions for Steel Frames*.

Retrieved from Steel Door Institute: <https://www.steeldoor.org/T-DOC/ansi-250-11.php>

Bhandari, B. (2016). *Full Scale Door Testing Under Flooding Conditions to Develop Testing Protocols*. Pocatello.

PACTware. (n.d.). *PACTware*. Retrieved from PACTware:

<http://www.pactware.com/en/products/pactware.html>

Siemens. (2012). *Application Guide: Setting Up & Working with HART networks*. Guide.

Slack, B. (2014). *Internal Flooding Flood Area Definition*. Excel Energy.

Slack, B. (2014). *Internal Flooding Walkdown Summary Report*. Excel Energy.

Suresh, S. (2017). *Development of an Interior Component Flooding Fragility Model of Component Flooding Evaluation Laboratory Safety Circuit*. Pocatello.

Szilard, R. H., Coleman, J., Smith, C. L., Prescott, S., Kammerer, A., Youngblood, R., & Pope, C.

(2015). *Industry Application External Hazard Analyses Problem Statement*. INL. Idaho

Falls: INL. Retrieved from

[https://lwrs.inl.gov/RiskInformed%20Safety%20Margin%20Characterization/INL-EXT-](https://lwrs.inl.gov/RiskInformed%20Safety%20Margin%20Characterization/INL-EXT-15-)

15-

36101%20Industry%20Application%20External%20Hazard%20Analyses%20Problem%20Statement.%20July%202015.pdf

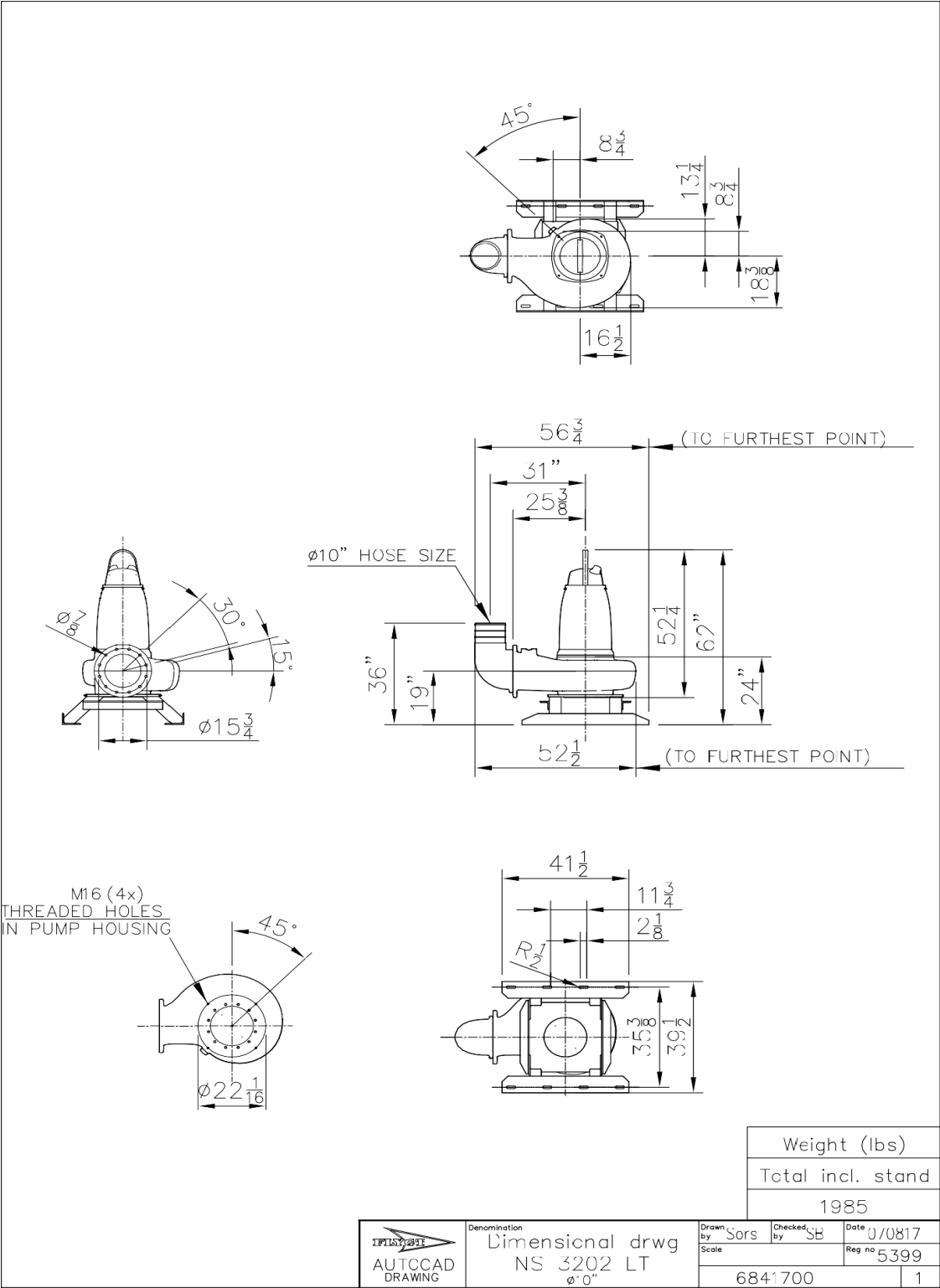
Tahhan, A., Nichols, L., Muchmore, C., Ryan, E., Wells, A., Roberts, G., . . . Pope, C. (2017). Development of Experimental and Computational Procedures for Nuclear Power Plant Component Testing Under Flooding Conditions. *ICONE25* (p. 9). Shanghai: ASME.

Wells, A. (2016). *Nuclear Power Plant Flooding Events*. Pocatello. Retrieved from [https://drive.google.com/drive/u/1/folders/0B\\_3V-pKLJhGhRWdTTjU1TIhpTDQ](https://drive.google.com/drive/u/1/folders/0B_3V-pKLJhGhRWdTTjU1TIhpTDQ)


World Nuclear Association. (2012, March). *Fukushima: Industry Response*. Retrieved from World Nuclear Association: <http://www.world-nuclear.org/focus/fukushima/fukushima-response-introduction.aspx>

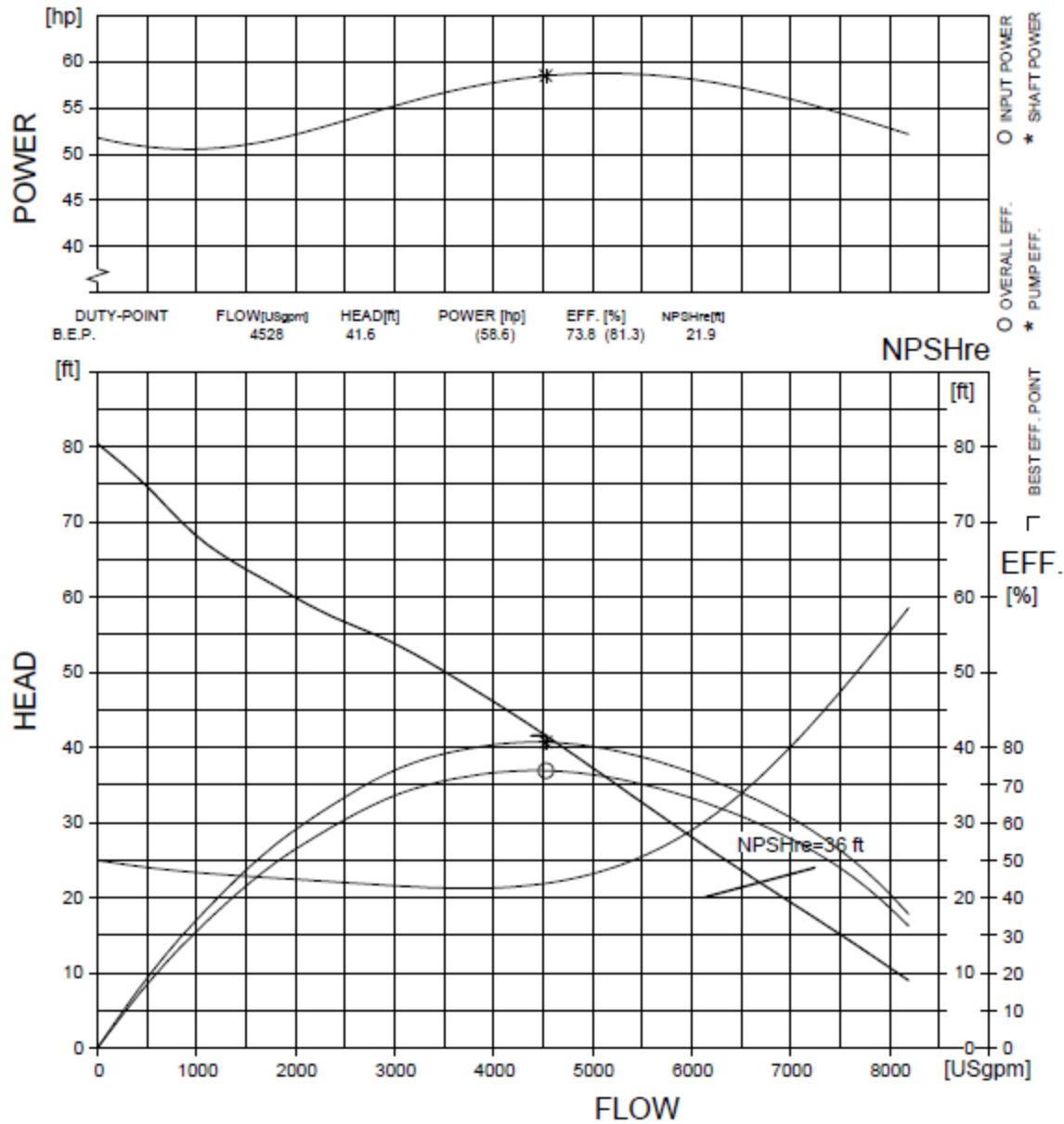
World Nuclear Association. (2017, October). *Fukushima Accident*. Retrieved from World Nuclear Association: <http://www.world-nuclear.org/information-library/safety-and-security/safety-of-plants/fukushima-accident.aspx>

Appendix #1: Flygt Pump, Performance Curve & Specs





				PERFORMANCE CURVE				PRODUCT NS3202.185			TYPE LT			
DATE 2010-08-02				PROJECT FLYGT US Catalog						CURVE NO 63-614-00-7010			ISSUE 2	
POWER FACTOR EFFICIENCY MOTOR DATA		1/1-LOAD		3/4-LOAD		1/2-LOAD		RATED POWER ..... 60 hp			IMPELLER DIAMETER 356 mm			
		0.88		0.83		0.74		STARTING CURRENT ... 420 A			MOTOR #		STATOR	REV
		90.5 %		91.0 %		91.0 %		RATED CURRENT ... 72 A			30-29-6AA		1 D	10
COMMENTS				INLET/OUTLET - / 12 inch		RATED SPEED ..... 1170 rpm			FREQ.	PHASES	VOLTAGE		POLES	
NEMA Code Letter: F				IMP. THROUGHLET ---		TOT. MOM. OF INERTIA ... 0.65 kgm2			60 Hz	3	460 V		6	
				NO. OF BLADES 2			GEARTYPE ---		RATIO ---					



NPSHre = NPSH3% + min. operational margin  
Performance with clear water and ambient temp 40 °C



**CURVE**

## N-3202

### Materials of Construction

Components	Cast Iron Pump
Major Castings:	Cast iron, A48, Class 35B
Pump Lifting Handle:	Stainless steel
Motor Cable:	Chloroprene rubber jacketed
Cable Entry Grommets:	Nitrile rubber
Shaft:	Stainless steel ASTM A479 S43100-T
Impeller:	Hard Iron™ (25 ASTM A-532 (Alloy III A) 25% chrome cast iron)
Insert Ring	Hard Iron™ (25 ASTM A-532 (Alloy III A) 25% chrome cast iron)
O-Rings:	Nitrile rubber
Lubricant Plug	316 Stainless steel
Screws, studs and nuts	316 Stainless steel
Inner Mechanical Shaft Seal:	*Tungsten carbide/ *Tungsten carbide
Outer Mechanical Shaft Seal:	*Tungsten carbide/ *Tungsten carbide

\*All corrosion and abrasion resistant

Appendix #2: Global Pump, Performance Curve & Specs

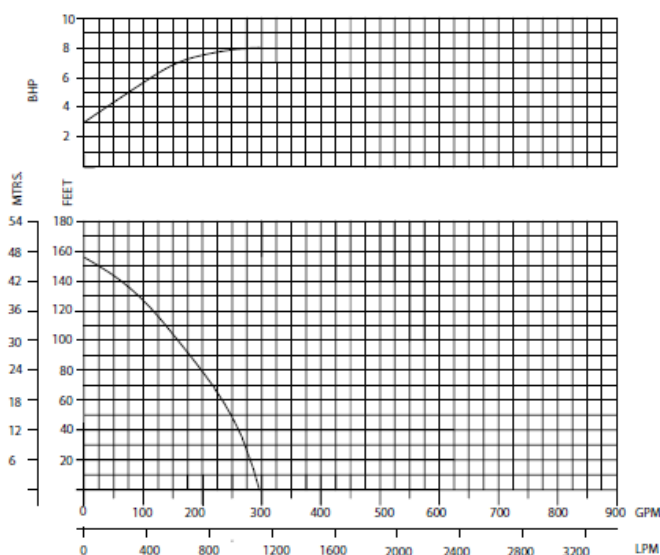
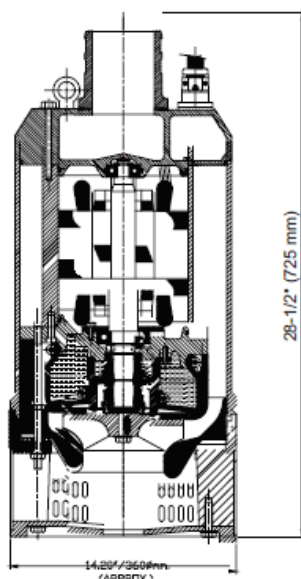


Global Pump® portable electric submersible pumps are ideal for corrosive and abrasive applications.

The Model 4GSUBHD75 pump with 3" NPT and a 7.5 hp (5.5 kW) motor is ideal for low volume, high head applications.

FEATURES	OPTIONS
Stainless steel strainer, shaft, impeller, outlet and hardware for maximum corrosion resistance	Choice of impeller materials including 316 stainless steel for sea water and corrosive applications
Mechanical seals in wholly enclosed pressure compensated oil chamber	Available in complete 316 stainless steel construction with silicon carbide/silicon carbide mechanical seals and viton elastomers
Nitride hardened 410 stainless steel impeller for abrasive applications	Automatic ON/OFF/ON thermal overloads embedded in stator winding (requires 6 core or control cable and external controls)
Tandem tungsten carbide/tungsten carbide and tungsten carbide/tungsten carbide mechanical seals	Polyurethane diffusers and wearplates available
Field adjustable nitrile rubber-lined diffuser/wearplate optimizes efficiency throughout the life of the pump	
Equipped with sacrificial zinc anodes for maximum life in a saline fluid environment	

# 4GSUBHD75 HIGH PRESSURE DEWATERING



## SPECIFICATIONS

Size	4" (100 mm)
Power	7.5 hp (5.5 kW)
Max Flow	350 gpm (28 m <sup>3</sup> /h)
Max Head	165' (50 m)
Motor	2-pole induction continuous rated motor with squirrel cage rotor. Stator insulation class 'H' (180°C)
Speed (motor)	3,400 RPM @ 60 Hz, 2,800RPM @ 50Hz
Power Rating (motor)	7.5 hp @ 60 Hz, 5.5 kW @ 50 Hz Full Load
Current FLA (motor)	11 Amps @ 460v, 12.5 Amps @ 400v
Max. temperature of the pump liquid (motor)	104°F/40°C
Max. start/stop per hour (motor)	15 Start: Delta starting optional
Power Supply	3 phase, 50/60 Hz, AC Supply. Available in any voltage frequency combination (208/220/230/380/415/460/575/1,000V)
Power Cable	50' (15 m) length standard
pH Range	5 - 8
Submergence	Submergence below liquid surface min. 5" (127 mm) max. 50' (15 m)
Weight (approx. w/o cable)	135 lbs. (61Kg)

## PUMP MATERIAL

Outer Casing	Epoxy-coated aluminum
Stator Casing	Epoxy-coated extruded aluminum
Diffuser/Wearplate	Nitrile rubber-lined (polyurethane optional)
Shaft	431 Stainless steel
Shaft Seal	Tandem tungsten carbide/tungsten carbide and tungsten carbide/tungsten carbide mechanical seals wholly enclosed in an oil chamber
Hardware	304 Stainless Steel
Impeller	Nitride-hardened 410SS to 56HRC (Standard)
Ball Bearings	Two single row deep groove ball bearing. Bearings enclosed with high temperature grease-containing special anti-corrosion additive
Power Cable	Waterproof/oil proof, rubber-insulated, neoprene-sheathed copper conductor flexible cable. Type SOOW in North America, EPR in the Middle East and HO7RN in the EU. 6 Core or Control cable with thermal overloads optiona
Strainer	304 Stainless Steel with 0.25" (6 mm) round holes

**GLOBAL PUMP**

**GLOBAL PUMP**  
10162 East Coldwater Road, Davison, MI 48423  
Tel: 810.653.4828 Fax: 810.658.0632  
**1.866.360.PUMP** [www.globalpump.com](http://www.globalpump.com)

© 2016 Global Pump  
Specifications reflect model pictured, and are subject to revision without notice. Global Pump is not liable for any consequential, incidental or indirect damages relating to these specifications.

## Appendix #3: PACTware Interface

(Note: Before using PACTware, it must be known whether the flowmeters are connected in a multidrop or point-to-point style. In a multi-drop connection, several flowmeters are connected to the same HART modem; in this case, each flowmeter must be setup with its own unique HART channel other than zero. In the case of a point-to-point connection, each flowmeter is connected to a single HART modem, in this case, the HART channel of each flowmeter must be set to zero).

The program that is used in the lab to record the flow meters is called PACTware. Figure 86 below shows the screen when the program is first opened.



Figure 86. PACTware Welcome Screen

To connect to the flow meters, the HART modems must be added first. Make sure that the physical connections are correct as described before. Next, right click on “HOST PC” on the left, as in Figure 87, and repeat next two steps for as many HART modems are in the system.

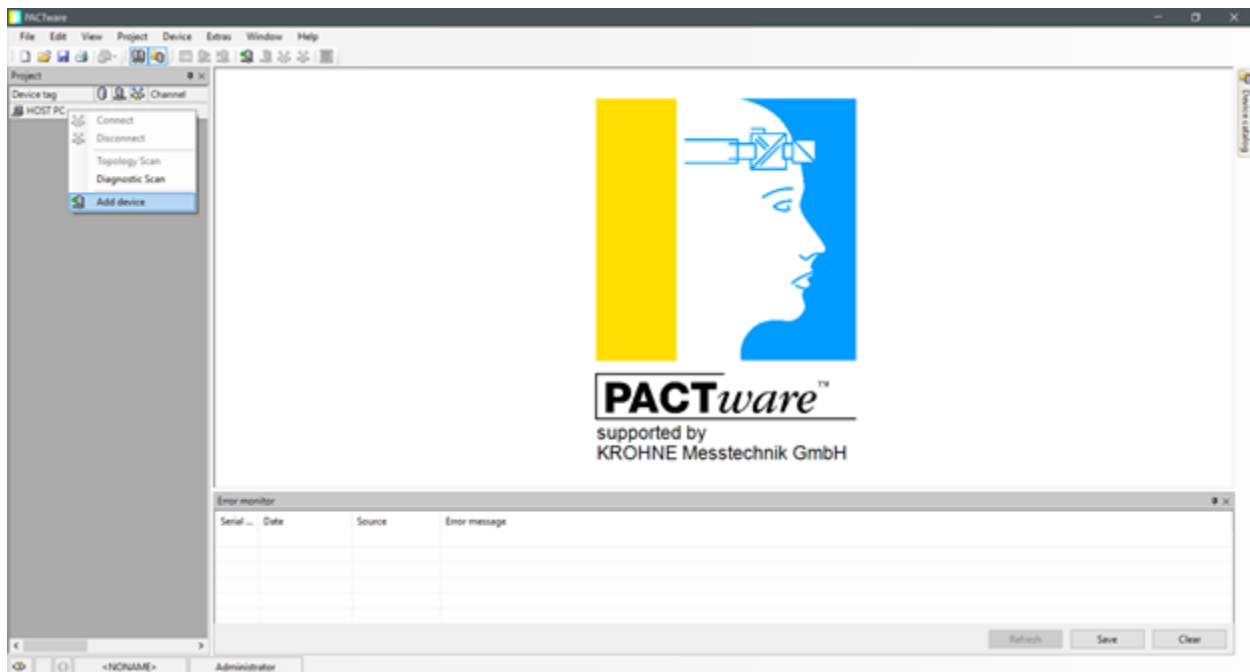


Figure 87. PACTware- adding the HART modems

In the menu that opens click add device. A window will open with several device types, as in. The device that is used is the HART Communication.

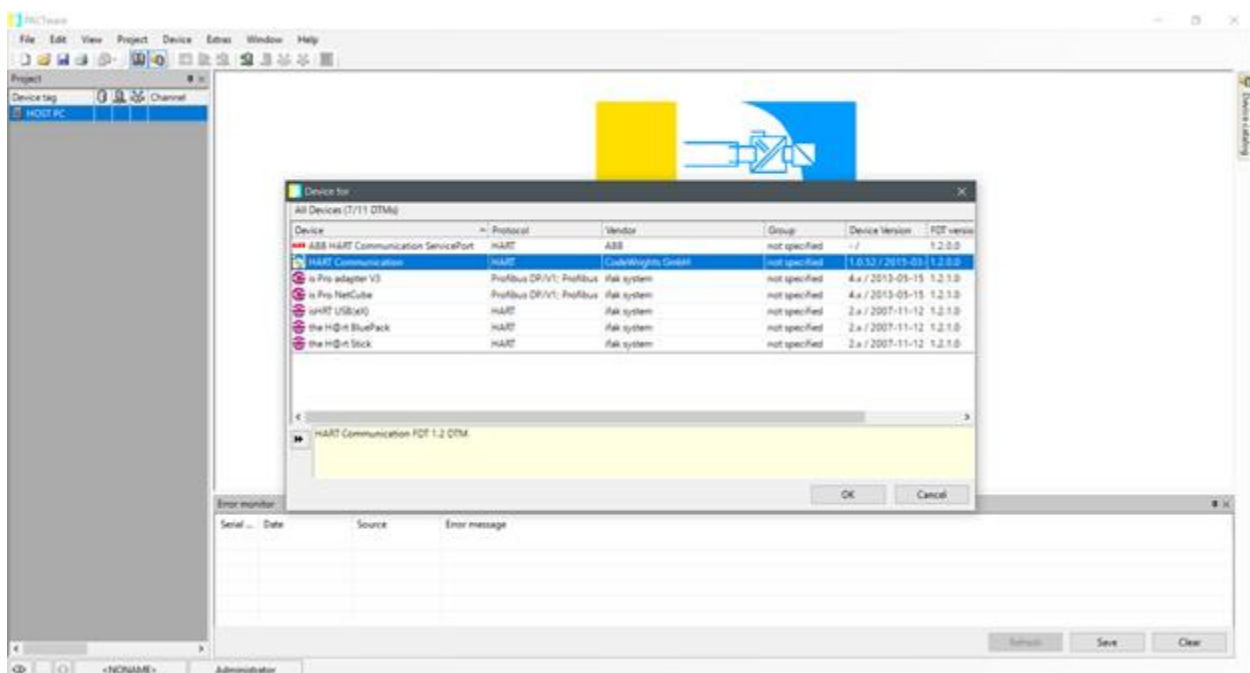


Figure 88. PACTware - Add HART modem DTM

The HART Communication device will now appear under the host PC with the name COM1. This represents the com port that the USB HART modem is plugged into the computer, but it is not likely that the modem will be in port 1. In the case of this example, the modem is connected in com port 3, but that may not always be the case. Open the device manager via the Windows control panel to find which com port the modem is in. Back in PACTware, double click the modem device, or right click and select the parameters page.

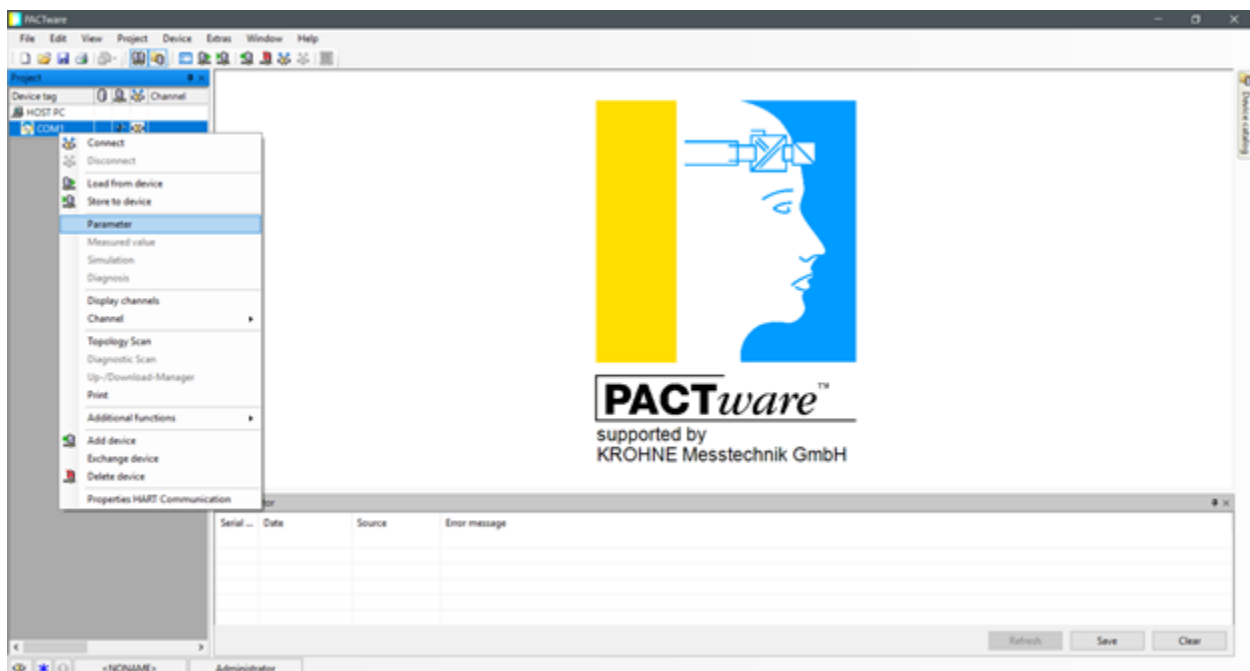


Figure 89. PACTware – HART Communication Device

The parameters page allows you to select the correct com port for PACTware to attempt to find the HART modem.

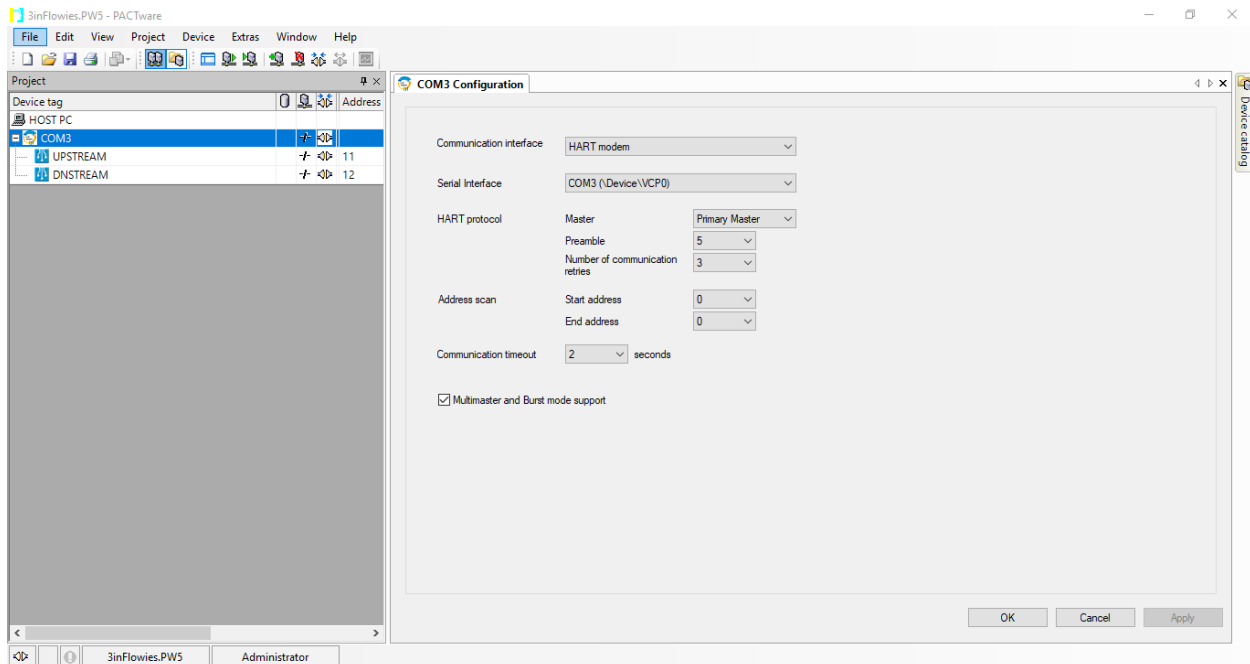


Figure 90. Device 'Parameters' Screen

The above figure also shows the address scan. If multidrop is to be used, be sure to set these to a range appropriate to encapsulate the addresses used. 0 is reserved for point to point connections, and one to 15 is for multidrop. Other than that, address designation is up to the user's discretion.

Once the correct port is chosen, the right click menu, clicking 'Connect' should connect the HART Communications Device. At this point, if the connection is successful, disconnect it again; otherwise, troubleshoot and try to find the error in the setup.

IT IS EXTREMELY IMPORTANT TO DICONNECT THE MODEM AT THIS POINT. IF THE MODEM IS CONNECTED THE NEXT STEP WILL NOT WORK.

The next step is to connect to the flowmeters themselves. Right click the modem and select add device. From the window that opens choose the Microflex Generic HART DTM 6 as the device. These are referred to as the DTMs.



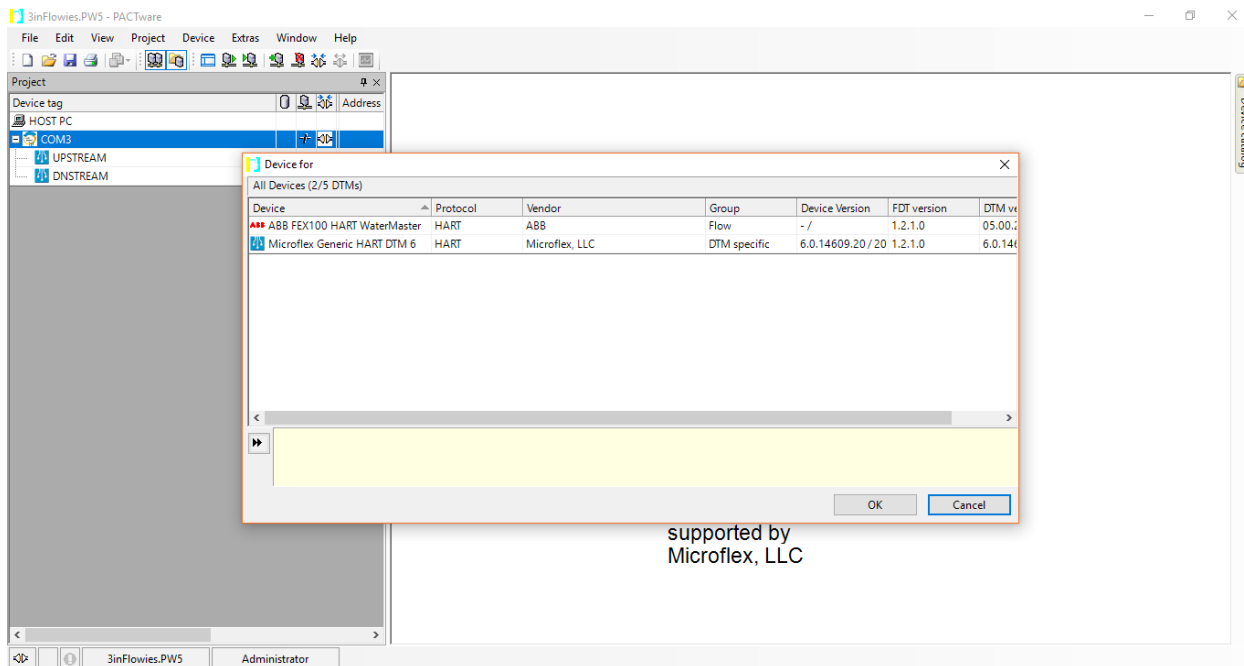


Figure 91. PACTware - Add Flowmeter DTM

If connecting to several flow meters via multidrop method, now is the time to set the address of the DTMs. Right click again on the COM device. Under 'Additional Functions' is the option 'Change DTM Address'. Open this window and change the new DTMs' addresses to match those of the devices. **If the modem is connected at this point, it is impossible to change the address of the DTMs.**

If multiple modems are in use, repeat the steps that add the modem and just one DTM, being sure to observe the different ports for each modem. This setup will allow for faster recording times for each flow meter, bypassing the inherent flaw in the HART protocol.

At this point, connecting to each flow meter should be possible. Right click each device you wish to connect to and click connect.

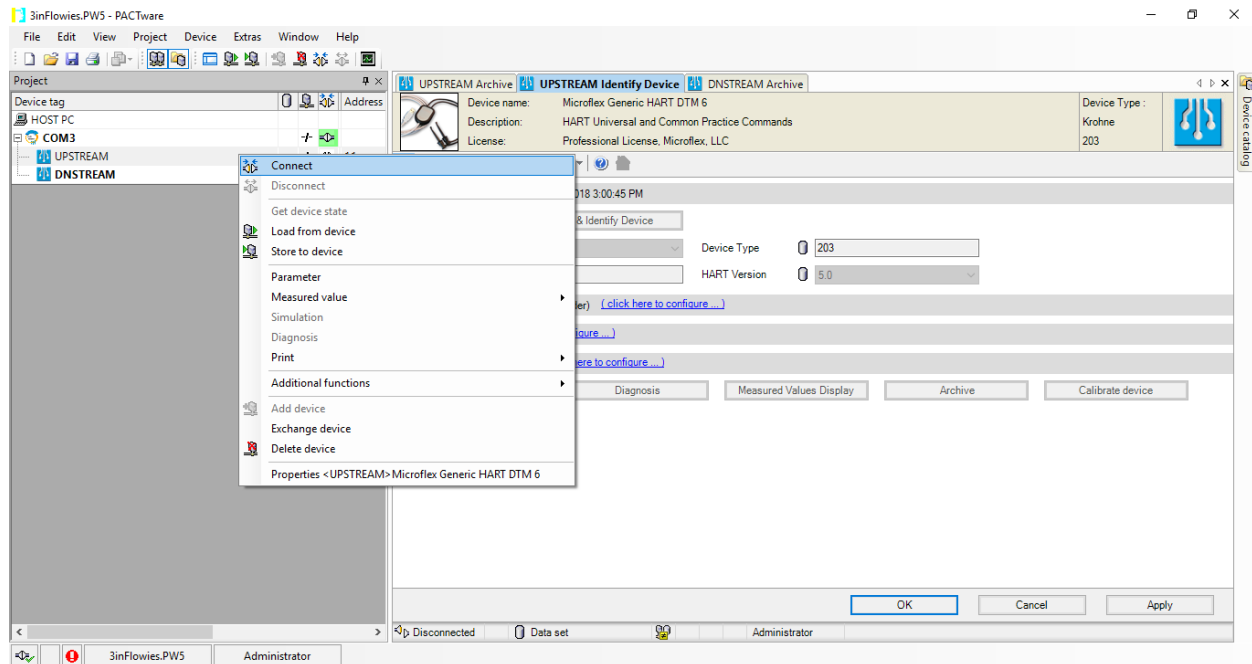


Figure 92. PACTware - Connecting to Flowmeters

To record the values of the flow meters then right click them again, mouse down to the 'Measured Value' tab, and click 'Archive' to open a new tab. In this tab, it is possible to see the flow value for a flow meter and to save the resulting data. Each flow meter will open it its own tab. To update the screen refresh interval, the 'Refresh' button must be pressed, when the arrow next to it is pressed, the refresh interval may be changed.

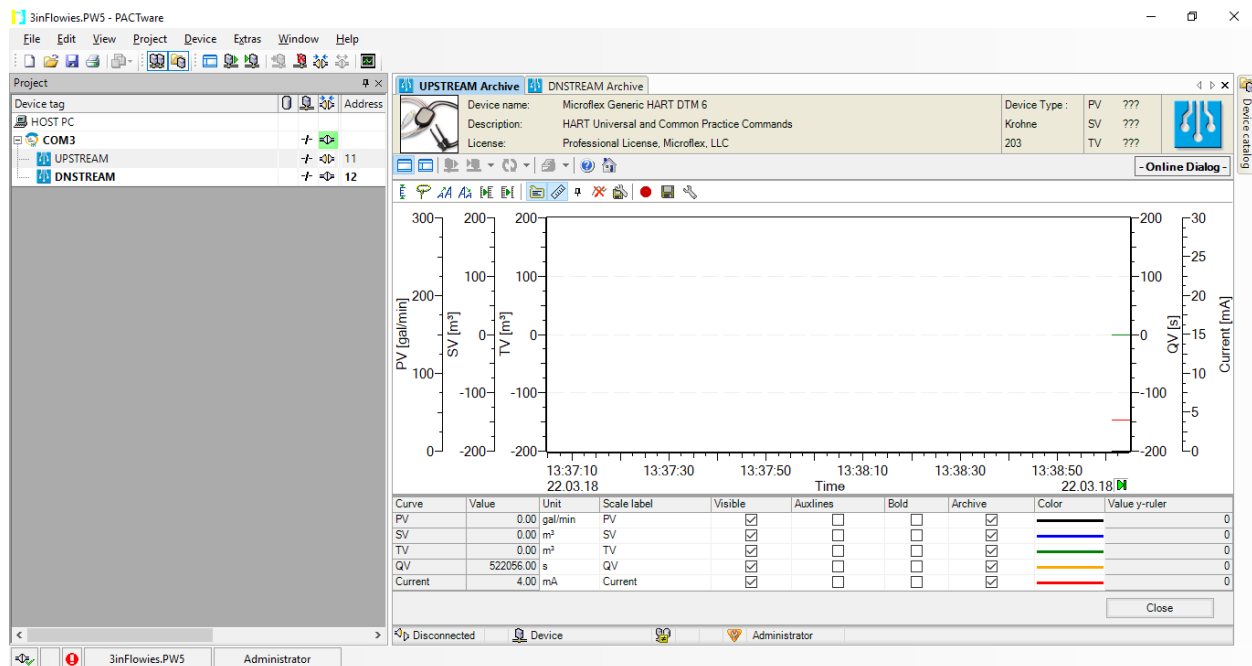


Figure 93. PACTware - 'Archive' Screen

After data is collected, clicking the save button will save a file called My Trend to a default location. If it is pressed again, it will attempt to do the same thing, but will be unable to. Saying no to overwriting the previous file will open a dialog allowing the user to save to a location of their choice. The file type is a CSV and opens best in Excel if the decimal and comma field are changed to a period and a comma from a decimal and a semicolon, respectively.

The save settings can also be modified at any time by pressing the 'Save Settings' icon (the one that has a wrench on top of a floppy disk).

<UPSTREAM> @11 [Microflex Generic HART DTM 6]: Archive settings

CSV File

CSV File

C:\Users\hijon\Documents\My Trends\Trend.csv

☒ User defined formats:

Date format: dd.MM.yyyy CSV separator: .

Time format: HH:mm:ss Decimal symbol: |

Date time e.g.: 22.03.2018 13:38:21 Number e.g.: 1234,56

Data Field	Name	Unit
<b>Time stamp</b>	Time stamp	
PV	PV	gal/min
State PV	State PV	
SV	SV	m <sup>3</sup>
State SV	State SV	

☒ Attach unit to data field

Ok Cancel

Figure 94. PACTware - 'Archive' Save Settings

## Appendix #4:CR1000 Interface: Device Configuration Utility, Shortcut & PC200W

**(Note: The three Software packages presented below 'Device Configuration', 'ShortCut' and 'PC200W' perform can perform similar functions. Since the datalogger and pressure transducer have already been connected to the computer, and the configuration is working properly, it is recommended to only use PC200W when collecting data. Device Configuration is used to get the status of the datalogger, whether the program that it is running is collecting data, updating its OS, and other datalogger functions. ShortCut should only be used to create programs for the datalogger(CR1000) to run. The PET computer is running ShortCut version 4.0, the programs produced by this version are incompatible with the CR1000 OS; it is recommended to first update the datalogger OS, before creating new programs using ShortCut. If that does not allow ShortCut to upload the program to the datalogger, troubleshooting will be necessary).**

## Device Configuration Utility



Figure 95. Device Configuration Utility - Welcome Screen

Device Configuration Utility allows connection to several Campbell Scientific dataloggers. The left panel shows information about the compatible dataloggers and other devices. To connect to the CR1000 all that is necessary is to specify at the bottom left corner the 'Communications Port' and the 'Baud Rate'. The communications port can be found by looking in the Windows Device Manager, which is located in the Control Panel, the Baud Rate that has been used is 9600, so that one should work. Once those two settings have been specified, click 'Connect' and the following screen should appear.

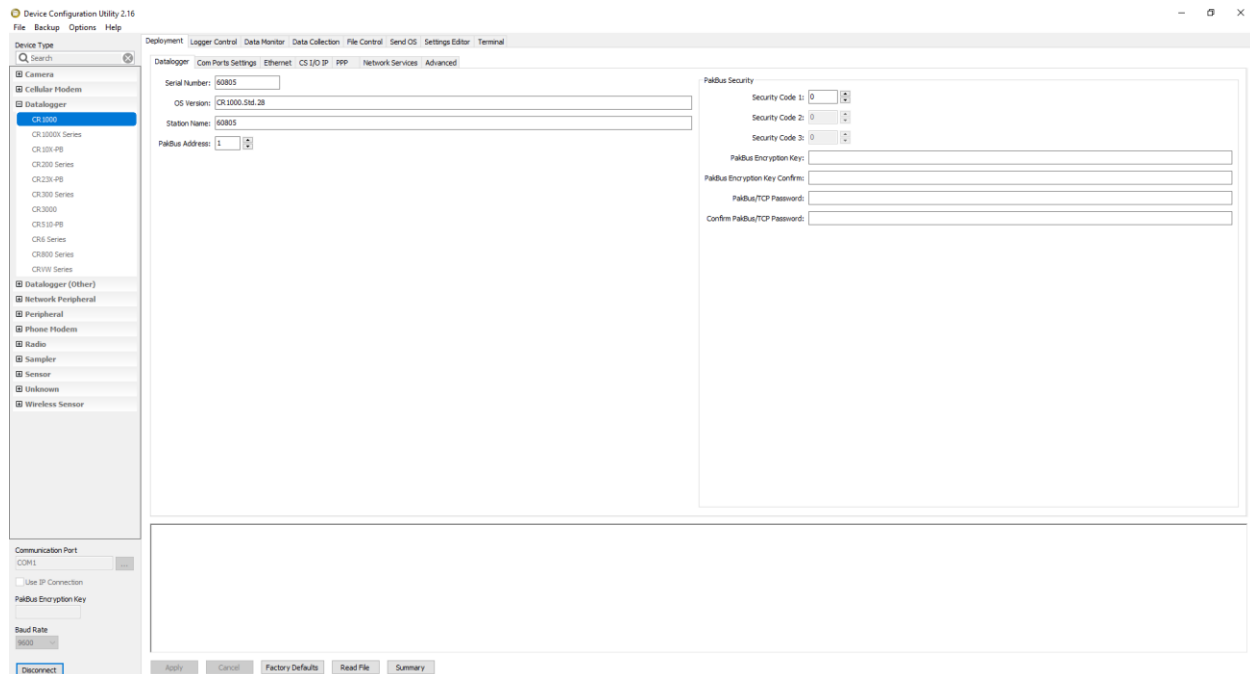


Figure 96. Device Configuration - Connected to the CR1000

Once connected to the datalogger, Device Configuration offers several tools. Figure 97 below shows the 'Logger Control' tab, in this section it is possible to send and retrieve the programs sent to the datalogger, as well as see what is program that the datalogger is currently running. The following picture Figure 98, shows the 'Data Monitor' tab, in which the users can see the data being recorded by the devices connected to the datalogger. In its current configuration, two tables of data are being collected, the data within the tables should be updated in real-time, if this is not happening there is an error either in the connection to the datalogger, or in the program it is running.

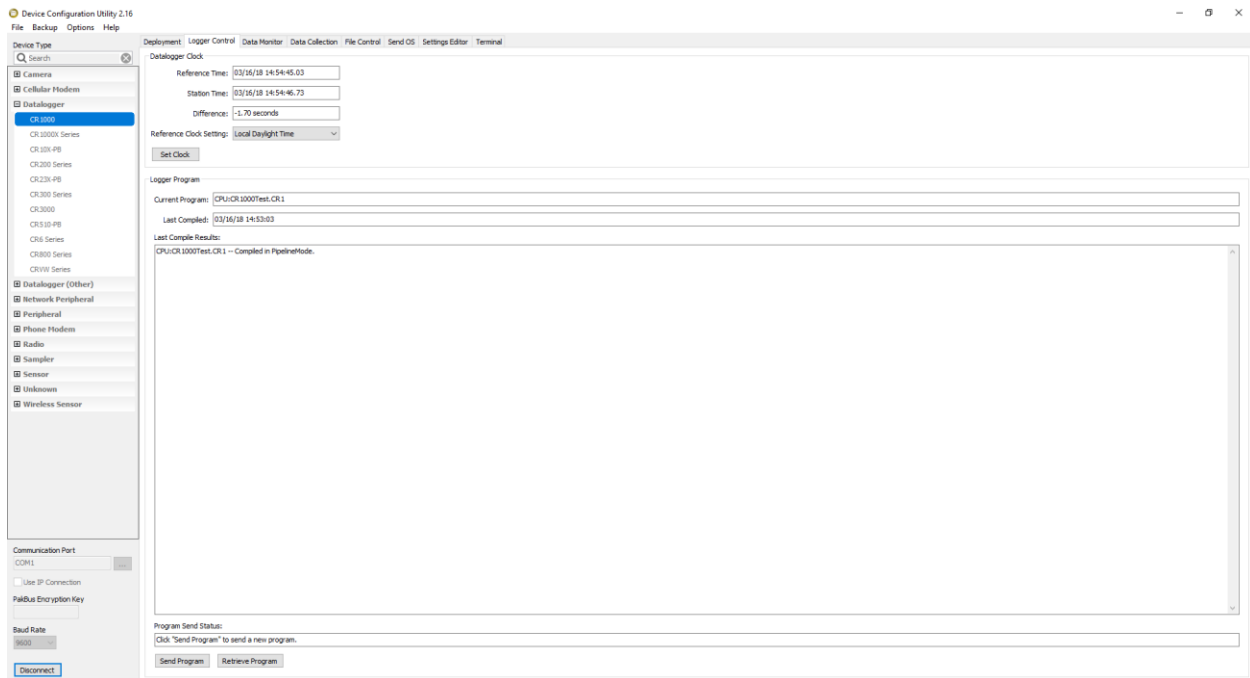


Figure 97. Device Configuration - 'Logger Control' Screen

Other useful tabs are 'Send OS' which allows the user to update the OS of the datalogger's OS.

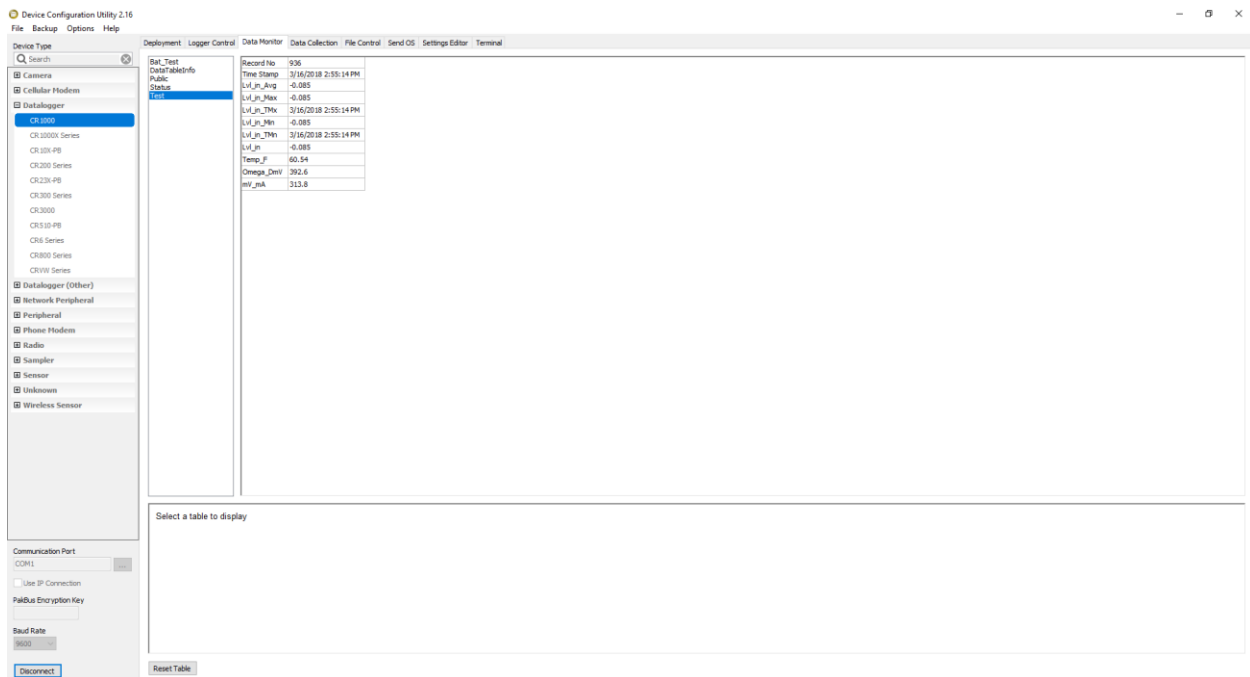


Figure 98. Device Configuration - 'Data Monitor' Screen



## ShortCut

ShortCut is the software that creates programs for the datalogger(CR1000) to run. It also shows the correspondent wiring diagram to connect the available sensors to the datalogger, Figure 99 below shows the welcome screen. **The current version of ShortCut installed in the PET computer will create programs that are not compatible with the CR1000. The datalogger's OS should be update first.**

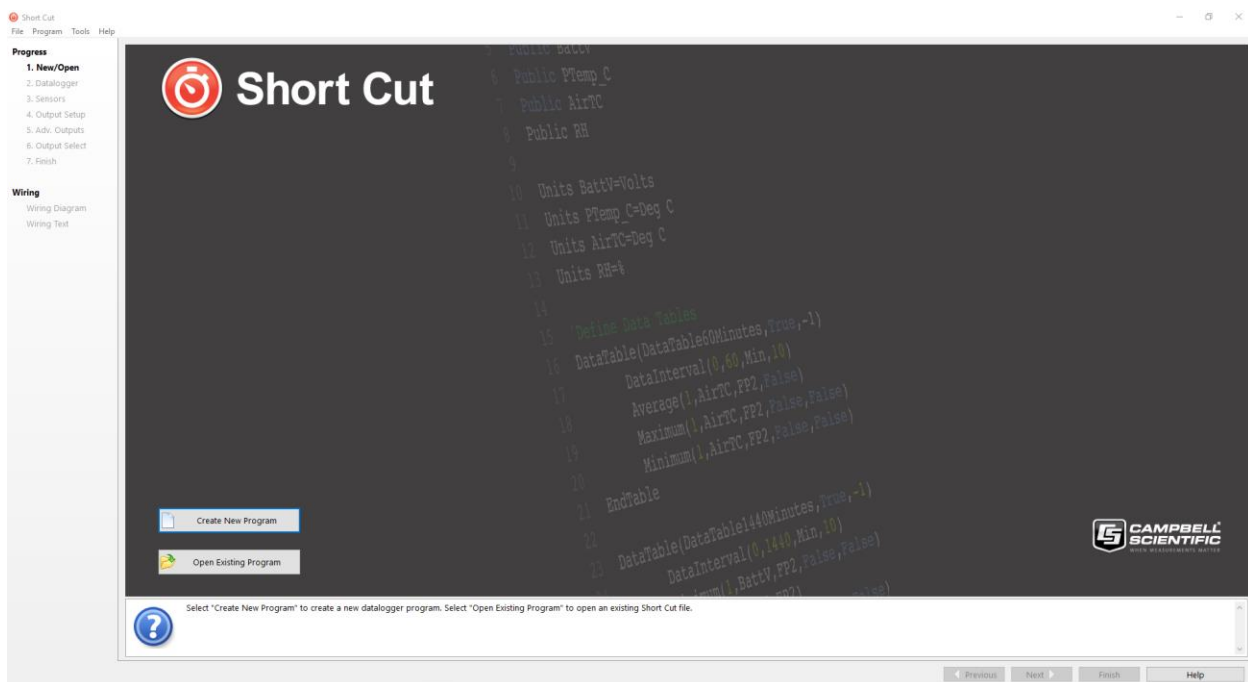


Figure 99. ShortCut - Welcome Screen

The first step is to select whether to create a new program or modify an existing one, by pressing on the correspondent button on the bottom left corner. The next two steps are to select the datalogger model and include the sensors connected to it; if the sensor is not supported, general voltage or current measurements may be added to the datalogger. The current program utilizes both a current and voltage measurements to interpret the data from the Omega Pressure Sensor. The voltage measurement is the one utilized, since the current one is not setup properly.

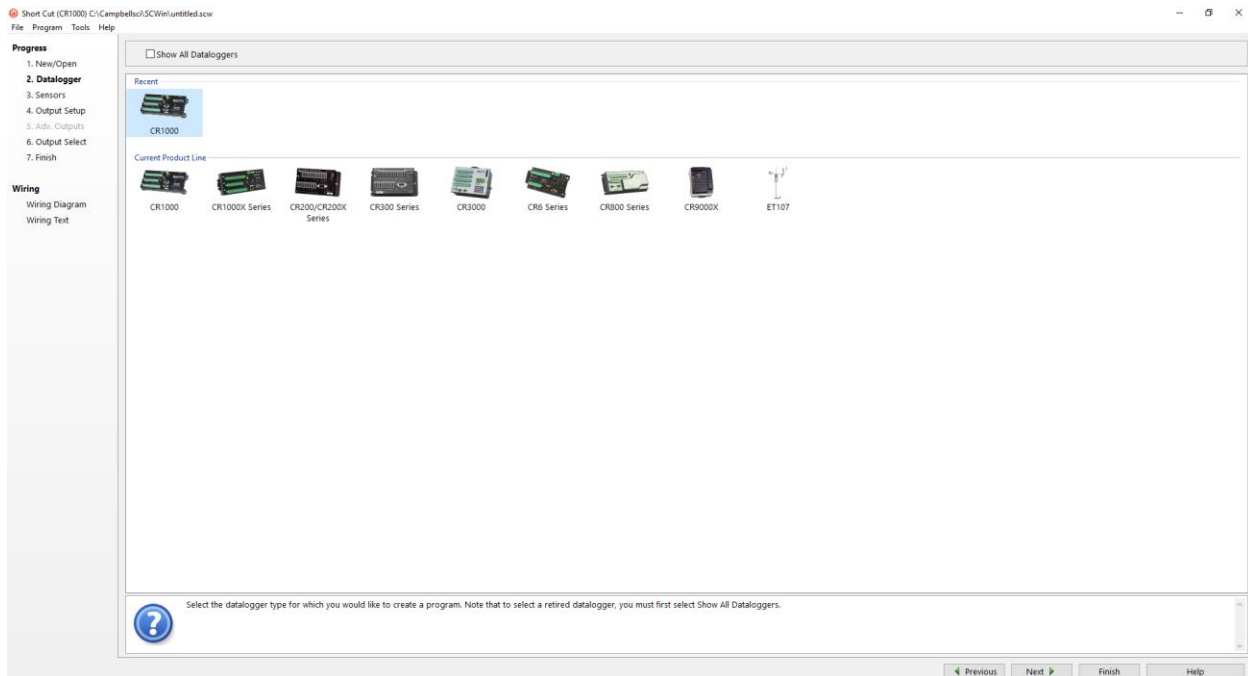


Figure 100. ShortCut - Datalogger Selection Screen

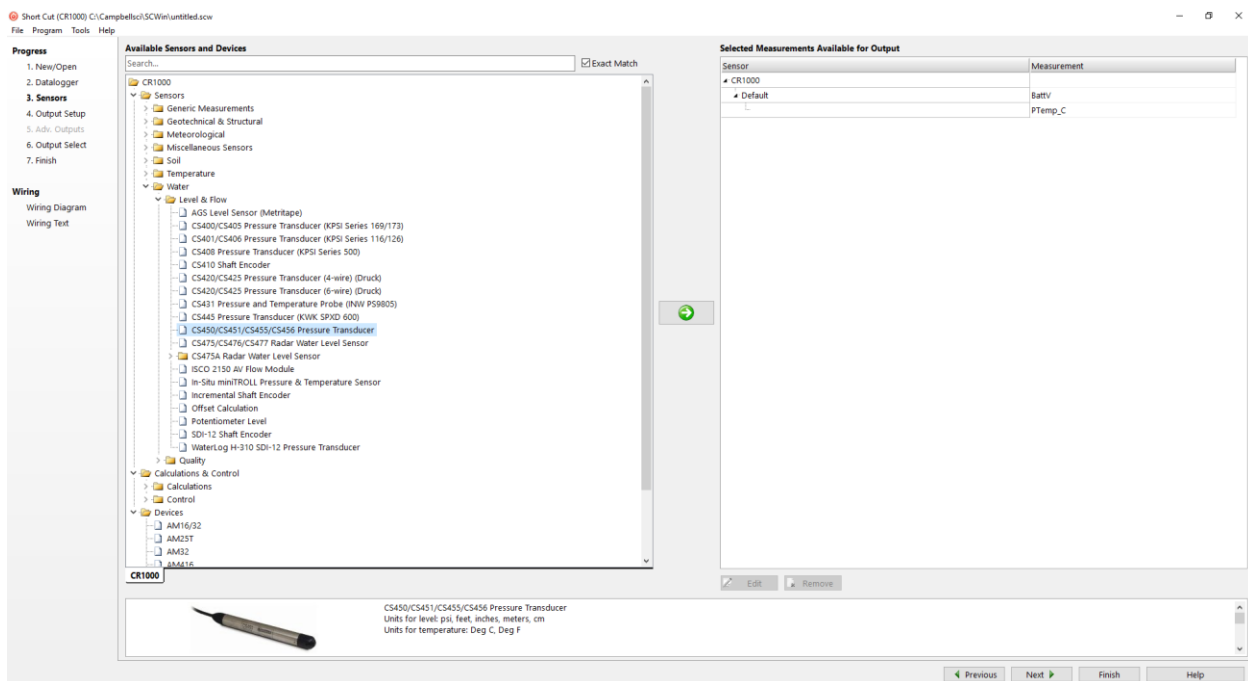


Figure 101. ShortCut - Sensor/General Measurements Selection Screen

Once all the sensors are accounted for, ShortCut asks for the user to select and organize the outputs of the program. The default is two tables; the first one contains data of the datalogger, such as its battery level, while the second one will contain the data from the sensors.

The sensors supported by ShortCut will usually offer a wide possibility of data measurements, for the CS451, on top of the pressure, the user can select in ShortCut the units of the measurement as well as other properties to measure such as the fluid temperature. This screen will also allow the user to select the recording interval of the datalogger.

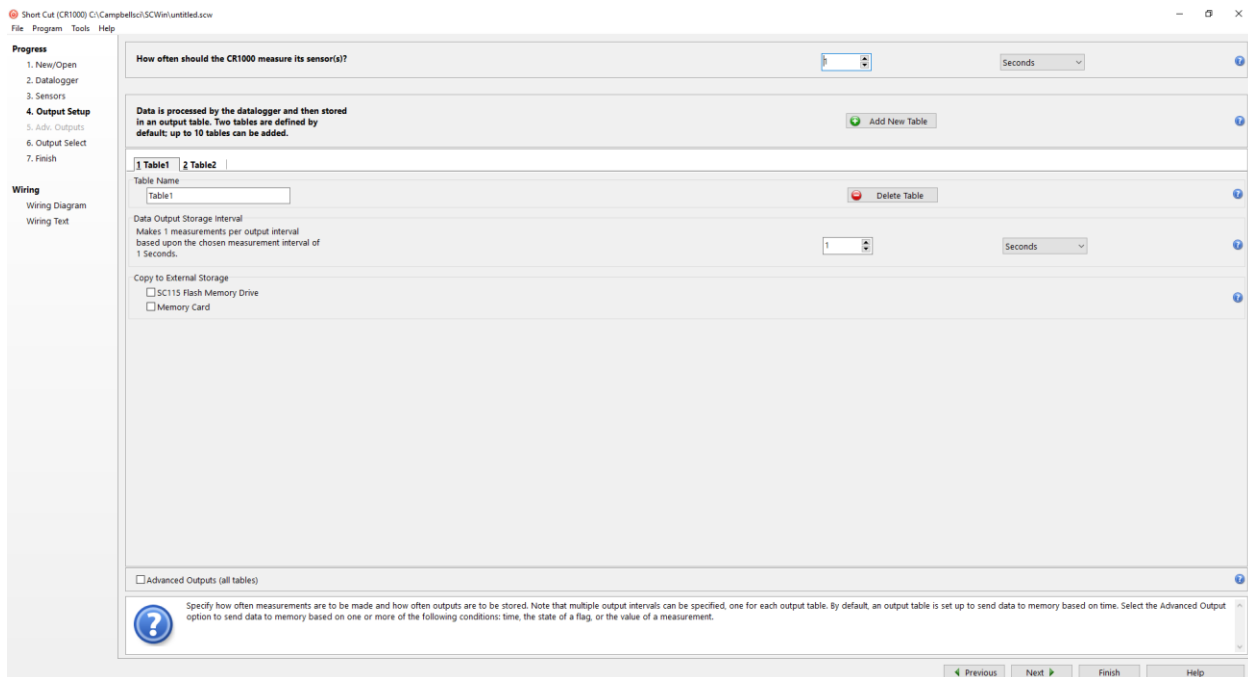


Figure 102. ShortCut - Output Setup Screen

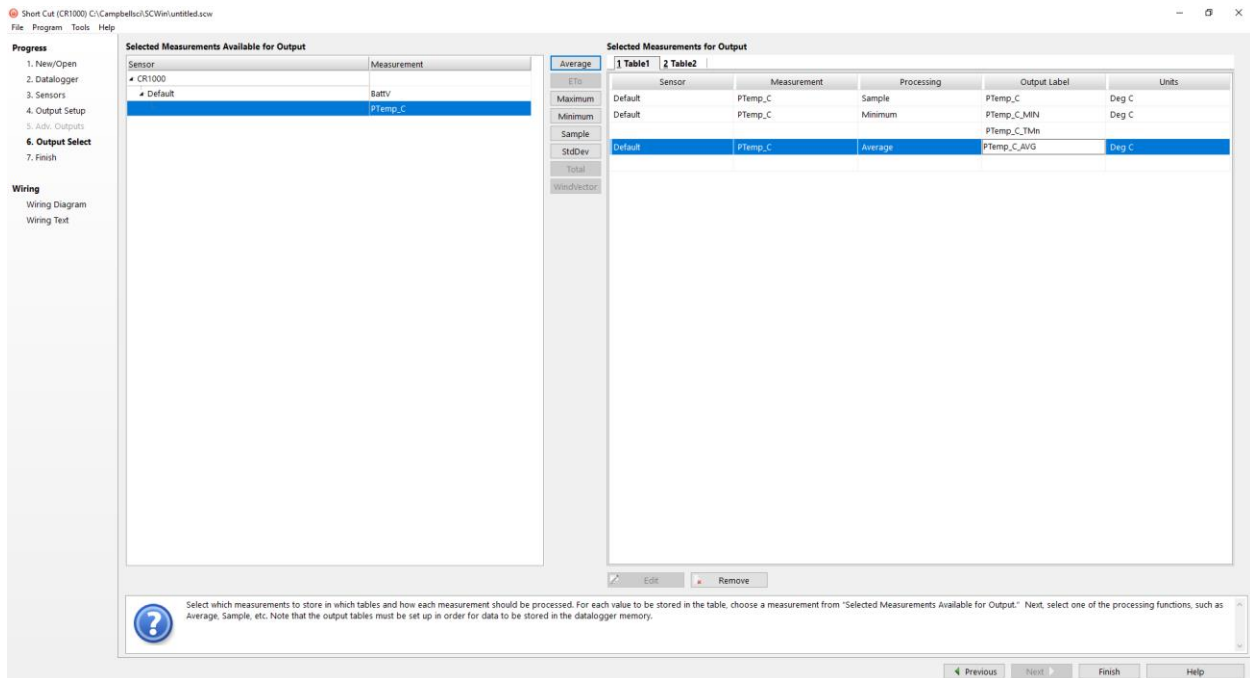


Figure 103. ShortCut - Output Select Screen

The program can then be saved anywhere in the system. ShortCut will also allow the user to send the program directly to the datalogger, for that work, ShortCut will need to connect to the datalogger, **only one software at a time can be connected to the datalogger, if either PC200W or Device Configuration are connected to the datalogger, ShortCut will not be able to send the program.**

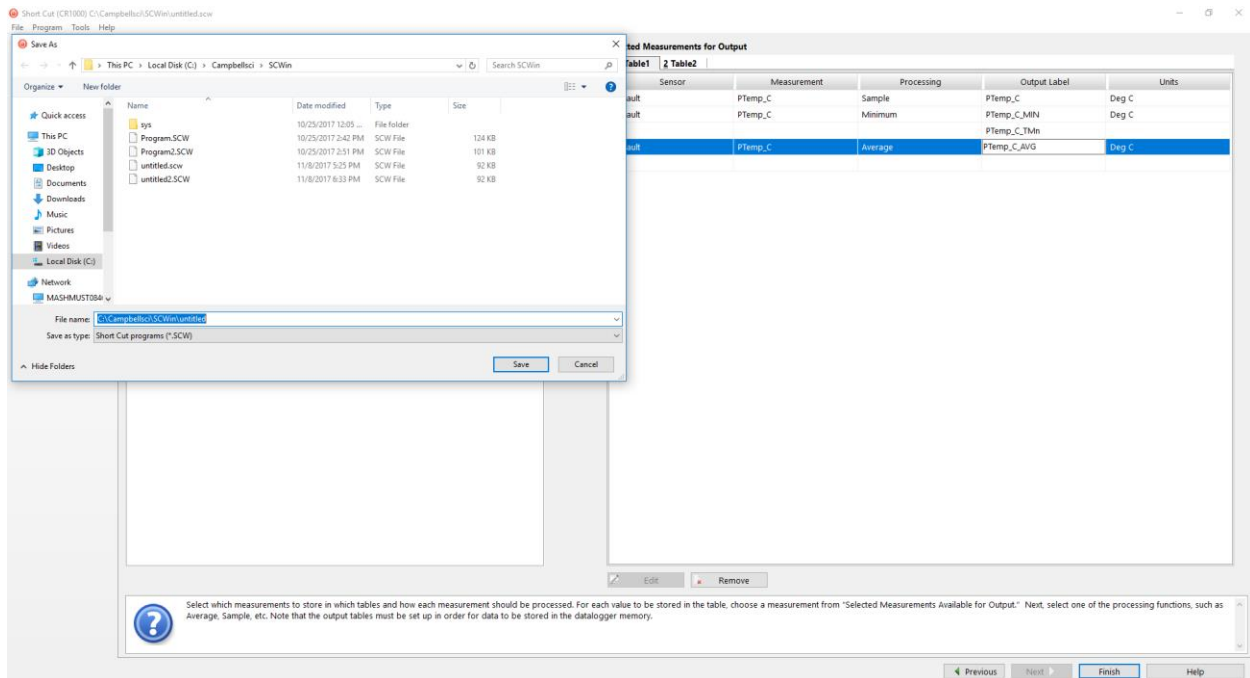


Figure 104. ShortCut - Save Screen

ShortCut also shows the user how to correctly wire the sensors into the datalogger. This can be done by pressing the 'Wiring Diagram' or 'Wire Text' tabs. Both of these options will provide the user with the specific location in the datalogger, of where each wire must be connected.

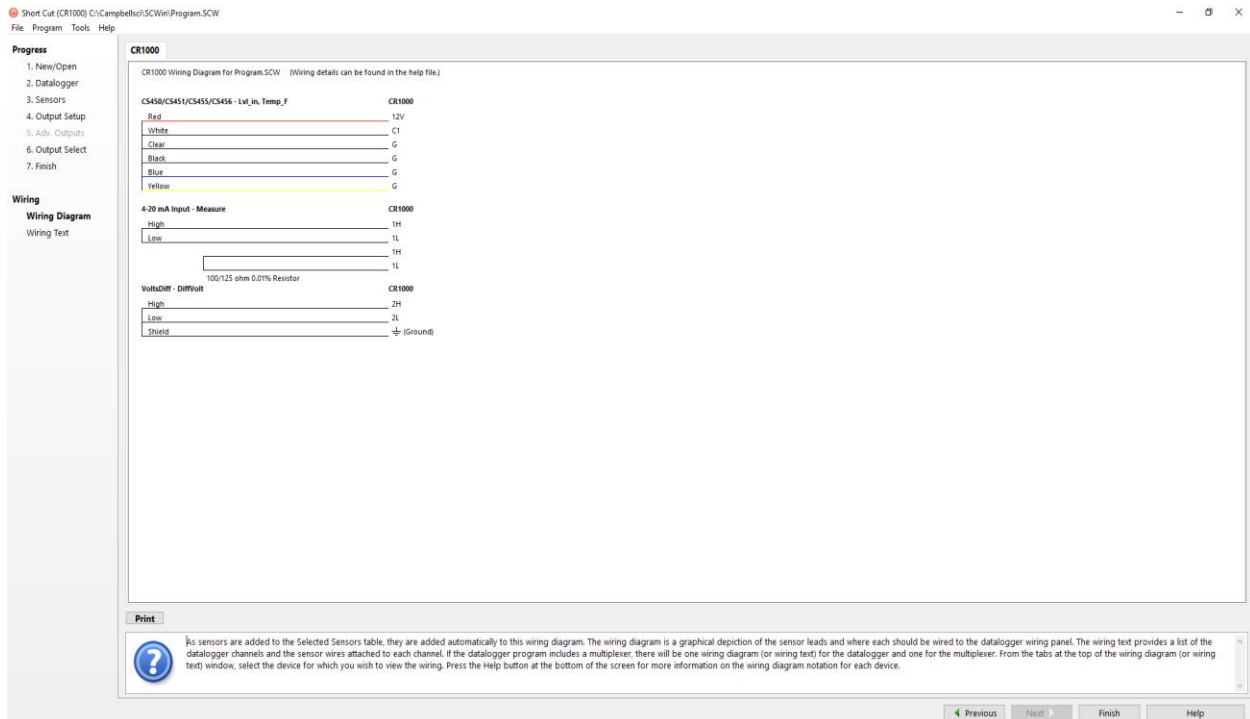


Figure 105. ShortCut - Wiring Diagram Screen

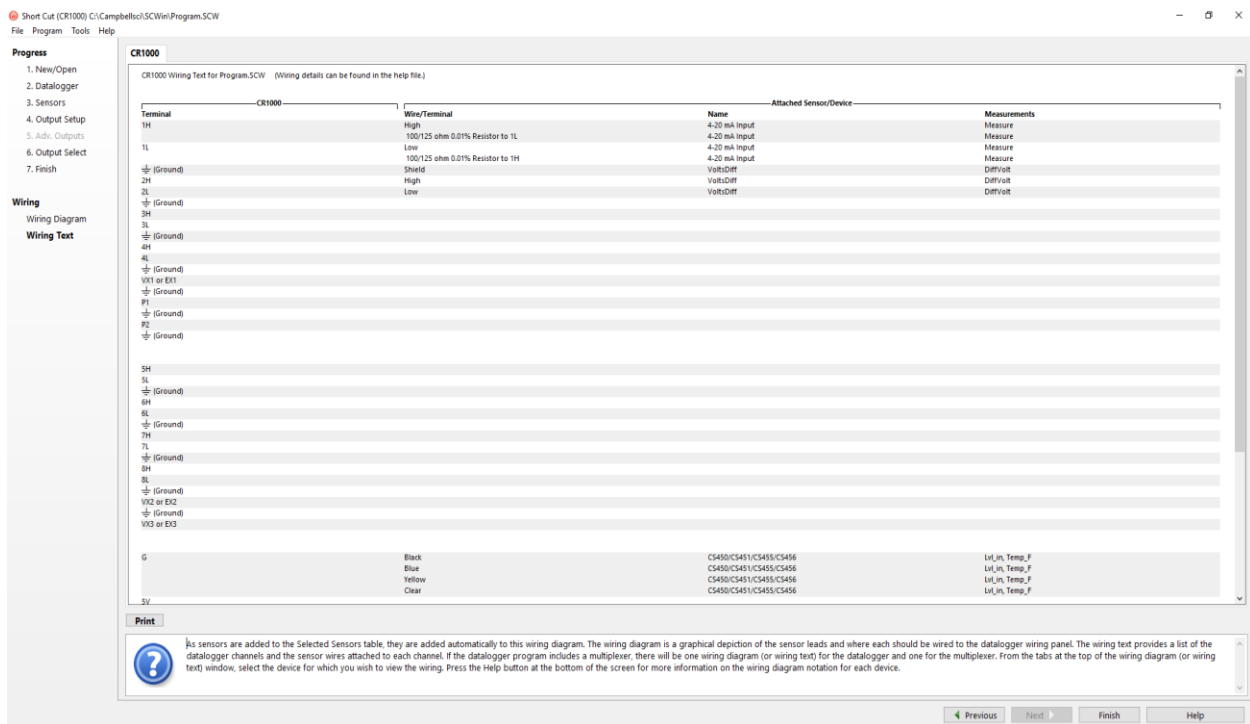


Figure 106. ShortCut - Wire Text Screen

## PC200W

This software is only used to start the datalogger when an experiment is to be performed. The picture below shows the welcome screen of PC200W. When first setting up the datalogger, the user must add it manually to the software by clicking in the button that has the plus sign. Once added, a datalogger will remain in the software until removed.

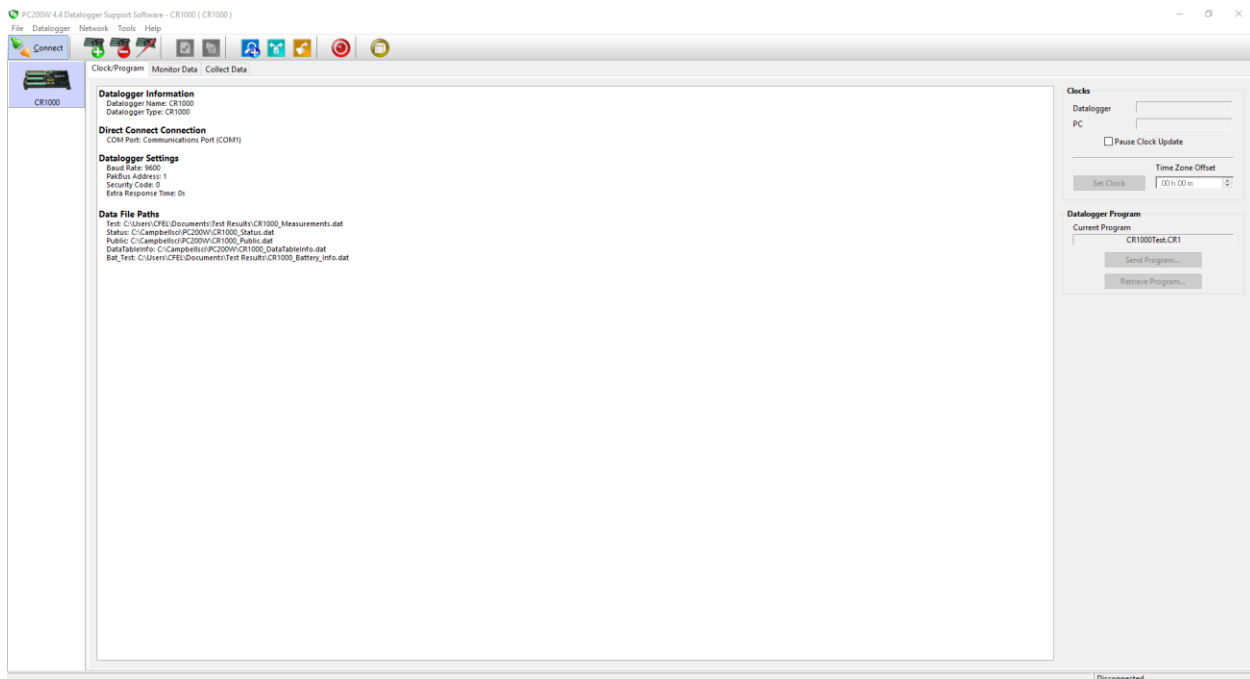


Figure 107. PC200W - Welcome Screen

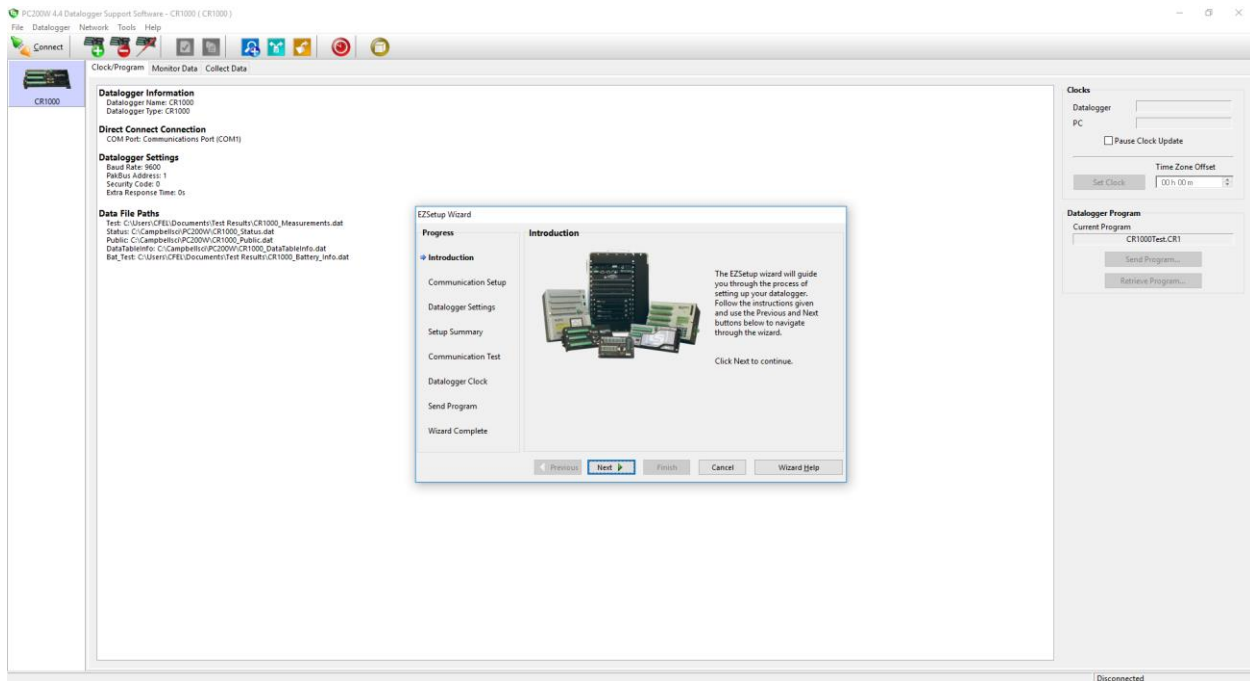
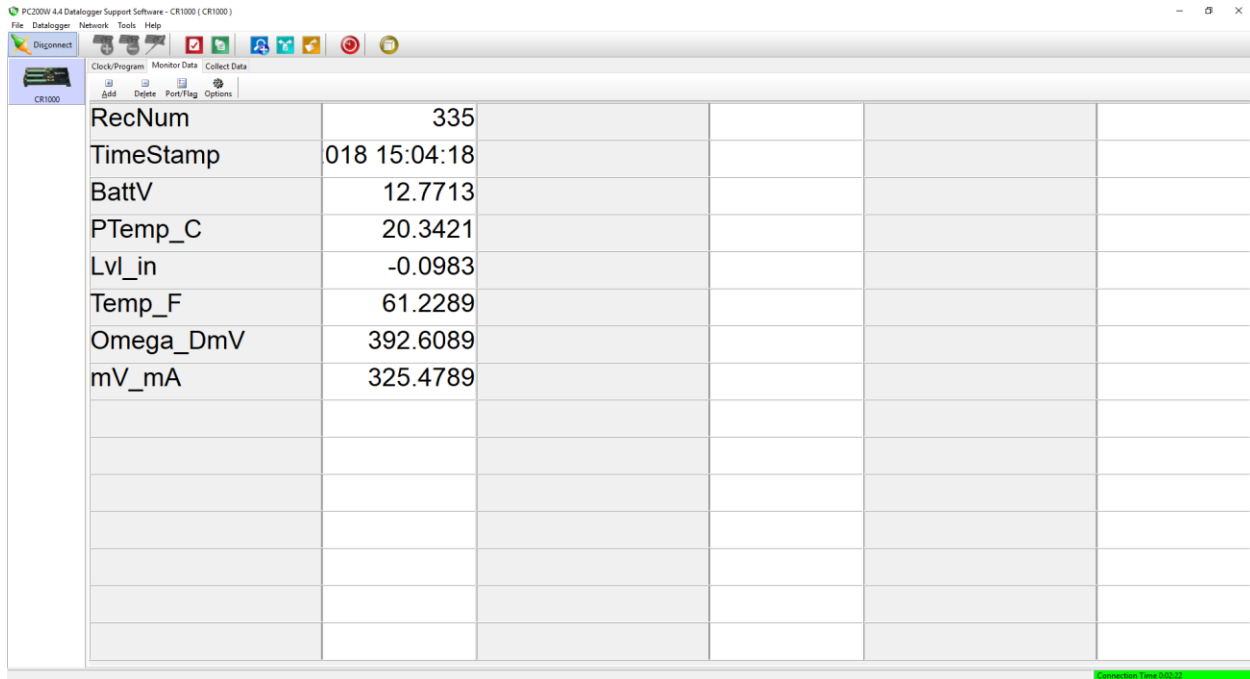


Figure 108. PC200W - Adding a Datalogger

Since the datalogger has already been added, the only necessary step to do when opening PC200W is to click the 'Connect' button. After clicking the connect button, the 'Set Clock' button should be pressed to synchronize the datalogger's clock with the one from the computer. After doing both these steps, the data retrieved by the datalogger can be observed in real-time using the 'Data Monitor' tab.





When saving the data go into the 'Collect Data' tab, in the main screen it is possible to select the data tables that the user wants saved, it is useful to remember from the program running in the datalogger, which are the data tables that will be filled, since PC200W shows all the data tabled from all the programs stored in the datalogger. For anyone using this software, it is recommended to not making any changes to the current working configuration. PC200W gives the user two options, to append the data to the current file, or to create a new one, from all the tests performed so far, both options keep append the data to the existing file, in order to truly reset the files, it is better to resend the program to the datalogger, this can be accomplished by going to the 'Monitor Data' tab.

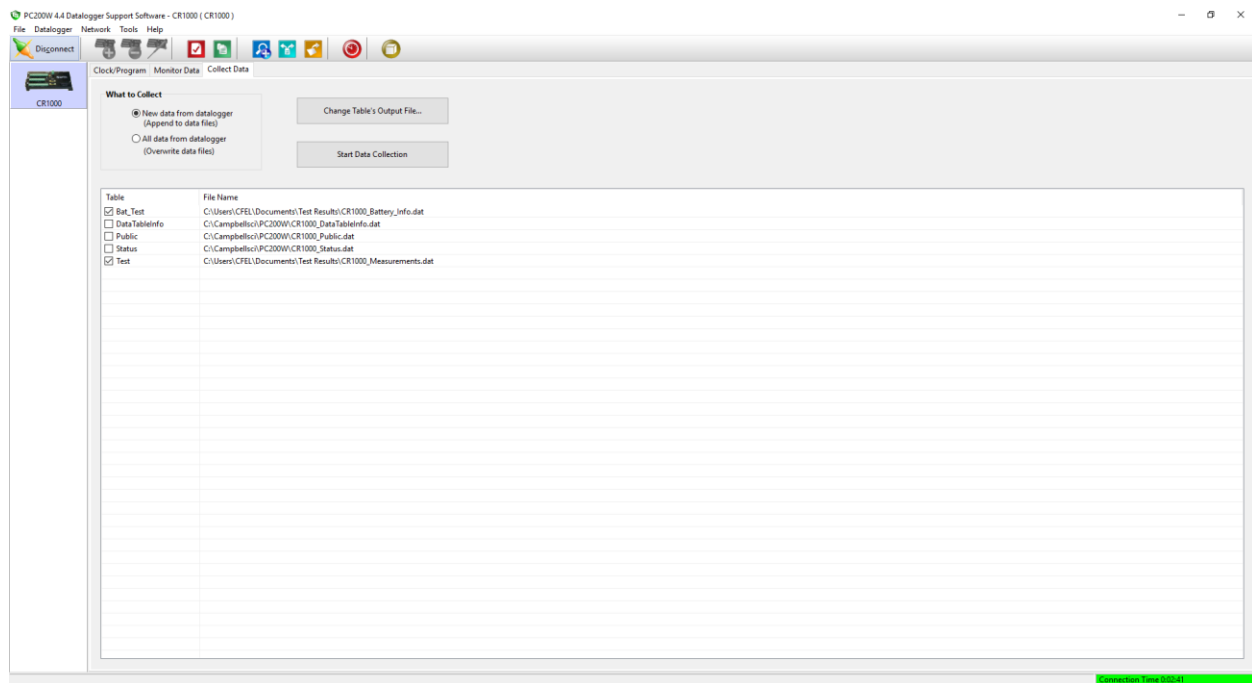


Figure 110. PC200W - Saving the Data

## Appendix #5: Additel Land Wireless & Additel 680 Wireless Transmitter Setup

This appendix will describe the methods used to setup the equipment of the experiment. Some of the instruments that were used for this were difficult to setup, usually due to a lack of help in manuals. Such as, with the flow meters, things that seem self-evident held up work for several weeks.

The gage used in this experiment is the Additel 680 Digital Pressure Gauge. It requires a ¼ inch female threaded port to be used and are externally water proof up to a depth of 1 meter. To setup the gauges to record, two additional items are required, a USB receiver and the software they come with. By going through the settings, the pressure gauge can be put on a specific channel. When more than one gauge is being used, they should be allocated to the same channel. The pressure gauge records data locally, then uploads it to the software via the USB transmission when requested. The software handles receiving and saving the data from two gauges, as well as starting and stopping the data recording. It is unknown how many gauges the software can handle.

The gages transmission must be turned on each time that they are turned on. This is done by holding the settings key on the device. The menu can be navigated through with the same settings key until a symbol that resembles a wi-fi signal is found.



Figure 111. Additel 680 Pressure Transmitter- Turning On transmission



Figure 112. Additel 680 Pressure Transmitter - Selecting Channel

The wireless menu can be entered using the zero key. Several different options are available, most importantly the option to turn it on, and the option to change the channel. It is unknown whether the channels themselves are important, but all gauges in use need to be set to the same channel. The wireless transmission will be activated when the same symbol as the menu is flashing in the top left. The software will then be able to find all gauges on each channel, then serial number can differentiate the gauges.

Once the USB is connected to the computer there is a green “play” button on the bottom right of the screen. Using this starts the transmission to the devices once a channel is selected.

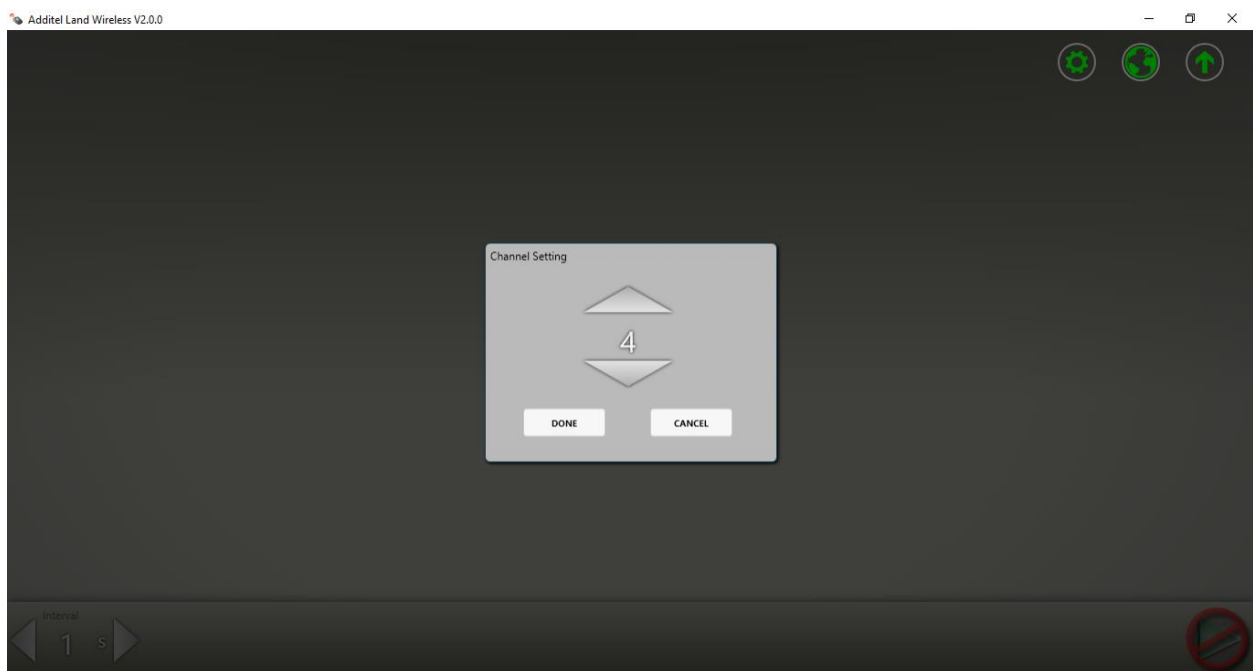


Figure 113. Additel Land Wireless - Channel Selection

An icon representing a computer then appears, and once they connect, so do icons for each pressure gauge.

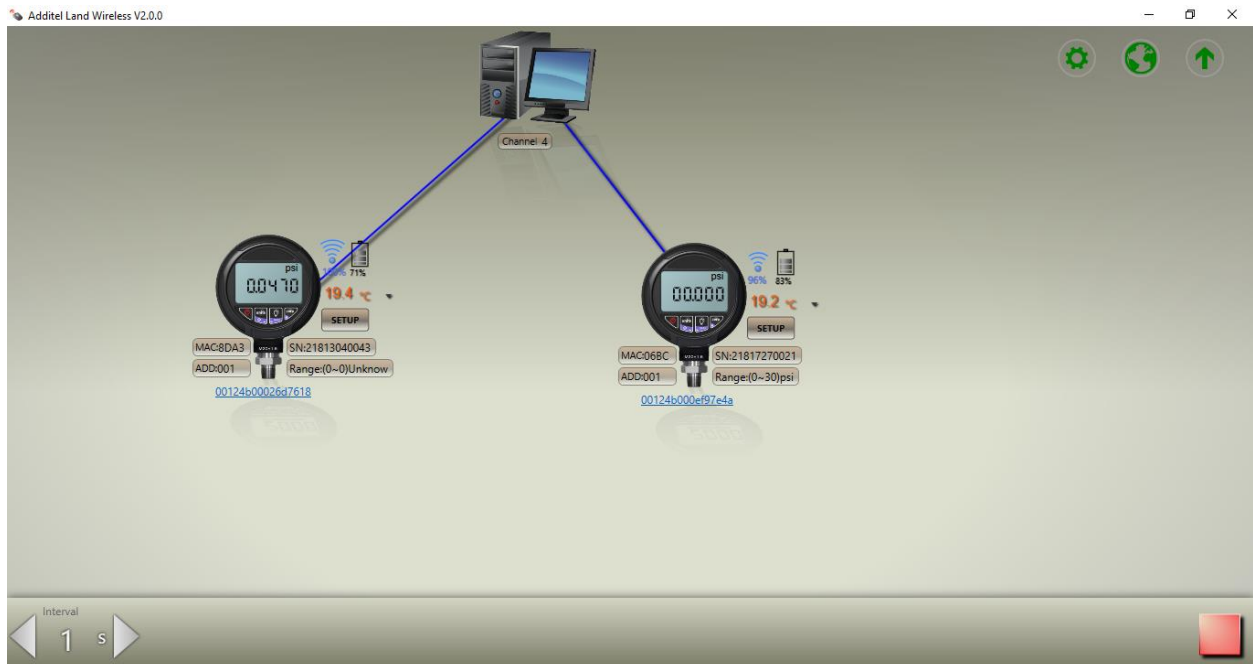


Figure 114. Additel Land Wireless Transmitters Screen

Clicking the 'Setup' button will open the menu on the device on the left in the figure below. The two most important options are Data Log and Export Data. Clicking Data Log opens the menu next to the right device. Clicking the 'Log Setting' toggle will start the device recording pressure data. Clicking it again will end it.

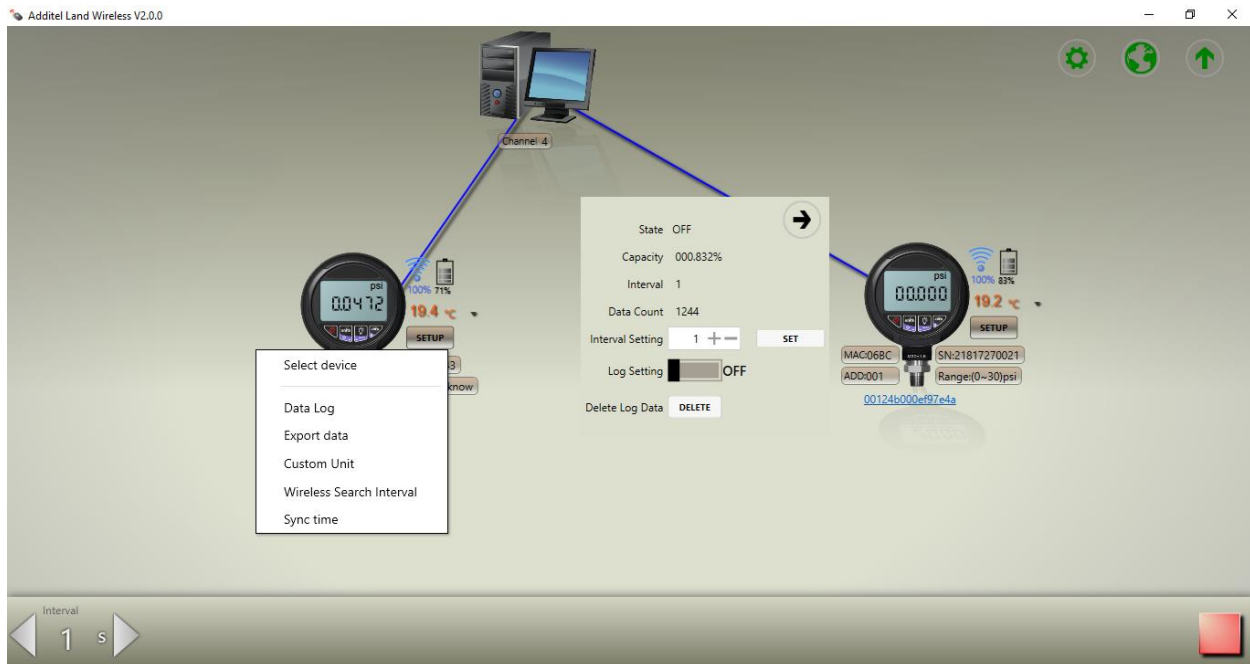


Figure 115. Additel Land Wireless - Start to Record

If it is wished to delete the old data on the device and start fresh, a password is required.

The password is 218 by default.

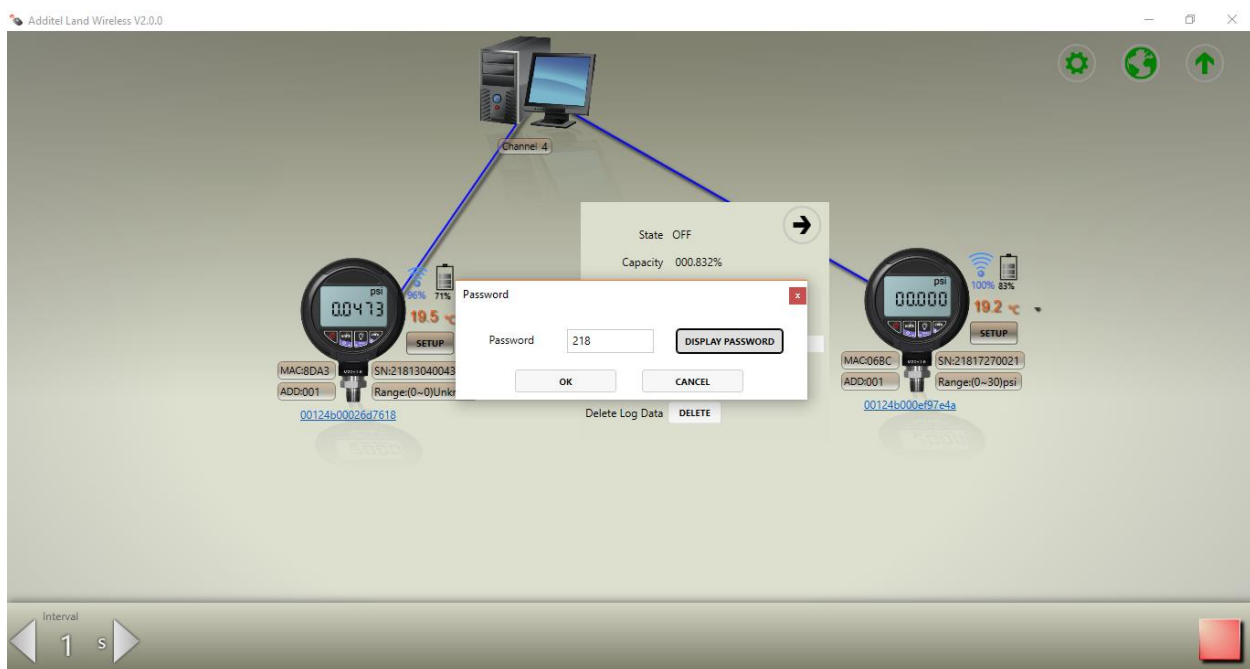


Figure 116. Additel Land Wireless - Password Screen

Once the data has been recorded to the device, it can be exported as a CSV file from the 'Export Data' tab. The data will be loaded from the device and a window will open as seen below. Clicking 'Export' will open a save dialog window allowing the file to be saved wherever with a name of choice. Sometimes instead of a table window opening, a chart window will open by default. This will show the most previously recorded session, with options to scroll through previous recordings. This is the only difference; a CSV file can still be exported from this window.

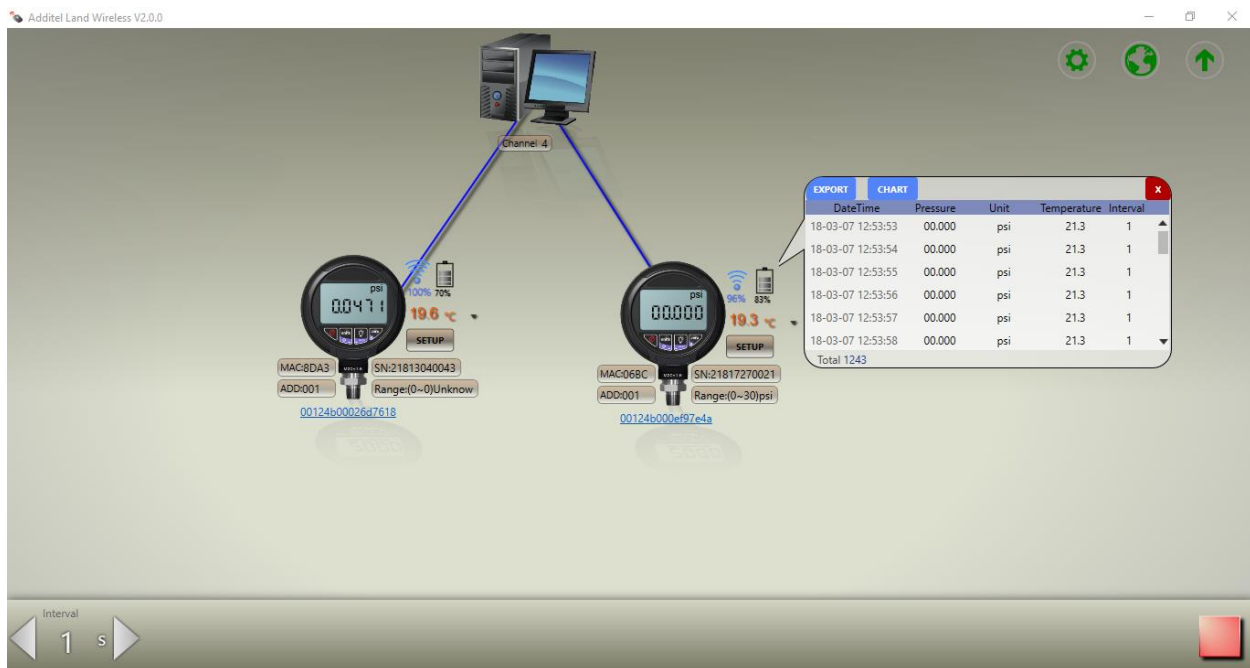


Figure 117. Additel Land Wireless - Export/Save Data



## Appendix #6: Saving Experiment Results into Excel Workbook

The first thing to do is create a new worksheet. This is accomplished by copying an existing worksheet (preferably the last one). In order to copy the worksheet, right-click the mouse on top of the name of the worksheet to copy, and click “Move or Copy”, select the option ‘Create a Copy’ and move the new worksheet to the end of the workbook.

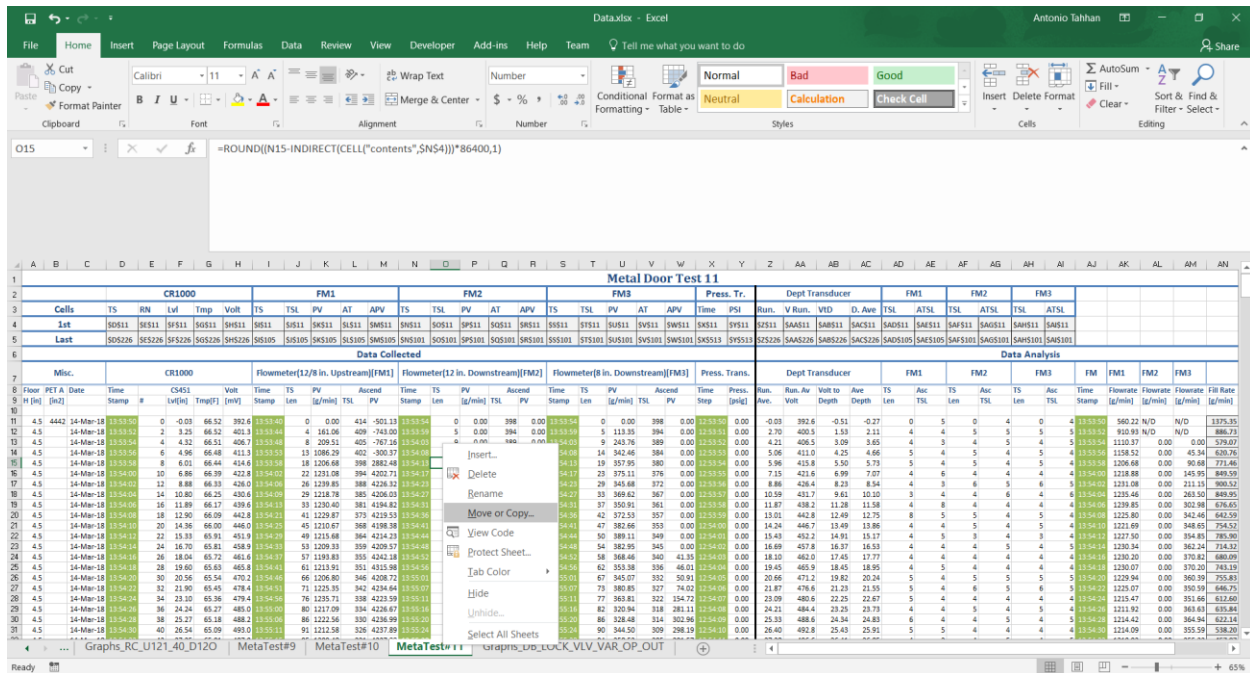


Figure 118. Excel - Copying a Worksheet

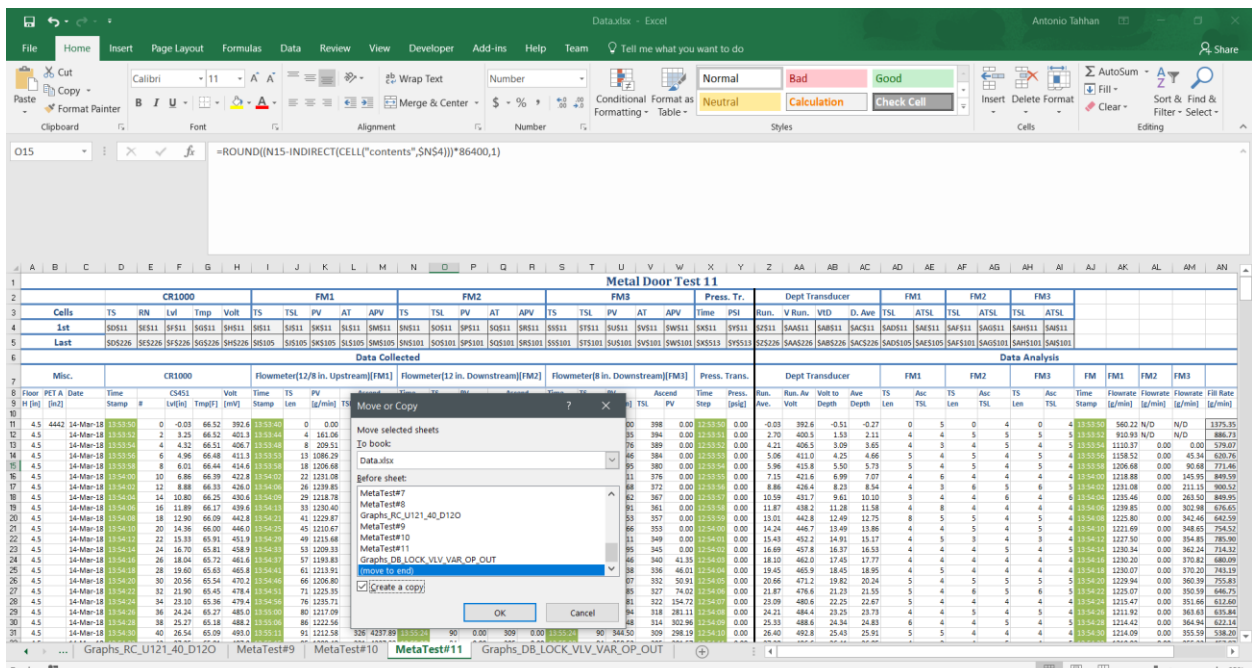


Figure 119. Excel - Selecting the Position of the New Worksheet

Once the worksheet has been created, rename it by right-clicking on the worksheet name, and selecting 'Rename'. The following step is to copy or cut the data into the appropriate columns.

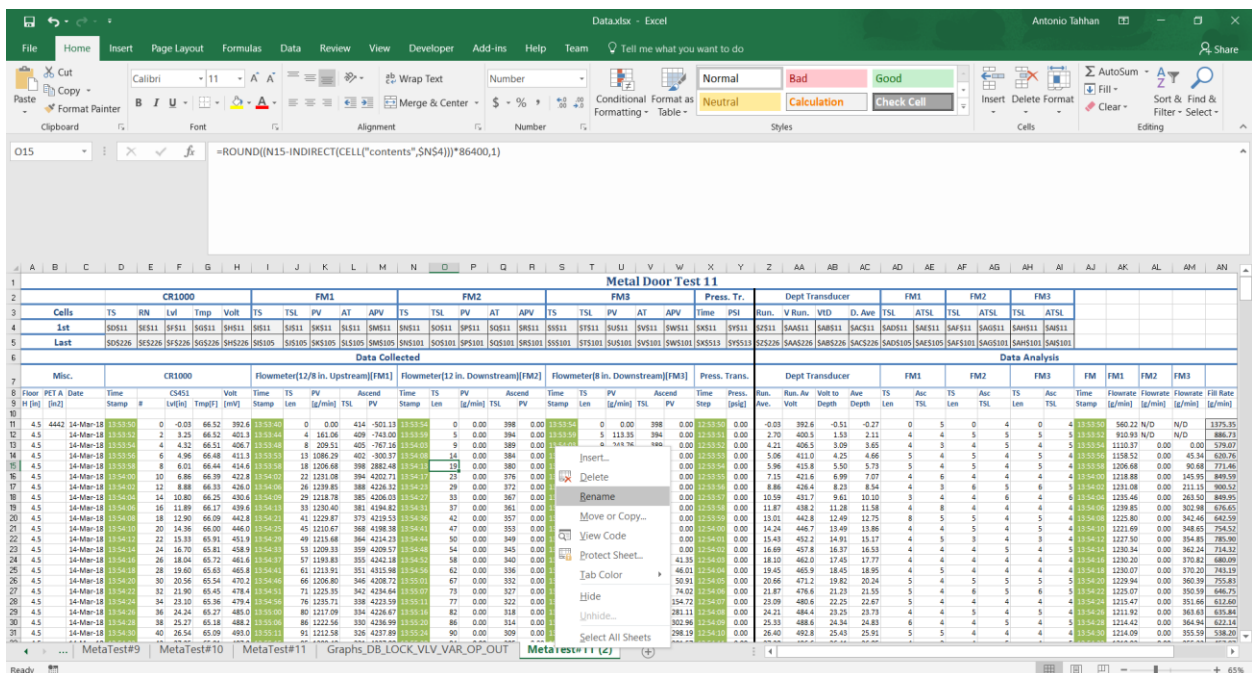


Figure 120. Excel - Renaming the New Worksheet

The last two steps are to 'Sort' the data in the 'Ascend PV' columns and enter the corresponding cell addresses for each column in rows 4 and 5. After these two steps are done, the worksheet should analyze all the data automatically.